EXPLORING THE ROLE OF SYNDECAN IN *DROSOPHILA* NERUAL AND GLIAL DEVELOPMENT

by

DUO CHENG

B.Sc., The University of Guelph, 2018

A THESIS SUBMITTED IN PARTIAL FULFILLMENT OF THE

REQUIREMENTS FOR THE DEGREE OF

MASTER OF SCIENCE

in

THE FACULTY OF GRADUATE AND POSTDOCTORAL STUDIES

(CELL AND DEVELOPMENTAL BIOLOGY)

THE UNIVERSITY OF BRITISH COLUMBIA

(Vancouver)

May 2021

The following individuals certify that they have read, and recommend to the Faculty of Graduate and Postdoctoral Studies for acceptance, a thesis entitled:

Exploring the role of Syndecan in *Drosophila* neural and glial development

submitted by Duo Cheng in partial fulfillment of the requirements for

the degree of Master of Science

in Cell and developmental biology

Examining Committee:

Vanessa Auld, Professor, Zoology, UBC
Supervisor

Calvin Roskelley, Professor, Cellular and Physiological Sciences, UBC
Supervisory Committee Member

Matthew Ramer, Associate Professor, Zoology, UBC
Supervisory Committee Member

Hakima Moukhles, Associate Professor, Cellular and Physiological Sciences, UBC
Additional Examiner

Abstract

Glia are dynamic modulators required for the development and function of the nervous system, and various cell surface receptors which interpret the extracellular landscape are integral to their actions. However, the mechanisms by which glia accomplish such tasks remain to be fully characterized. This thesis explores the function of a major transmembrane heparan sulfate proteoglycan (HSPG) protein, Syndecan (Sdc), and its function in the *Drosophila* nervous system.

In the central nervous system, where Syndecan is robustly expressed, I have shown that its downregulation in glia leads to a reduction in neuroblasts population, resulting in shrinkage of the brain lobe. In parallel, I observed elongation of the ventral nerve cord, indicative of disruption to the glial-ECM interactions.

Syndecan is also found in high levels in various glial membranes within the peripheral nervous system, where I observed distinctive and cell-autonomous defects upon downregulation of Syndecan expression within each glial layer. Our results suggest Syndecan is required for the maintenance of blood-nerve barrier integrity, as Syndecan knockdown disrupted separate junction morphology of peripheral subperineurial glia. Moreover, I showed Syndecan is required for the ensheathment by multiple glial populations, including perineurial and wrapping glia. In particular, laminin deposition in the basal lamina surrounding the peripheral nerve was reduced upon knockdown of Syndecan in the outermost (perineurial) glial layer. Overall, these results demonstrate several novel aspects of Syndecan's role *in vivo* during neural and glial development.

Lay Summary

Cells use various receptors to sense their surroundings and communicate with other cells. This is also true for glial cells, the main non-neuronal cell type in the nervous system. I studied a protein called Syndecan which is highly conserved across different species and can be found on the cell surface of neurons and glia. I found that when I removed Syndecan from the glia, the neighboring neural stem cells which can give rise to neurons, are unable to maintain or expend their cell numbers. I also found that Syndecan is needed for glia to wrap around their associated neurons, and to maintain the shape and structural integrity of the nervous system. Overall, the work in this thesis uncovered that Syndecan as a necessary protein for glia to perform their different functions in the development of the nervous system.

Preface

Chapter 2: **Exploring the role of Syndecan in *Drosophila* neural and glial development**

Work in this chapter contributes to the ongoing investigation into characterizing Syndecan's expression and subcellular localization in the *Drosophila* nervous system and elucidating Syndecan's function in glial interactions and development. For this chapter, I made major contributions to experimental design, data collection and analysis, writing and editing. Jaimy Coates contributed to data collection. Dr. Mary Gilbert and Dr. Mriga Das made significant contribution editing. Vanessa J Auld contributed to experimental design, data interpretation and analysis, writing and editing.

Table of Contents

List of Tables

List of Figures

List of Abbreviations

ADAMTS	A disintegrin and metalloproteinase with thrombospondin motifs metallopeptidase with thrombospondin
AG	Astrocyte-like glia
BBB	Blood brain barrier
BL	Brain lobe
BMP	Bone morphogenetic protein
BNB	Blood nerve barrier
CASK	Calcium/calmodulin-dependent serine protein kinase
cDCP-1	cleaved Death caspase-1
CG	Cortex glia
chk	Chaski
CNS	Central nervous system
Cyto	Cytoplasmic domain
Dcr2	Dicer-2
dilp	*Drosophila* insulin-like peptide
Dlp	Dally-like protein
Dpn	Deadpan
ECM	Extracellular matrix
Ecto	Ectodomain
EG	Ensheathing glia
EGF	Epidermal growth factor

EGFR	Epidermal growth factor receptor
EM	Electron microscopy
ER	Endoplasmic reticulum
FGF	Fibroblast growth factor
FGFR	Fibroblast growth factor receptor
FRET	Förster resonance energy transfer
Fyn	Fyn proto-oncogene, Src family tyrosine kinase
GAG	Glycosaminoglycans
GFP	Green fluorescent protein
HB-GAM	Heparin-binding growth-associated molecule
HER2	Human epidermal growth factor receptor-2
HGF	Hepatocyte growth factor
HRP	Horseradish peroxidase
HS-GAG	Heparan-sulfate glycosaminoglycans
HSPG	Heparan-sulfate proteoglycan
Htl	Heartless
HUVEC	Human umbilical vein endothelial cells
if	Inflated
IGF	Insulin-like growth factor
IL	Interleukin
InR	Insulin-like receptor
mAb	Monoclonal antibody

mCD8	Mouse lymphocyte marker cluster of differentiation 8
MFA	Muscle field area
MSC	Myelinating Schwann cell
MMP	Matrix metalloproteinases
mys	Myospheroid
NB	Neuroblast
NCKX	$Na^{+}Ca^{2+}K^{+}$ exchanger
NB	Neuroepithelium
NER	Nerve extension region
NF1	Neurofibromin 1
NG	Neuropile glia
NLS	Nuclear localized signal
Nrg	Neuroglian
Nrv2	Nervana 2
NrxIV	Neurexin IV
NMJ	Neuromuscular junction
nMSC	Non-myelinating Schwann cells
PDGF	Platelet-derived growth factor
PDZ	Post synaptic density protein-95, *Drosophila* disc large tumor suppressor-1, Zonula occludens-1
PG	Perineurial glia
pHis-3	phosphohistone-3

PIP_2	Phosphatidylinositol 4,5-biphosphate
PIP_3	Phosphatidylinositol 3,4,5-triphosphate
PKCα	Protein kinase C-α
PNS	Peripheral nervous system
Pys	Pyramus
repo	Reverse polarity
RFP	Red fluorescent protein
RNAi	RNA interference
RTK	Receptor tyrosine kinase
Sdc	Syndecan (*Drosophila*)
SHh	Sonic hedgehog
shRNAi	Short hairpin RNAi
SJ	Septate junction
SG	Surface glia
SPARC	Secreted-protein acidic cystine-rich
SPG	Subperineurial glia
TFL	Trophic factor ligand
TFR	Trophic factor receptor
TGF-β	Transforming growth factor-β
Tiam1	T-cell lymphoma invasion and metastasis-1
TM	Transmembrane domain
Tret1-1	Trehalose transporter 1-1

TOR	Target of rapamycin
UTR	Untranslated region
VEGF	Vascular endothelial growth factor
VNC	Ventral nerve cord
wb	Wing blister
WG	Wrapping glia
Wnt	Wingless/Integrated
YPet	Yellow fluorescent protein
zyd	Zydeco

Acknowledgements

Of most, I offer my greatest gratitude to my supervisor Vanessa for taking me on as a student and providing guidance and insight into the scientific field during our numerous discussions throughout my time in her lab. Through our numerous discussions, not only it opened my eyes to new directions in the project, and made me to think like a scientist, but also allowed me to understand and able to navigate the scientific field and academia.

I would also like to thank my advisory committee members Dr. Calvin Roskelley and Dr. Matt Ramer for their valuable time and insightful feedback, special shoutout to Matt for letting me use his fancy super-resolution microscope for my project pro bono.

To my follow lab members Murry, Mriga, Amelia, Katie, Sravya and Rosalie and fellow cohort, thank you for teaching and helping me troubleshoot my experiments, and dealing spicy meme in the group chat, special thanks to Murry and Mriga for editing and providing the necessary feedback on this thesis

Though most special thanks of them all are owed to my parents, who worked endlessly and sacrificed so much to provide the support (financial or otherwise) I needed throughout my years of education.

fruit fly trap

pour one cup of apple cider vinegar with a few drops of soap into a container

roll one sheet of paper into a cone, cut away the excess and place onto the opening

Chapter 1: Introduction

Glia (derived from Greek for "glue") are the main cell type within the nervous system apart from neurons. Glia were historically mislabeled by Virchow in 1846, who coined the term "nervenkitt" to describe the abundant connective structure within the brain as "the glue that holds neurons together" (Somjen, 1988). For more than a century, proposed glial functions were confined to providing passive structural and metabolic support to the neurons they surround. However, this paradigm has shifted dramatically where we now appreciate that glia are active and highly dynamic regulators of nervous system development, function, and disease (Magnusson et al., 2014; Saab et al., 2016; Fernandes et al., 2017; Cui et al., 2018). Regardless of our recent advancements, numerous questions remain as to the molecular machineries and pathways required for glial function. For instance, the ability to communicate with neighboring glia and the extracellular environment (i.e., the extracellular matrix or ECM) is a vital for glia to properly encase/isolate neurons and provide the necessary protection. Yet, the mechanisms utilized by glia to interact with their environment are still being elucidated. Cellular adhesion and growth factor mediated signaling has been shown to play a pivotal role in the glial development. This thesis focuses on characterizing a heparan-sulfate proteoglycan (HSPG) ECM receptor, Syndecan (Sdc), and the role Sdc plays in modulating cell-ECM adhesion and growth-factor mediated pathway in *Drosophila* nervous system development.

1.1 Glia of the *Drosophila* Nervous System

Drosophila melanogaster is an invaluable model organism to test our understanding of principles of neurobiology as its nervous system shares many broad structural and functional similarities to vertebrates (Freeman and Doherty, 2006; Freeman, 2015). In both the larvae and

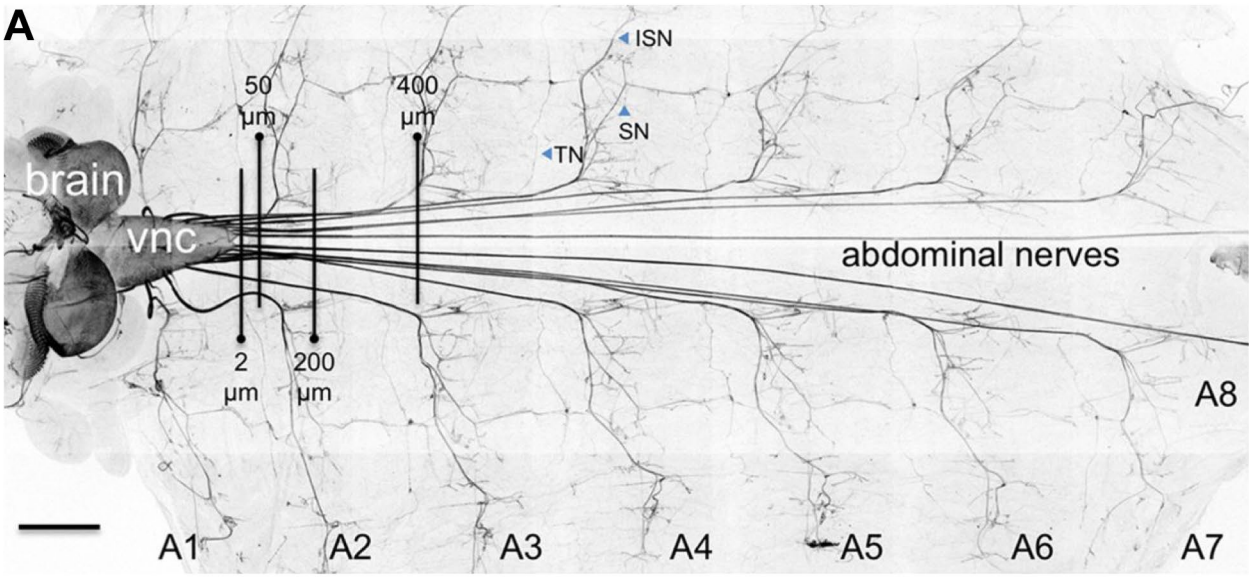
A
ISN
50 µm
400 µm
SN
TN
brain
vnc
abdominal nerves
2 µm
200 µm
A8
A1
A2
A3
A4
A5
A6
A7

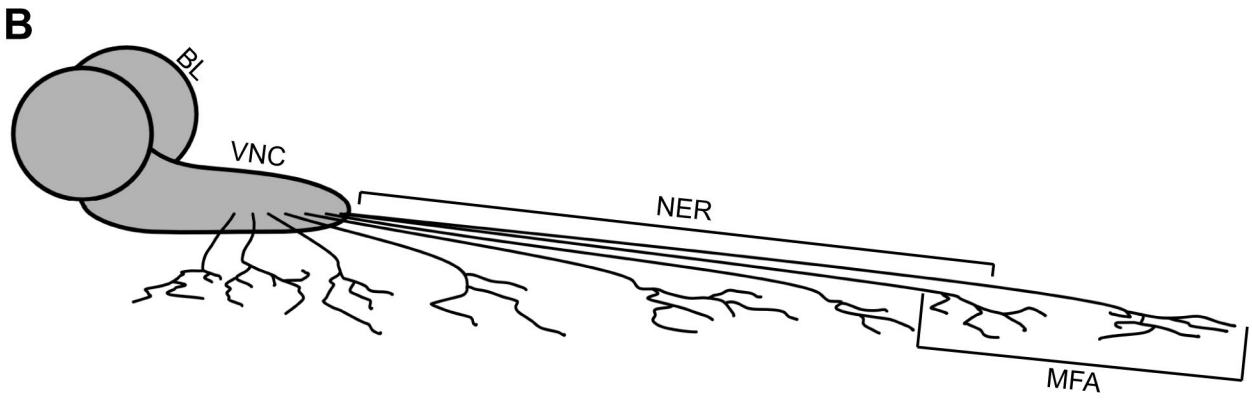
B
BL
VNC
NER
MFA

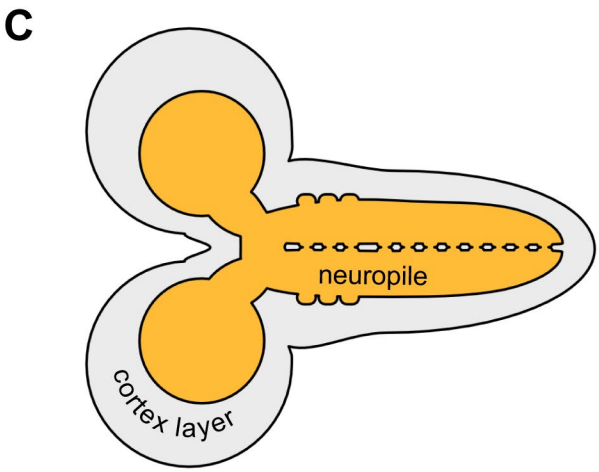
C
neuropile
cortex layer

Figure 1.1: The major compartments of the *Drosophila* larval nervous system

(**A-B**) Image of a larval fillet with the entire nervous system visualized through horseradish peroxidase (HRP) staining. At the third instar stage, the central nervous system is comprised of two brain lobes (brain/BL) and the ventral nerve cord (VNC). Eight pairs of abdominal nerves (A1-A8) branch off from the VNC and contain both motor and sensory axons. The nerve extension region (NER) is defined as the segment of the nerve between the VNC and the muscle field area (MFA). ISN, intersegmental nerve; SN, segmental nerve; TN transversal nerve. Scale bar = 200µm. (Adapted from (Matzat et al., 2015)) (**C**) The CNS contains two distinct structures, the neuropile (yellow) contains all synapses and neuronal somata are found within the cortex layer (light grey).

adult stages, the *Drosophila* central nervous system (CNS) contains a diverse range of glial cell types categorized mainly by their morphology and their association with neurons. The CNS of *Drosophila* larvae is made up of two brain lobes (BL) and the ventral nerve cord (VNC) (**Fig. 1.1A, B**). Most neuronal cell bodies are found in the cortex of the CNS and the synapses are within the neuropile at the core (**Fig. 1.1C**). Within the CNS, glial cells are divided into three main classes: neuropile glia (NG), cortex glia (CG), and surface glia (SG). Neuropile glia can be further categorized into ensheathing glia (EG) and astrocyte-like glia (AG). *Drosophila* astrocyte-like glia behaviour resembles in parts vertebrate astrocytes. Though morphologically distinct, both regulate synaptic function, and both extend membrane projections that surround synapses and actively regulate neurotransmitter homeostasis (Awasaki et al., 2008; Stork et al., 2012, 2014; Yildirim et al., 2019). Ensheathing glia dwell mainly along the neuropile-cortex interface. Consequently, EGs' main functions are thought to provide compartmentalization by separating the neurite and synapse-dense neuropile from the soma-packed cortex, and divide major groups of axons into discrete commissures (Doherty et al., 2009; Stork et al., 2012). Ensheathing glia also regulate axon fiber tract formation and guidance within the developing

CNS (Spindler et al., 2009). Cortex glia directly enwrap multiple neuronal somata (Pereanu et al., 2005; Hartenstein, 2011; Stork et al., 2012) and associated nerves as they exit the ventral nerve cord (**Fig. 1.2A**) (Freeman, 2015). Due to their close proximity, cortex glia are thought to provide trophic and metabolic support to the neurons (Pereanu et al., 2005; Hartenstein, 2011).

The last class of CNS glia, the surface glia, ensheathe the entire CNS and are responsible for forming the blood-brain barrier (BBB) (Hindle and Bainton, 2014). Surface glia are comprised of two sub-types: the outer perineurial glia (PG) and the inner subperineurial glia (SPG) (Hindle and Bainton, 2014) (**Fig. 1.2A-C**). Perineurial glia directly contact the overlying ECM that coats the entire nervous system. Together with the ECM, perineurial glia contribute to the overall CNS morphology through regulation of cell-ECM interactions (Xie and Auld, 2011; Hunter et al., 2020). Subperineurial glia are located directly below the perineurial glia and their most notable function is to maintain the ionic homeostasis within the nervous system, they do this by virtue of septate junctions (SJ), which create a permeability barrier (Auld et al., 1995; Baumgartner et al., 1996; Stork et al., 2008). For this thesis, I will mainly be focusing on both perineurial and subperineurial glia, collectively known as surface glia, and cortex glia when discussing the CNS glia function during *Drosophila* development.

The peripheral nervous system (PNS) is comprised of mixed sensorimotor nerves, with axons ensheathed by three glial layers (**Fig. 1.2B**). Each nerve can be further broken down into the nerve extension region (NER) and the muscle field area (MFA) (**Fig. 1.1A, B**). The muscle field is where the motor axons branch off each nerve to innervate their associated muscles and the sensory axons enter each nerve. The glial ensheathment of each PNS nerve is comparable to the CNS, with the surface glia forming the blood-nerve barrier (BNB) in a similar manner (**Fig. 1.2A, B**). Positioned at the center of each nerve are wrapping glia (WG). Wrapping glia are in

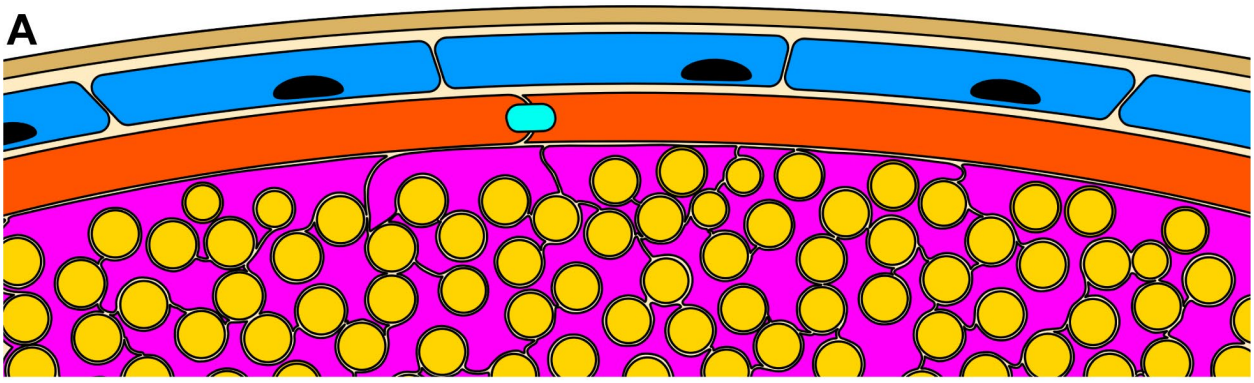
A

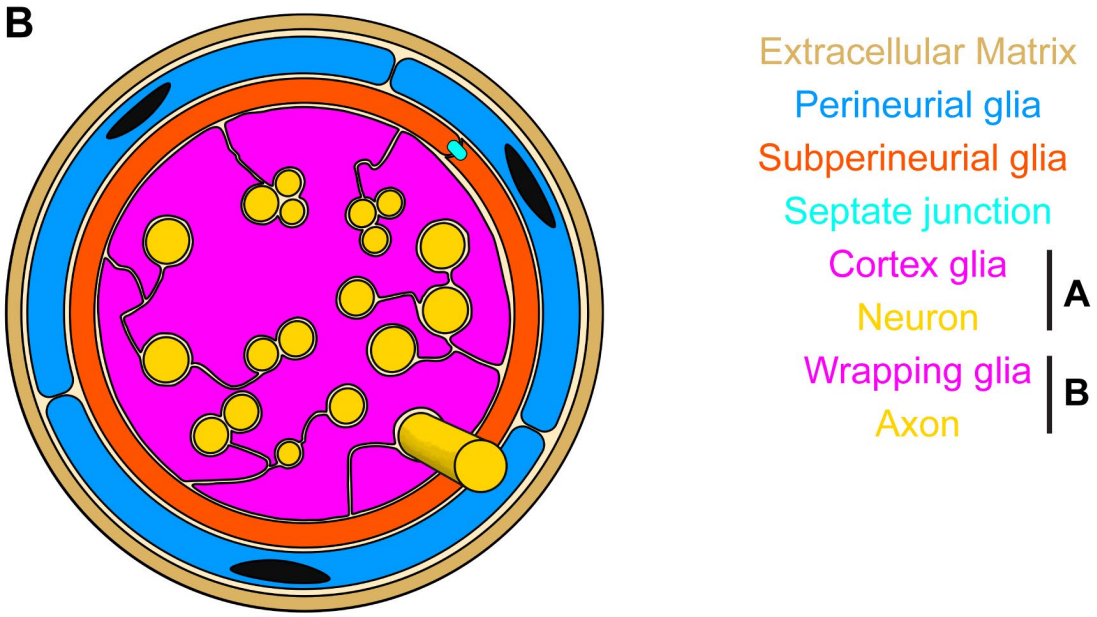
B
Extracellular Matrix
Perineurial glia
Subperineurial glia
Septate junction
Cortex glia
Neuron
A
Wrapping glia
Axon
B

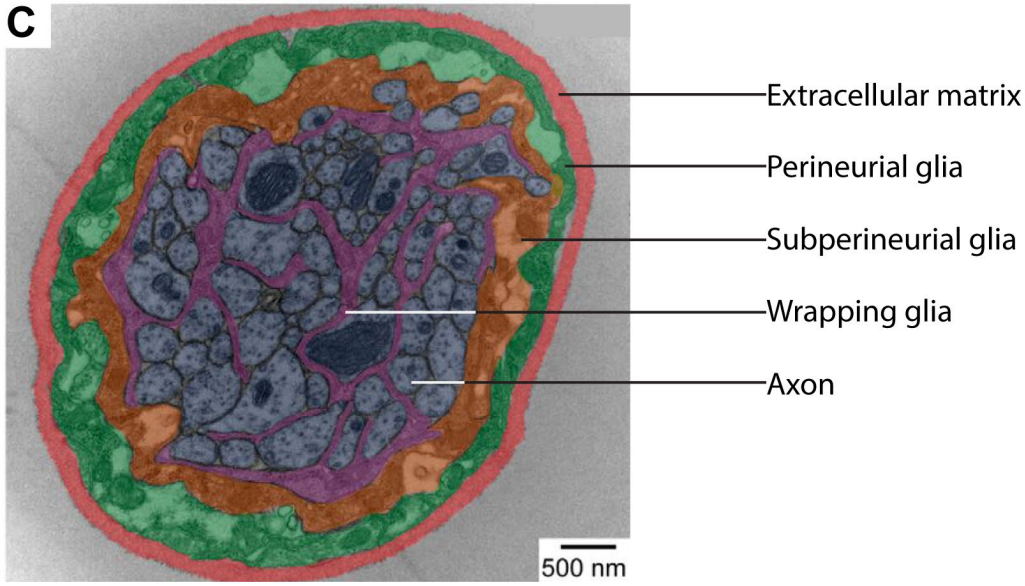
C
Extracellular matrix
Perineurial glia
Subperineurial glia
Wrapping glia
Axon
500 nm

Figure 1.2: An overview of superficial glial populations within the *Drosophila* the CNS and PNS

(**A-B**) Illustrations showing subset glial position and morphology within CNS cortex and PNS. The ECM (light brown) covers the nervous system in its entirety. Residing below are the perineurial glia (blue) which in turn ensheathe the subperineurial glia (orange). The subperineurial glia establishes the septate junction (cyan) forming a tight seal as the blood-brain/nerve-barrier. Below the subperineurial glia are the cortex glia (magenta in **A**) and wrapping glia (magenta in **B**) within the CNS and PNS, respectively. Cortex/Wrapping glia sort neurons/axons into individual compartments or small bundles. (**C**) Electron microscopy image of a peripheral nerve section showing the layering of different glial cell types illustrated in B. Scale bar = 500 nm. (Adapted from (Petley-Ragan et al., 2016))

close association with axons and directly ensheathe them (Stork et al., 2008). In the late larval stages, each wrapping glial cell is capable of ensheathing individual axons or small bundles. While loss of wrapping ensheathment has no deleterious effects, the loss of wrapping glia themselves can affect axonal conduction (Stork et al., 2008; Matzat et al., 2015; Kottmeier et al., 2020). The ensheathment of *Drosophila* wrapping glia resembles that of non-myelinating Schwann cells (nMSC) in vertebrates. This is an important yet poorly understood class of glia that ensheathe small-caliber axons such as C-fibers (Nave and Salzer, 2006; Nave and Trapp, 2008). Therefore, *Drosophila* is often used as a model to study the underlying molecular mechanisms of glial ensheathment during vertebrate development (Xie and Auld, 2011; Matzat et al., 2015; Kottmeier et al., 2020). Though all the glial subtypes mentioned above are important for nervous system function, the underlying mechanisms that glia utilize to direct such function remains to be fully decrypted. The following sections will explore the development and function of those *Drosophila* glial classes that are the focus of this thesis.

1.1.1 Perineurial glia

Late in embryonic development, perineurial glial cells arise in part from the lateral edge of the CNS. After several rounds of symmetric cell division, perineurial glia then migrate over the surface of the CNS and along the peripheral nerves (von Hilchen et al., 2013). Mature perineurial glia are elongated with many fine cell processes (Stork et al., 2008) (**Fig. 1.3A, B**), and completely cover the nervous system by the third instar larval stage (Awasaki et al., 2008; Stork et al., 2008; von Hilchen et al., 2013). Individual perineurial glial cell are highly mobile and able to migrate over large distances; more than half of the length of the larva in some cases (von Hilchen et al., 2013). The mitotically active nature of perineurial glia is in contrast with other glia (i.e., wrapping glia, subperineurial glia) which are polyploid and undergo hypertrophy as the larva grows (von Hilchen et al., 2013; Matzat et al., 2015). The division and differentiation of the perineurial glia are controlled by a number of signaling pathways. The activation of Insulin-like receptor (InR) / Target of rapamycin (TOR) pathway is required for perineurial glial proliferation, as loss of function mutants of the InR pathways reduced their numbers (Avet-Rochex et al., 2012). Acting in parallel, fibroblast growth factor (FGF) signaling regulates perineurial glia growth through paracrine signaling by the FGF ligand Pyramus (Pys) and the fibroblast growth factor receptor (FGFR), Heartless (Htl) (Avet-Rochex et al., 2012). Together the combined activity of InR/TOR and Htl generates the perineurial pool in the larval and adult stages (**Fig. 1.3C**) (Avet-Rochex et al., 2012).

As the most superficial glial layer, perineurial glia contribute to the formation of the ECM by secreting laminin, a core ECM component, into the extracellular space (Petley-Ragan et al., 2016). Other ECM components such as Perlecan, Collagen, Nidogen, and secreted-protein acidic cystine-rich (SPARC) are secreted by adipocytes and haemocytes (i.e. macrophages)

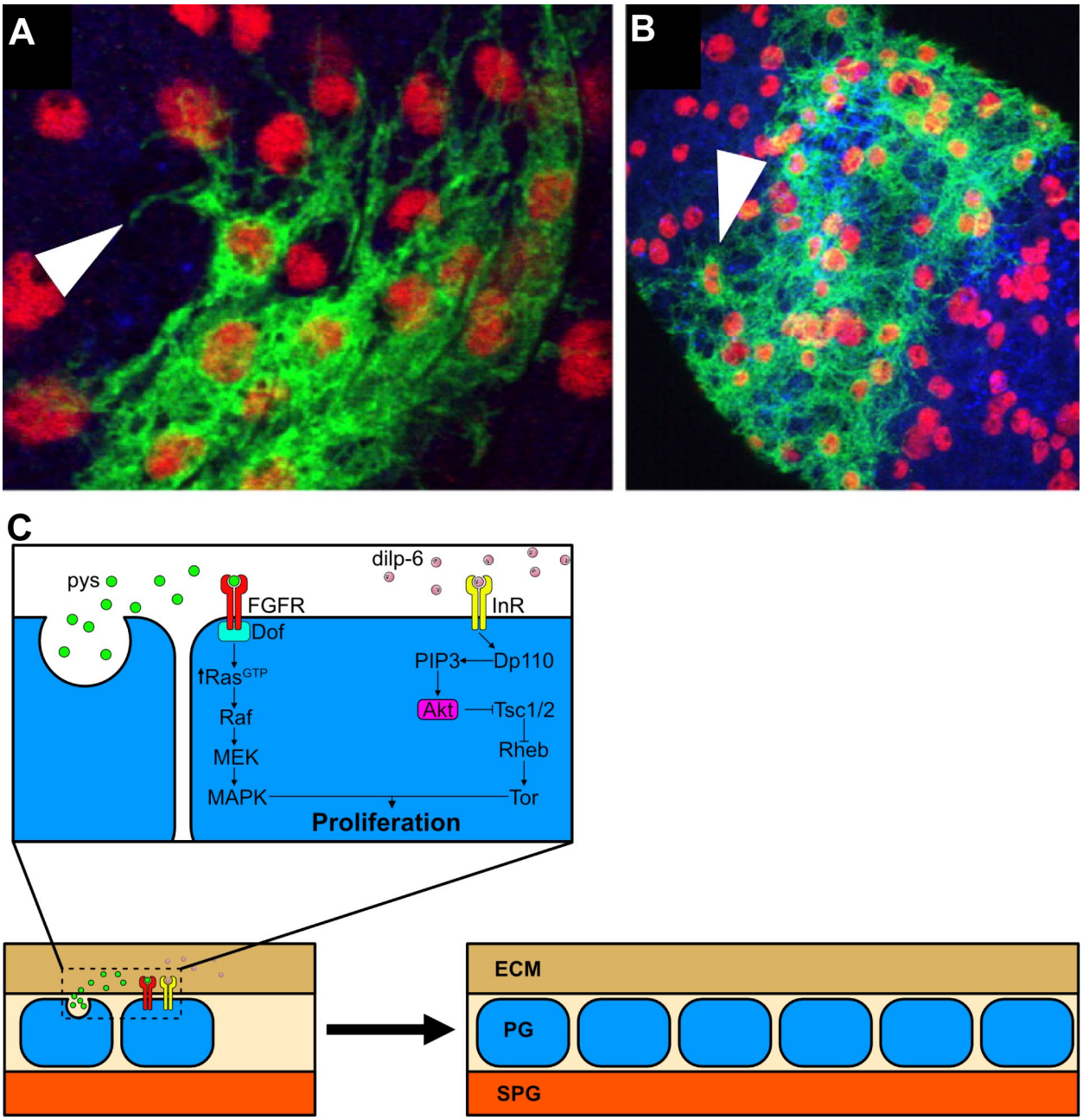
A
B
C
pys
dilp-6
FGFR
InR
Dof
RasGTP
Raf
MEK
MAPK
PIP3
Dp110
Akt
Tsc1/2
Rheb
Tor
Proliferation
ECM
PG
SPG

Figure 1.3:The growth and morphology of *Drosophila* perineurial glia

(**A-B**) Fluorescent images of perineurial glia (green) in the brain lobe (A) and VNC (B). Individual perineurial glia (green) were labeled with actin::GFP showing extensive cell projection (white arrowhead). All glia nuclei are stained using an anti-repo antibody (red)(Stork et al., 2008). (**C**) Illustration showing the proliferation of perineurial glia (PG) is controlled by Fibroblast growth factor (FGF) and InR/TOR pathways. Pyramus (Pys) activates Ras-MAPK signaling cascade via FGFR in a paracellular signaling manner. In conjunction, the InR/TOR pathway is activated through *Drosophila* insulin-like peptide 6 (dilp-6), acting in parallel to promote perineurial glial division for the ensheathment of the underlying subperineurial glia (SPG). Dof, Downstream of FGFR, an FGF scaffolding protein necessary for FGFR signal transduction; Dp110, a catalytic subunit of Phosphatidylinositol 3-kinase; PIP3, Phosphatidylinositol (3,4,5)-triphosphate; Tsc1/2, Tuberous sclerosis complex 1/2, an inhibitor of the TOR pathway; Rheb, Ras homolog enriched in brain, activate the growth regulator, Target of rapamycin (Tor).

(Broadie et al., 2011). Collectively the extensive and cross-linked ECM surrounding the nervous system is known as the "neural lamella" (Broadie et al., 2011; Zang et al., 2015). Additionally, perineurial glia express various ECM receptors, such as integrin (Xie and Auld, 2011; Meyer et al., 2014; Hunter et al., 2020), and modulate the neural lamella by secreting matrix metalloproteinases (MMPs) (Meyer et al., 2014; Skeath et al., 2017). Loss of ECM adhesion or degradation of ECM by overexpressing a membrane-bound MMP (i.e., MMP-2) on perineurial glial cells results in an elongated ventral nerve cord and deformed brain lobes. In the PNS, disruption of glia-ECM interactions leads to incomplete ensheathment by perineurial glia, peripheral nerves prone to mechanical damage and lethality at larval stages (Xie and Auld, 2011; Meyer et al., 2014).

Despite not being in direct contact with neurons, perineurial glia influence neuron survival, and behaviour (Brankatschk et al., 2014; Volkenhoff et al., 2015; Kanai et al., 2018; Parkhurst et al., 2018). Perineurial glia express a variety of nutrient transporters such the sugar

Trehalose transporter 1-1 (Tret1-1), and metabolic enzymes such as pyruvate kinase (Volkenhoff et al., 2015). Moreover, perineurial glia can influence neuroblast growth and division through the expression and release of Dally-like protein (Dlp) and Insulin-like peptides (dilp) (Chell and Brand, 2010; Kanai et al., 2018). While more and more evidence points to the importance of perineurial glia in the development and function of the nervous system, many questions remain with respect to the mechanisms perineurial glia use to communicate with their surroundings.

1.1.2 Subperineurial glia

Subperineurial glia are large, flattened cells that surround each nerve and the entire CNS (**Fig. 1.4 A**). During embryogenesis, subperineurial glia are in direct contact with axons and the neural lamella. As development proceeds, wrapping glia, cortex glia, and perineurial glia expand their region of ensheathment reducing subperineurial contacts with neurons and the ECM. The subperineurial glial population is established through the ventral neuroectodermal neuroblast progenitor population (von Hilchen et al., 2013). Fully differentiated, subperineurial glia do not divide; rather they undergo hypertrophy in order to accompany the dramatic growth of the animal (Brink et al., 2012; von Hilchen et al., 2013). One of the subperineurial glia's most notable functions is maintaining ionic balance through septate junctions that span the entire nervous system and stop just short of the neuromuscular junction (**Fig. 1.4 B, C**). Septate junctions act as a paracellular diffusion barrier that isolates the neurons from the high concentration of K+ in the hemolymph (Auld et al., 1995; Baumgartner et al., 1996; Stork et al., 2008). Insect septate junctions are functionally analogous to the tight junctions forming the blood-brain barrier in vertebrates. However, they are molecularly similar to paranodal junctions that flank vertebrate Nodes of Ranvier flanked by myelinating Schwann cells (MSC) and

oligodendrocytes (Hortsch and Margolis, 2003). The core adhesion components of the septate junction in subperineurial glia consist of a complex of membrane proteins including Neurexin IV (NrxIV), Contactin, Neuroglian (Nrg) and the Na^+/K^+ ATPase pump (the α-subunit (ATPα) and β-subunit-Nervana 2 (Nrv2)) (**Fig. 1.4 D**). Loss of any of these core proteins compromises the junction, and disrupts the blood-nerve barrier, leading to the hindrance of action potential conduction and paralysis (Baumgartner et al., 1996; Genova and Fehon, 2003; Faivre-Sarrailh, 2004; Banerjee, 2006). The process by which the septate junction is assembled and maintained remains an active area of research with recent investigations showing that the architecture of the septate junction changes from "Mr. Noodle™ ramen-like" parallel fibers in the late embryonic stage to a more linearized restaurant-style ramen later on (Babatz et al., 2018). However, the machinery by which subperineurial glia maintain septate junction integrity throughout this drastic remodeling phase remains to be described.

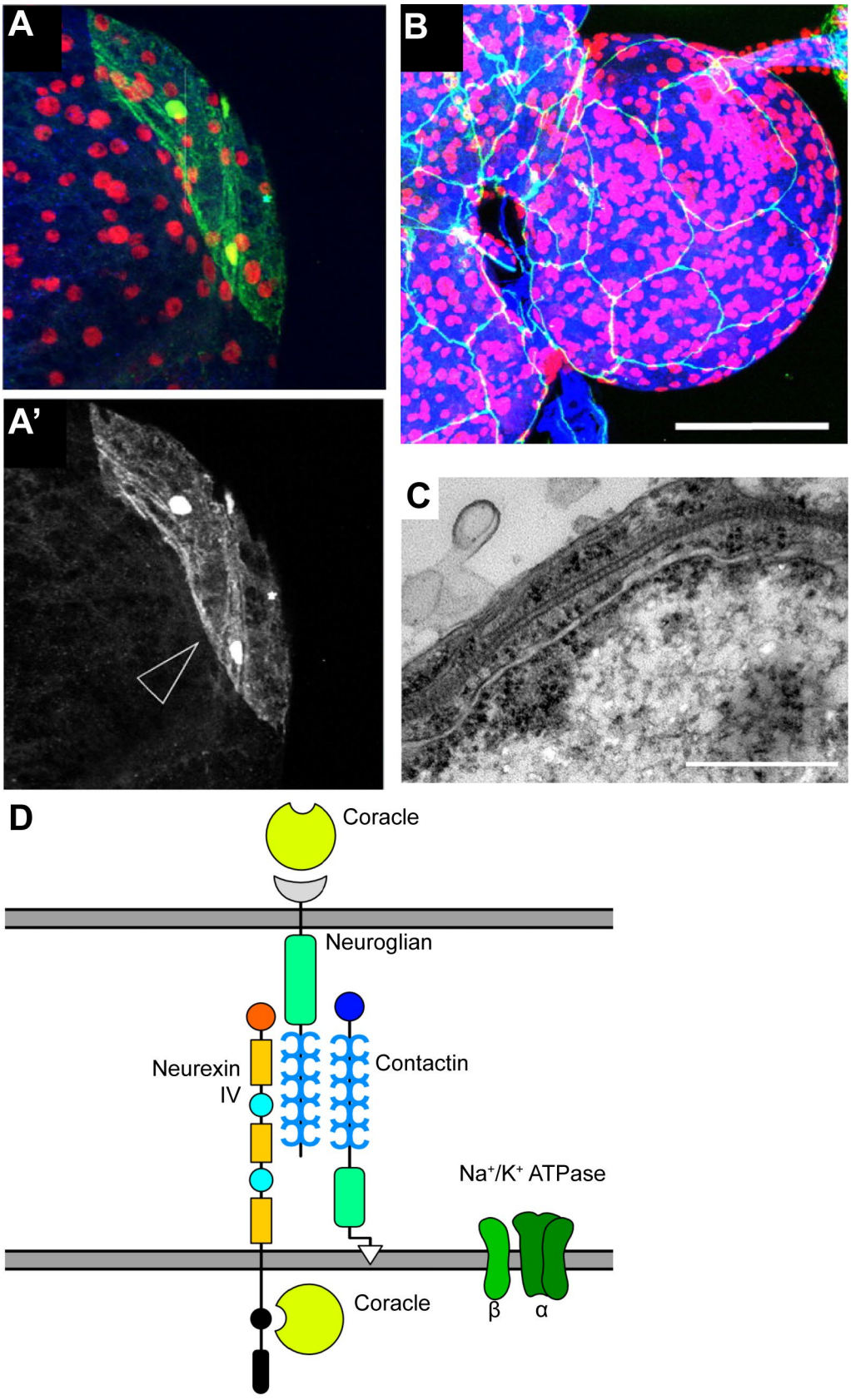
A
B
A'
C
D
Coracle
Neuroglian
Neurexin
IV
Contactin
Na+/K+ ATPase
Coracle
β
α

Figure 1.4: Subperineurial glial morphology and core components of the septate junction

(**A, A'**) Fluorescent image of an individual subperineurial glia (green) label with actin::GFP with all glial nuclei stained using repo (red). Subperineurial glia do not have cell projections (A') unlike perineurial glia. (**B**) Fluorescent image of septate junctions (green) morphology in the CNS visualized via Neurexin-IV::GFP, all glial nuclei (red) are labeled with anti-repo antibody, neurons are labeled with HRP (blue). Scale bar = 85µm. (Stork et al., 2008) (**C**) EM image of the ultrastructure of the septate junction of a peripheral nerve demonstrating adhesion proteins as an electron-dense pleated sheet between the two opposing cell membranes. Scale bar = 85µm. (Babatz et al., 2018) (**D**) illustration showing the core components of the bicellular septate junction. Transmembrane adhesion protein Neurexin-IV and Neuroglian along with membrane-linked adhesion receptor Contactin, and Na^+/K^+ ATPase forming the pleated ladder structures visualized in (**C**). Both Neurexin-IV and Neuroglian are shuttled to the membrane by coracle, an intracellular adaptor protein.

1.1.3 Wrapping glia

Wrapping glia reside within each peripheral nerve and enwrap individual nerve fibers or small fiber bundles (**Fig. 1.2 B, C**) (Stork et al., 2012). These resemble "Remak fibers" formed by non-myelinating Schwann cells in vertebrates. A few wrapping glia, like cortex glia, can also encase a limited number of neuron somata near the peripheral nerve roots in the ventral nerve cord (Stork et al., 2012). Peripheral wrapping glia arise near the end of embryogenesis and are born in the ventral nerve cord. Using mechanisms that are still unknown, wrapping glia migrate to the periphery and initiate the ensheathment of the PNS axons. They ensheathe almost all axons of the nerve simultaneously by the third instar stage (Matzat et al., 2015). Like subperineurial glia, wrapping glia do not proliferate. Rather, they are polyploid and grow to over 1mm in

length. Similar to other glial cell types, both FGF and epidermal growth factor (EGF) signalling serve critical roles in the ensheathment process. EGF acts mainly through autocrine signaling with the release of Vein (the *Drosophila* homologue of mammalian neuregulin) from wrapping glia and binding to epidermal growth factor receptor (EGFR) on the wrapping glia surface (Matzat et al., 2015). Blocking EGF signaling results in the complete absence of wrapping glial ensheathment, with the cells collapsing into a single strand in the center of the nerve (Matzat et al., 2015). Similar results can be seen by reducing the function of FGF signalling (Kottmeier et al., 2020); FGFR-mediated ensheathment relies on activation of Htl expressed by the wrapping glia, though the specific FGF ligand is still unclear.

1.1.4 Cortex glia

At the late larval stage, cortex glia span the thickness of the cortex and forms a structure called the "trophospongium" – a honeycomb-like network of cell membrane projections, where each cell surrounds upward 50 to 100 neurons and neural stem cells (**Fig. 1.5 A, B**) (Freeman, 2015). Cortex glia are closely associated with the subperineurial glia and the tracheal vasculature as it penetrates the CNS (Freeman, 2015). Cortex glia provide metabolic support to neurons by expressing various nutrient transporters, such as Chaski (chk), a lactate/pyruvate transporter (Delgado et al., 2018). Cortex glia also directly modulate neuron activity. For instance, Zydeco (zyd), a $Na^+Ca^{2+}K^+$ (NCKX) exchanger expressed by cortex glia, produces microdomain Ca^{2+} oscillations. Loss of zyd leads to seizure-like behaviour through accelerated K^+ influx in neurons (Melom and Littleton, 2013). Neuroblast proliferation is also reliant on cortex glia, and their ablation is lethal (Coutinho-Budd et al., 2017; Spéder and Brand, 2018).

Like perineurial and wrapping glia, cortex glial cell proliferation and ensheathment occurs in late embryonic and early larval stages; and these are one of the few glial cell types that remain during metamorphosis and into adulthood (Coutinho-Budd et al., 2017). Cortex glia growth relies on similar pathways to those of perineurial glia including InR/TOR and FGF signaling. However, Pys and InR signaling differ from that of perineurial glia, as signaling from both ligands converge on the Ras/MAPK pathway to control cortex glial cell proliferation (**Fig. 1.5 C**) (Avet-Rochex et al., 2012). Cortex glia are key to neuronal development and function by providing structural and metabolic support to neurons along with modulating circuit formation and neuron behaviour (Spindler et al., 2009; Melom and Littleton, 2013; Coutinho-Budd et al., 2017; McLaughlin et al., 2019; Nakano et al., 2019). Thus, while cortex glia have no clear vertebrate homologue they do share some functional similarities with astrocytes, microglia, and even oligodendrocytes, who perform those same roles in the vertebrate CNS.

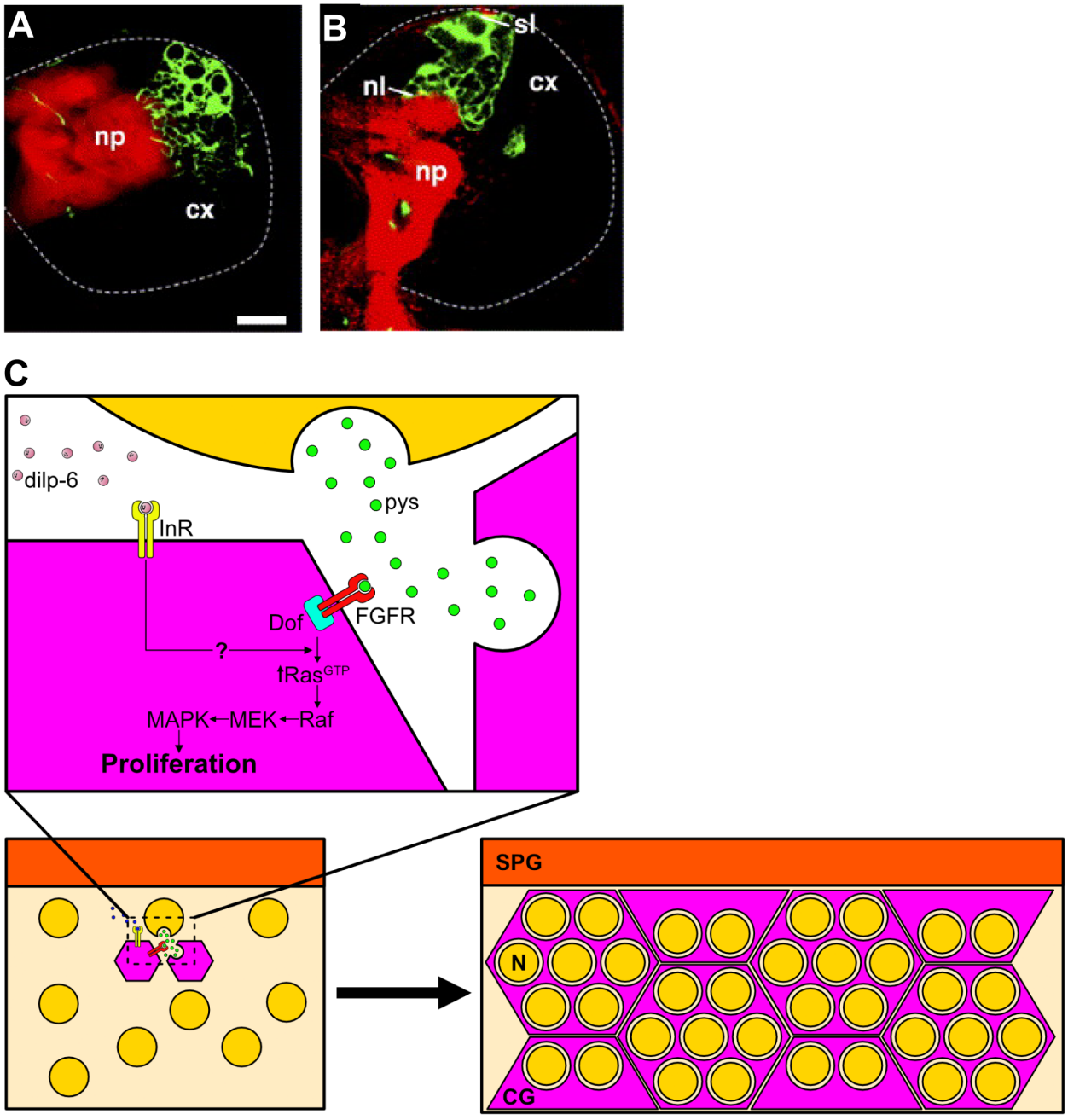
A
np
cx
B
sl
nl
cx
np
C
dilp-6
pys
InR
Dof
FGFR
?
↑Ras^GTP
MAPK←MEK←Raf
Proliferation
SPG
N
CG

Figure 1.5: The morphology and proliferation of cortex glia

(**A-B**) Fluorescent images of a GFP-labelled cortex glial cell clone (green) with neuropile (red) stained using an anti-Syntaxin antibody. Note the sponge-like morphology of cortex glia, suggesting it envelops many neuron cells bodies and can span the entire thickness of the cortex (cx), from the surface lamella (sl, white dotted line) to the neuropile lamella (nl). Scale bar = 25µm. (Pereanu et al., 2005) (**C**) Schematics of cortex glia (CG) proliferation pathways. Pyramus (Pys) from neighboring cortex glia and neurons triggers the proliferation signaling cascade through FGFR> Ras-MAPK signaling pathway. Similar to perineurial glia, InR and dilp-6 also play a role in cortex glia proliferation, though it is suggested that the pathway converges onto the Ras-MAPK signaling cascade through other pathways canonical InR/TOR downstream mutants shows no difference in cortex glial populations.

1.2 Glia-extracellular matrix interactions

The extracellular matrix not only operates as a structural barrier but also as a conduit for intercellular communication, as many matrix proteins carry crucial information via cell-ECM interactions (Theocharis and Karamanos, 2019). The key components of the ECM are large fibrillar glycosylated proteins including collagen, laminin, fibronectin, and proteoglycans (GAGs), forming a highly complex and dynamic, yet organized molecular network (Theocharis et al., 2016). The ECM also directly binds numerous growth factors, cytokines, and proteolytic enzymes (Wilgus, 2012; Theocharis et al., 2016). The ECM prevents degradation of trophic factors and aid in establishing trophic factor concentration gradients (Wilgus, 2012). Thus, extracellular matrix components are capable of influencing all aspects of cellular behaviour and function, in addition to modulating tissue homeostasis (Frantz et al., 2010; Clause and Barker, 2013; Pickup et al., 2014). It is theorized that variations in regional ECM deposition or degradation can modulate tissue architecture and cell behaviour via alteration in the adhesive forces or concentration of growth factors (DuFort et al., 2011). Cell membrane receptors such as integrins, syndecan, and growth factor receptors interact with the ECM. Here I will highlight the relevant processes and components related to ECM-cell adhesion that are the focus of this thesis.

1.2.1 ECM components

In *Drosophila* there are range of well characterized ECM components in the basal lamina surrounding the nervous system. These include Perlecan, Collagen IV (Viking), and Laminin. Both viking and perlecan are major components of the basal membrane and produced by adipocytes and hemocytes (Pastor-Pareja and Xu, 2011). The incorporation of Viking and perlecan into the ECM is a major determinant in tissue morphology and in particular in CNS

morphology (see following section). Though perlecan seem to counteract collagen IV's function by reduce the tensile strength of the ECM, the deposition of perlecan during embryogenesis is dependent on collagen IV (Martinek et al., 2008; Pastor-Pareja and Xu, 2011).

Laminin is one of the key ECM proteins known to be produced by glia. Laminins are heavily glycosylated heterotrimeric ECM proteins consisting of an α, a β, and a γ subunit. In *Drosophila*, there are only 2 unique isoforms, as there are just two α-subunits (*wing blister*, *wb* and, *laminin A, LanA*), one β-subunit (*LanB1*), and one γ-subunit (*LanB2*) (Yamada and Sekiguchi, 2015). In comparison to vertebrates in which there are 16 potential isoforms (Hohenester and Yurchenco, 2013). All subunits contain a laminin N-terminal domain, subunit-dependent repeats of laminin EGF-like (LE) domains, followed by α-helical domains that mediates the coiled-coil structure. Unique to the α-subunits are five-tandem globular (LamG) domains that contain binding sites for ECM receptors, such as integrins and Syndecan (Yamashita et al., 2004; Yamada and Sekiguchi, 2015). For laminin to be released into the extracellular environment, β, γ, and α-subunit need to trimerize within the endoplasmic reticulum (ER). The α-subunit of laminin is independently secreted and drives the secretion of its β- and γ-partners (Yurchenco et al., 1997). Conditional deletion of laminin in Schwann cells causes hypomyelination as Schwann cells fail to extend processes and initiate ensheathment (Yu et al., 2005). Equivalently, deletion of laminin in non-myelinating Schwann results in peripheral nerves devoid of ensheathment (Yu et al., 2009). In *Drosophila*, the absence of β- or γ- subunit leads to accumulation of the other subunits within the glial ER, subsequent swelling and ER stress often accompanied by ensheathment defects in perineurial and wrapping glia (Petley-Ragan et al., 2016). The engagement of laminin is critical to the glial cell ensheathment and different adhesion complexes has been implicated in the laminin signaling cascades in vertebrate myelinating and

non-myelinating Schwann cell wrapping, with integrin and dystroglycan having been best studied (Colognato and Tzvetanova, 2011).

1.2.2 ECM receptors in glia

Along the extensive ECM surrounding both vertebrate and *Drosophila* glia, there are also a range of ECM binding receptors present on the glial membrane that mediate ECM to cell signaling. The major ECM receptor in glia in all animals are the integrins. Integrins are a superfamily of heterodimeric receptors composed of α and β subunits. They bind to many ECM ligands based on the specificity of individual α and β subunits, and through various adapter proteins including talin and paxillin, connect to the intercellular actin network. Upon activation by Talin (i.e., inside-out activation), the integrin heterodimer changes conformation (Ginsberg et al., 2005). This allows for the integrin complex to bind its ECM ligand with high affinity and establishing a physical coupling between the extracellular environment and the cytoskeleton (Takada et al., 2007). The focal adhesion formed by integrin directs cell migration via the Rho GTPases which coordinate actin dynamics as well as adhesion itself (Abram and Lowell, 2009; Huveneers and Danen, 2009). Compared to vertebrates, *Drosophila* possesses a relatively small integrin family with five alpha (αPS1-αPS5) and two beta (βPS and βν) subunits. The αPS2βPS and αPS3βPS heterodimers are expressed in the *Drosophila* peripheral glia (Xie and Auld, 2011), with *inflated* (*if*) and *scab* (*scab*) encoding the αPS2 and αPS3, respectively; βPS is produced by *myospheroid* (*mys*) (Brown, 2000; Takada et al., 2007). However, the respective ligand(s) that bind to these integrin heterodimers has yet to be conclusively demonstrated. Overall integrins play a central role in glial ensheathment in *Drosophila* (Xie and Auld, 2011). Down-regulating the β-subunit (*mys*) in glia blocks axon ensheathment by wrapping glia and nerve ensheathment

by perineurial glia. Consistently, downregulation of β1 integrin, the vertebrate homologue of *mys*, also impedes Schwann cell radial ensheathment and axon sorting (Milner et al., 1997; Feltri et al., 2002; McKee et al., 2012). In this system, β1 binds to laminin in the basal lamina and activates integrin-linked kinase to promote membrane process extension and radial sorting (Pereira et al., 2009; McKee et al., 2012). There are other cell surface laminin receptors critical for laminin-mediated myelination in vertebrates, such as dystroglycan and heparin-containing molecules (McKee et al., 2012). Conditional dystroglycan knockout mice resulted in various Schwann cell myelination abnormalities, including polyaxonal myelination and hypomyelination (Masaki and Matsumura, 2010). Similarly, treating cultured dorsal root ganglion cultures with laminin lacking LG4-5, which contains the dystroglycan and heparin-binding site, blocks myelination (McKee et al., 2012). Later in this chapter, I will discuss syndecan, a laminin interaction partner as a potential candidate in influencing glia-ECM communication.

1.2.3 Glia-ECM interactions and ventral nerve cord condensation

The shortening of the ventral nerve cord occurs during *Drosophila* development and relies heavily on glial-ECM interactions, but how this occurs is still unclear (Meyer et al., 2014; Skeath et al., 2017). During embryogenesis, as the ventral nerve cord becomes clearly defined, it spans approximately 80% of body length; however, by late embryogenesis, the ventral cord nerve shrinks to about 60%, eventually attaining a final size of just 10% of the body length (Olofsson and Page, 2005). The process of ventral nerve cord condensation is regulated in part by non-neural tissues, such as haemocytes, which transiently contact the ventral nerve cord around stage 12 of the *Drosophila* embryogenesis (Tepass et al., 1994; Olofsson and Page, 2005; Evans et al., 2010). Haemocytes secrete multiple ECM components, such as Perlecan, Nidogen,

Collagen IV, and laminin. Elimination of haemocytes reduces ECM glycoprotein deposition within the animal cavity resulting in an elongated ventral nerve cord (Olofsson and Page, 2005). The fat body also produces ECM proteins, and nerve cord elongation is a consequence of blocking adipocyte exocytosis (Pastor-Pareja and Xu, 2011; Zang et al., 2015). However, not all ECM components act in the same way. In perlecan (*trol*) loss of function mutants, the ventral nerve cord become over-condensed (Pastor-Pareja and Xu, 2011). In contrast to the over-condensed VNC triggered by loss of perlecan, the loss of collagen IV produces an elongation of the ventral nerve cord. This has led to a model where collagen cross-linking works to increase matrix stiffness and counteract the action of perlecan (Pastor-Pareja and Xu, 2011; Isabella and Horne-Badovinac, 2015). The *Drosophila's* ECM stiffness and tensile characteristics is a balance between perlecan and collagen IV, where perlecan serves to "soften" the basement membrane as observed using atomic force microscopy on the *Drosophila* egg chamber (Crest et al., 2017). In comparison, collagen IV acts to increase the basement membrane stiffness. Degradation of the collagen that surrounds embryonic columnar epithelium leads to rapid flattening and planar expansion (Pastor-Pareja and Xu, 2011). These studies emphasize that the structure and properties of the ECM are not set in stone and the cells that interact with the ECM can also alter these properties.. For example, in *Drosophila* ADAMTS-A (A disintegrin and metalloproteinase with thrombospondin motifs metallopeptidase with thrombospondin type 1 motif A) works to inhibit the accumulation of Viking and promotes perlecan in the basement membrane (Skeath et al., 2017).

Glia can also regulate ventral nerve cord architecture: as reducing glial cell numbers results in ventral nerve cord elongation (Campbell et al., 1994). Additionally, glia express ECM receptors such as integrin, and a suite of ECM modulators including ADAMTS-A (Xie and Auld,

2011; Skeath et al., 2017). Altering the composition of the integrin-mediated focal adhesion complex or ADAMTS-A results in defective ventral nerve cord condensation (**Fig. 1.6A-C**) (Meyer et al., 2014; Skeath et al., 2017). This effect is likely mediated by perineurial glia, as they express both integrin and ADAMTS-A, and are in direct contact with the neural lamella (Xie and Auld, 2011; Skeath et al., 2017). Though it is highly likely that there are non-integrin-mediated mechanisms working in parallel to regulate ventral nerve cord length, as integrin knockdown within the CNS produces a relatively mild elongation in comparison to the elimination of the ECM (**Fig. 1.6A-E**) (Xie and Auld, 2011; Meyer et al., 2014).

1.2.4 Extracellular matrix and glial ensheathment

Drosophila glial differentiation and ensheathment of peripheral nerve fibers occur mainly in the larval stages, with glia born in the CNS during embryonic stages then migrating towards the periphery along the established axon tracts (Sepp et al., 2000). The normal process of cellular migration also applies to glial migration, including lamellipodia contacting the extracellular substrates, and cytoskeleton contractility (Banerjee and Bhat, 2008). The actin cytoskeleton plays a key role in glial migration as changes to the small GTPase Rho-GTPase interferes with glial actin polymer structure and disrupts glial migration (Sepp and Auld, 2003). The integrin adhesion complex represents a logical link between the extracellular environment and the glial actin cytoskeleton as integrin influences Rho-GTPase activation via various effector kinases (Huveneers and Danen, 2009), and integrin itself is able to physically link the ECM with the cytoskeleton though various adaptor proteins including talin (Abram and Lowell, 2009). Disruption of integrin affects glial ensheathment in both *Drosophila* and vertebrates. Laminin reduction or mutation of laminins and integrins results in abnormal axonal sorting by non-

myelinating Schwann cells, and abnormal myelination by Schwann cells (Feltri et al., 2002; Wallquist et al., 2002, 2005; Yu et al., 2009). In *Drosophila*, integrin reduction impedes peripheral nerve ensheathment by both perineurial glia and wrapping glia (**Fig. 1.6F, G**) (Xie and Auld, 2011). It is unclear which extracellular ligands integrins are binding to activate migration of glia in *Drosophila*. There may be other ECM receptors expressed in the peripheral glia that mediate glia-ECM interactions such as the dystrophin/dystroglycan complex and syndecan. This thesis will focus on whether syndecan, a well-known receptor in mediating cell-ECM adhesion, plays a role in mediating glial function. Overall, glia-ECM interactions are key to glial migration and ensheathment of peripheral nerves, though the identity and role of potential ECM binding proteins have yet to be determined.

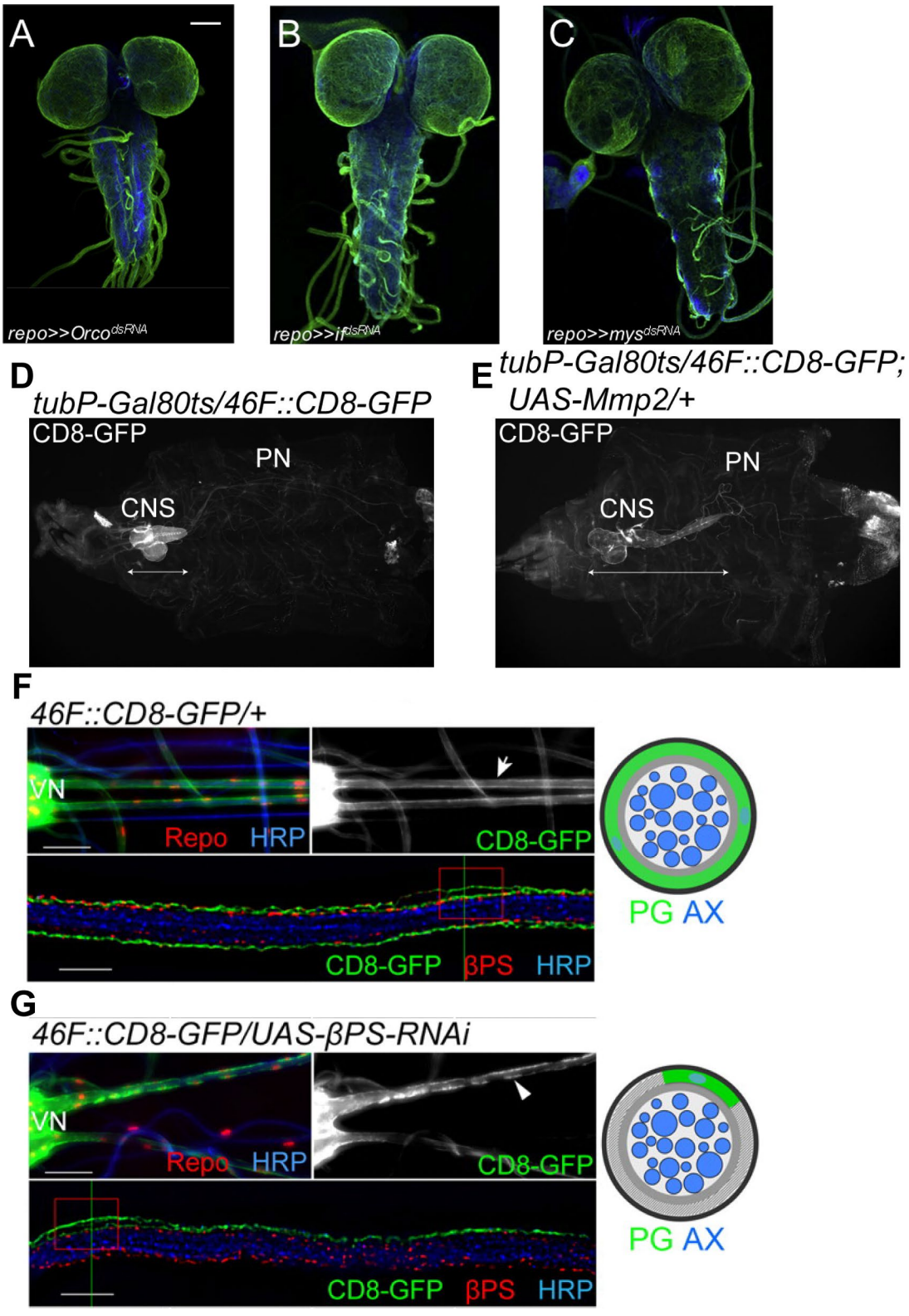
A
repo>>Orco dsRNA
B
repo>>if dsRNA
C
repo>>mys dsRNA
D
tubP-Gal80ts/46F::CD8-GFP
CD8-GFP
PN
CNS
E
tubP-Gal80ts/46F::CD8-GFP;
UAS-Mmp2/+
CD8-GFP
PN
CNS
F
46F::CD8-GFP/+
VN
Repo HRP
CD8-GFP
CD8-GFP βPS HRP
PG AX
G
46F::CD8-GFP/UAS-βPS-RNAi
VN
Repo HRP
CD8-GFP
CD8-GFP βPS HRP
PG AX

Figure 1.6: Disruption to glial-ECM adhesion cause structural defects and impaired ensheathment by perineurial glia

(**A-C**) Pan glial knockdown of integrin is associated with an elongation of the ventral nerve cord. All glia are labeled using repo-GAL4 induced CD8::GFP expression. Noticeable lengthening of the VNC occurs in the *inflated* (*if*) and *myospheroid* (*mys*) knockdown group (A). Scale bar = 50 μm (Meyer et al., 2014) (**D-E**) Degradation of the ECM caused large structural defects within the CNS. Using 46F-GAL4, which directs expression of MMP-2 in perineurial glia and depletes the ECM, caused the lengthening of the VNC (E) (Xie and Auld, 2011). (**F-G**) perineurial glial knockdown of integrin impairs its ensheathment in the PNS. Perineurial glia (green) are visualized using mCD8::GFP, upon expression of integrin-RNAi in perineurial glia, the cell membrane becomes restricted to one side of the nerve (lower panel in G) instead of the bilateral distribution in control (lower panel in F), overall showing a non-uniform distribution of the glial cell membrane. AX, axon; VN, ventral nerve cord. Scale bar = 50 μm (F,G, upper panels), 10 μm (F,G lower panel). (Xie and Auld, 2011)

1.3 Syndecan, a heavily glycosylated cell surface receptor

Syndecans are a small family of transmembrane heparan sulfate proteoglycan cell surface receptors. The vertebrate syndecan family is represented by four distinct syndecan genes (SDC -1, -2, -3, -4), whereas in invertebrates including *Drosophila*, there is a single gene (Spring et al., 1994; Couchman, 2003). In mammals, each syndecan has a temporal and spatial expression profile: SDC-1 is mainly expressed in epithelial and endothelial cell types, while SDC-2 is mainly expressed in mesenchymal cells, SDC-3 is expressed by neurons and glia, SDC-4 is ubiquitously expressed (Bernfield et al., 1999; Rapraeger, 2001; De Rossi and Whiteford, 2013; Chung et al., 2016). Syndecan has been implicated in regulating cell and ECM adhesion, migration, and proliferation. Yet, how syndecans mediate these functions in different tissues remains unknown (De Rossi and Whiteford, 2013).

All syndecan proteins share similar molecular architecture; an extracellular domain (i.e., ectodomain), a transmembrane domain, and a short highly conserved cytoplasmic domain (**Fig. 1.7**). The ectodomain ranges widely in size between the different family members, with little similarity between most of the protein sequence; yet, the attachment site for heparan sulfate glycosaminoglycan (HS-GAG) chains, Ser-Gly, is identical in all syndecan family members across species (Xian et al., 2010; Leonova and Galzitskaya, 2013). The single-pass transmembrane domain contains a motif "GxxxG", which is the main substrate for syndecan's dimerization. The functional relevance of syndecan dimerization remains controversial where forced heteromeric dimerization between different mammalian syndecan family members reduces cell migration and adhesion in comparison to homomeric dimerization (Choi et al., 2015). The cytoplasmic domain can be broken down into three mini-domains, the highly conserved C1 (proximal to the membrane) and C2 (distal to the membrane) flanking a V region. The V region peptide sequence is specific to each family member, suggesting distinct functional attributes (Couchman et al., 2015). All syndecan C2 mini domains contain a canonical PDZ binding motif (i.e., EFYA) that interacts with several PDZ proteins including Calcium/calmodulin-dependent serine protein kinase (CASK) and Syntenin, which coordinate syndecan trafficking and translocation to the membrane (Grootjans et al., 1997; Hsueh et al., 1998). However, such relationships have not been demonstrated in invertebrates. In the following sections, I will focus particularly on syndecan's contribution to cellular adhesion and growth factor signaling, as such processes are pivotal for glial development and ensheathment.

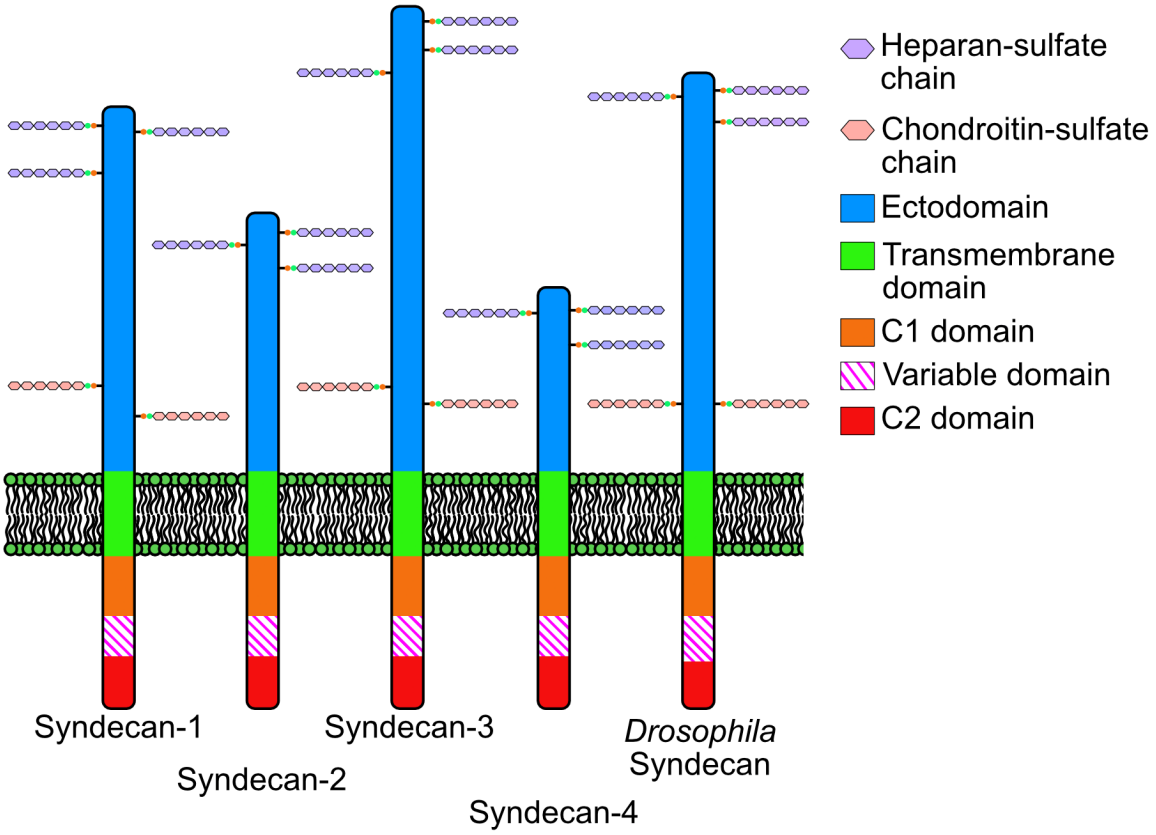

Figure 1.7: Mammalian and *Drosophila* syndecan family members

Syndecan is a family of single-passed transmembrane heparan sulfate proteoglycans. All family members share a similar protein structure. All Syndecan bear heparan sulfate chains, though some members (Syndecan-1/-3 and *Drosophila* Syndecan) also bear chondroitin-sulfate chains. The function of chondroitin-sulfate chains or the difference in the sulfate status between the different family members is currently unclear. The mammalian Syndecan family can be further divided into two subfamilies: syndecan-1/-3 in one and syndecan-2/-4 in the other.

1.3.1 Syndecan and cellular adhesion

The evidence supporting syndecan's role in integrin-mediated cellular adhesion has been more thoroughly investigated, albeit in cell culture. In fibroblasts, integrin-mediated adhesion is sufficient to direct fibroblast attachment and spread on fibronectin (Woods et al., 2000).

However, integrin alone was insufficient for focal adhesion and stress fiber formation. Rather the formation and maturation of adhesion complexes require the GAG chains and the syndecan's protein core (Woods et al., 2000; Mahalingam et al., 2007). The interaction between SDC-4 and the heparin-binding domain II of fibronectin in combination with integrin α5β1 leads to cytoskeletal rearrangement and ultimately, formation of focal adhesion and subsequent syndecan-mediated cell migration (Kwon et al., 2012). Various studies have shown different syndecans modulate different integrin complexes with different ECM substrates (**Fig. 1.8**). Although *in vitro*, SDC-1 can enhance α*v*β3 adhesion to Vitronectin, SDC-2 cooperates with α5β1 binding with Fibronectin, and SDC-4 itself can bind to the ECM and directly interacts with laminin through the globular domain. Though *Drosophila* Sdc shows similar interactions with laminin, its binding to other ECM proteins, such as collagen, has not been demonstrated (Munesue et al., 2002; Beauvais et al., 2004; Yamashita et al., 2004; Carulli et al., 2012; Yang and Friedl, 2016).

Syndecan's contribution to integrin-mediated adhesion and ECM organization has been well-described *in vitro*; in contrast, the *in vivo* contribution of syndecan to cellular adhesion is far less explored. Challenges to study any potential syndecan-integrin synergy *in vivo* arise as null mutants in any one of the single *syndecan* genes in mice are healthy and fertile with no apparent defects.. Only mild delays in cell migration is observed in wound healing in SDC-1 or -4 nulls, and impaired performance associated with long-term potentiation in the hippocampus with SDC-3 knockout (Echtermeyer et al., 2001; Kaksonen et al., 2002; Stepp et al., 2002; Melendez-Vasquez et al., 2005). The contrast in phenotypes between cultured cells and *in vivo* is theorized to reflect the functional redundancy between the different mammalian syndecan family members. As mentioned previously, while the four mammalian syndecans are expressed predominantly in

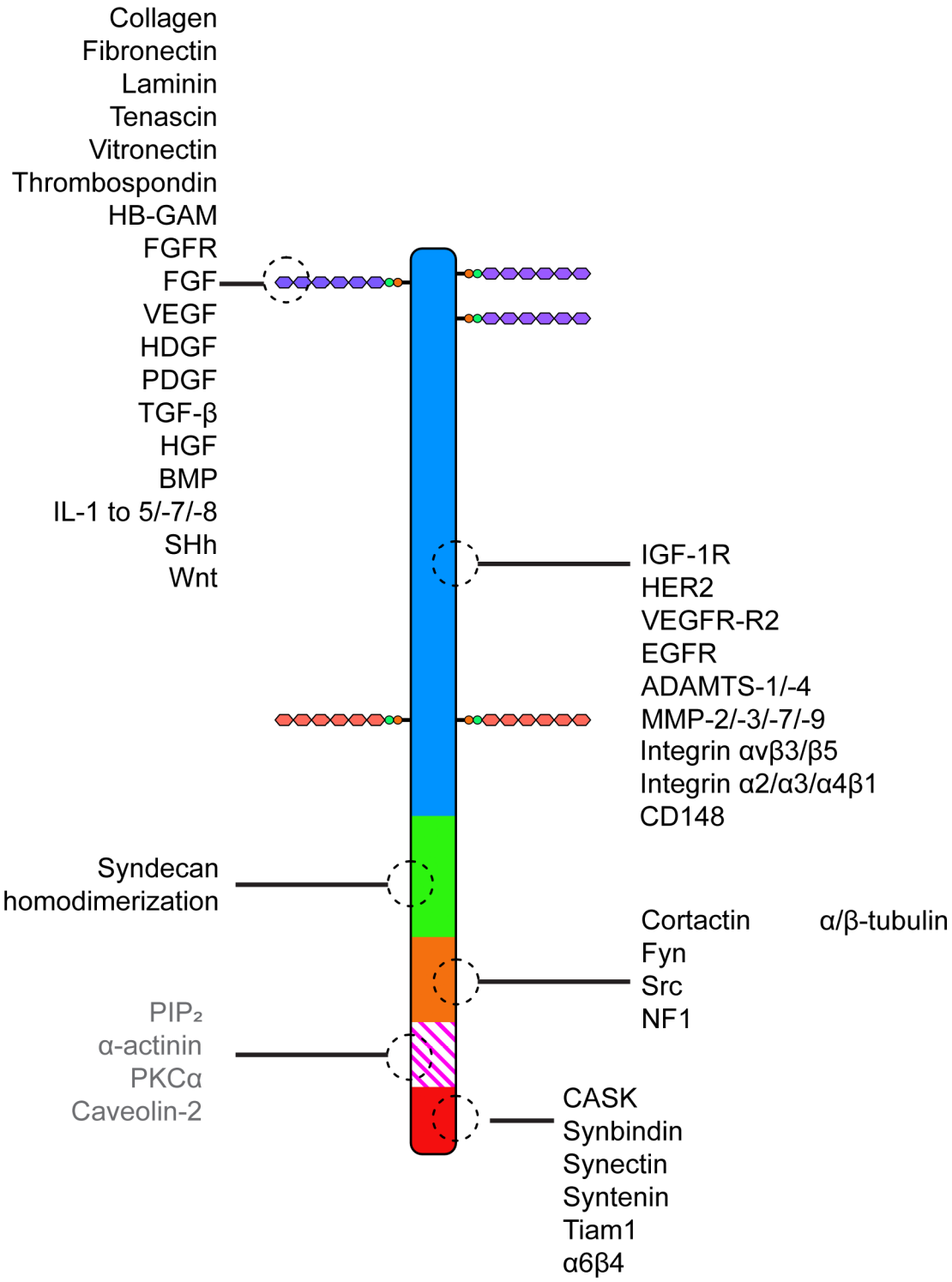
Collagen
Fibronectin
Laminin
Tenascin
Vitronectin
Thrombospondin
HB-GAM
FGFR
FGF
VEGF
HDGF
PDGF
TGF-β
HGF
BMP
IL-1 to 5/-7/-8
SHh
Wnt
IGF-1R
HER2
VEGFR-R2
EGFR
ADAMTS-1/-4
MMP-2/-3/-7/-9
Integrin αvβ3/β5
Integrin α2/α3/α4β1
CD148
Syndecan
homodimerization
Cortactin
α/β-tubulin
Fyn
Src
NF1
PIP2
α-actinin
PKCα
Caveolin-2
CASK
Synbindin
Synectin
Syntenin
Tiam1
α6β4

Figure 1.8: List of the interaction partners of mammalian syndecan

The heparan sulfate chains (purple hexagon) can span from 40 to 500 nm away from the core protein and can bind to a wide array of ligands that contains a heparan-sulfate binding domain, including various chemokines, growth factor, morphogens, and ECM structural proteins (Stepp et al., 2015). The ectodomain itself is capable of interaction with different receptor tyrosine kinases, including EGFR and HER2. The ectodomain (blue) can also be cleaved by metalloproteases, in a process named: "shedding". The intracellular domains can bind to different adaptor protein with the C1 domain (orange) showing a preference for cytoskeleton linkage protein; the variable domain's (magenta bars) interaction partner (grey) are specific to each syndecan; the C2 domain (red) contains a PDZ-binding motif and mainly interaction with PDZ protein.

distinct cell types, the overlap in expression patterns is not to be dismissed. Indeed, the shared similarities in molecular architecture between the different syndecans make it very likely that the absence of one syndecan can be compensated by the others.

1.3.2 Syndecan and growth factor signaling

Syndecan is capable of controlling information flow between the cell and the environment and influence cellular events by acting as a co-receptor with receptor tyrosine kinases (RTK) signaling complexes, including growth factor receptors (**Fig. 1.8**) (Kwon et al., 2012). The HS-GAG chains can orchestrate the recruitment and anchoring of soluble growth factors, such as EGF and FGF to the membrane, subsequently allowing the growth factors to bind to their corresponding receptors, though the HS-GAG chains may also interact with growth factor receptors directly regardless of the ligand is present (Burgess and Maciag, 1989; Woods et al., 1998; Xian et al., 2010). The formation of a heparan sulfate-growth factor signaling complex has been well described with FGF-2 *in vitro* using various cell types. Syndecan-1, -2, -4 all support the binding of FGF-2 to FGFR, increasing FGFR activation (Steinfeld et al., 1996). The

syndecan-growth factor interaction does not elicit an intracellular signal, but rather, the binding of FGF-2 to syndecan results in a high local concentration of FGF-2 at the cell surface. This bolsters FGF-2 binding affinity to FGFR, triggering growth factor receptor clustering and activation (Reiland and Rapraeger, 1993; Filla et al., 1998). Similar associations have been identified *in vitro* between syndecan-2 and Vascular endothelial growth factor (VEGF), syndecan-1 and hepatocyte growth factor (HGF), and EGF related signaling, among others (Andersen et al., 2005; Kaji et al., 2006; Mahtouk et al., 2006; Corti et al., 2019). In comparison, the evidence for syndecan contribution to growth factor signaling *in vivo* is very limited. One study did find syndecan-2 is required for efficient VEGF-mediated signaling in the sprouting angiogenesis in zebrafish (Chen et al., 2004). Our limited understanding of syndecan's *in vivo* function, in the context of growth factor signaling is likely due to functional redundancy between the four vertebrate syndecans, where a single syndecan knockout has mild to no phenotype (Couchman et al., 2015). *Drosophila* as a model organism offers a platform in which there are limited Sdc functional redundancies, as it only possesses one *Sdc* gene. Similar to vertebrate syndecans, *Drosophila* Sdc has a modulatory role in FGF-FGFR signaling in astrocytes-like glia to regulate morphology (Stork et al., 2014) and in other tissues (Knox et al., 2011). The implication of Sdc's role in growth factor signaling in other glia requires further investigation to determine the breadth of Sdc function.

1.4 Thesis question

The purpose of this thesis is to characterize the *in vivo* function of Sdc in glial development and function within the *Drosophila* larval nervous system. Prior literature has highlighted Sdc's ability to modulate cellular adhesion and growth-factor mediated

signaling though its interaction with integrin and growth factor ligand/receptors *in vitro*. However, the function of Sdc in glia is not well characterized. Despite Sdc being robustly expressed by the *Drosophila* embryonic nervous system, its endogenous expression pattern within the larval nervous system, particularly in glia, has been inadequately described. Moreover, it is currently unclear whether Sdc is needed for overall glial development. Thus, **Chapter 2** of this thesis will characterize Sdc's endogenous expression within the *Drosophila* glia and address the functional role Sdc serves in different glial layers in the CNS and PNS to affect nervous system development.

Chapter 2: Exploring the role of Syndecan in *Drosophila* neural and glial development

2.1 Synopsis

Glia are active and dynamic modulators required for the function and development of the nervous system. However, the mechanism by which glia communicate and interpret the extracellular landscape remains to the elucidated. In this chapter, I showed *Drosophila* Sdc's expression within a range of central and perineurial glia. Knockdown of Sdc in all glia resulted in defective neuroblast proliferation. This indicates Sdc maybe a vital component to the maintenance and development of the neural stem cell niche. Additionally, the loss of Sdc in different glial layers resulted in disruptions in the morphologies of each glial layer. The absence of Sdc resulted in impaired ensheathment in wrapping glia and abnormal septate junction morphology in subperineurial glia. Moreover, I saw ensheathment defects and a reduction in glial numbers with Sdc knockdown in perineurial glia. Loss of Sdc in the perineurial glia also resulted in reduced laminin deposition within the peripheral ECM, suggesting perineurial glia play a role in ECM formation within the PNS. Thus, our results indicate Sdc has multiple roles in *Drosophila* nervous system development including as an integral component in regulating glial cell morphology, in mediating glial-ECM interactions and maintaining neuroblast populations within the optic lobe.

2.2 Introduction

For cells of all types, the ability to communicate among themselves and the extracellular environment is a pivotal aspect of their overall functioning. Glia are no exception as they rely heavily on efficient adhesion and communication with their surroundings to ensheathe, protect and modulate the nervous system. Yet, exactly how glia accomplish information exchange between themselves and the extracellular landscape stays obscured.

Neurons in the *Drosophila* nervous system are surrounded by multiple glial populations. Within the brain lobe and ventral nerve cord that makes up the CNS, individual neuron somata are ensheathed by cortex glia (Freeman, 2015). In the PNS, axons of both sensory and motor neurons are ensheathed by wrapping glia (Stork et al., 2012). Both the CNS and PNS are covered by a thin layer of large polyploid cells called subperineurial glia, which establishes a permeability barrier via the septate junctions, isolating the neurons from the circulating hemolymph filling the animal's cavity (Auld et al., 1995; Baumgartner et al., 1996; Stork et al., 2008). Lying beneath the ECM that blankets the entire nervous system are perineurial glial cells. Perineurial glia are small cells that are highly mobile and undergo mitosis throughout larval development, spreading across the surface of the entire nervous system by the late third instar stage (Awasaki et al., 2008; von Hilchen et al., 2013). To communicate with the overlying ECM, perineurial glia express transmembrane receptors and release metalloproteases, such as integrin and ADAMTS-A respectively, to direct CNS structural remodeling during development and structural integrity in the larval stages (Meyer et al., 2014; Skeath et al., 2017). Similarly, the perineurial glia interactions with the ECM are mediated by integrins. Disruption of glial-ECM adhesion in the PNS by mutant or RNAi reduction manifests as incomplete ensheathment by the perineurial glia (Xie and Auld, 2011). Though studies in both *Drosophila* and vertebrates have

delved into the importance of integrin-mediated focal adhesion in glial-ECM adhesion, questions remain about other transmembrane receptor candidates besides integrin contribute and how to the cell-ECM adhesion in glia during development.

The syndecan family proteins constitute a group of transmembrane heparan sulfate proteoglycans (HSPGs) cell surface receptors that consist of a core protein with heparan sulfate glycosaminoglycan chains covalently attached to the ectodomain. There are four mammalian syndecan, designated syndecan-1, -2, -3, and -4, with each having its unique characteristic structural and expression profiles, though similarities do exist. Challenges arise to study them *in vivo* as functional redundancy plagues attempt to delineate their functions, where the others may compensate for the lack of one, and to date, there is no double knock out model in vertebrates (Couchman et al., 2015). In comparison, *Drosophila* only contains a single *Sdc* gene. Despite its simplicity as a model organism, little is known regarding Sdc's expression pattern or cellular localization in *Drosophila*. Sdc is known to be present in the embryonic nervous system, and in the both larval neuropile and neuromuscular junction in late larva stages (Spring et al., 1994; Stork et al., 2014; Nguyen et al., 2016). Yet, the existence of Sdc in glial populations remains poorly explored.

Mammalian syndecans are enriched in focal adhesion and growth-factor signaling complexes, thus placing syndecan in multiple signaling pathways and cellular functions. Syndecan acts in cooperation with integrin to direct focal adhesion and stress fiber formation in fibroblasts to mediate cell migration (Morgan et al., 2007). Additionally, syndecan acts to concentrate local ECM-ligand and growth factor levels, allowing these ligands to bind to their corresponding receptors with higher efficiency (Wu et al., 2003; Cheng et al., 2016).

In comparison, how Sdc interacts with focal adhesions in *Drosophila* is not well explored. However, Sdc is important for a range of cell migration and adhesion pathways during *Drosophila* development, including axon migration and cardiogenesis (Johnson et al., 2004; Steigemann et al., 2004; Rawson et al., 2005; Chanana et al., 2009; Knox et al., 2011; Smart et al., 2011). Moreover, *Drosophila* Sdc plays a conserved role in trophic factor pathways such as FGF signaling, including tracheal cell migration (Lin et al., 1999; Schulz et al., 2011). Similarly, loss of HSPGs causes tracheal defects (Lin et al., 1999). In glia, Sdc directs astrocyte-like glia morphogenesis through FGF signaling and concentrates FGF ligands similar to vertebrate syndecan (Stork et al., 2014). However, the characterization of Sdc's role in other glia has not been carried out.

To understand the role of Sdc in mediating glial development I analyzed the distribution and function of Sdc in larval glia. I observed Sdc is present in multiple glial layers in the third instar larvae, particularly noticeable in the wrapping and perineurial glia. By reducing Sdc expression in glia using RNAi-mediated knockdown, I observed locomotion defects and nervous system abnormalities. Specifically, loss of Sdc in the CNS glia leads to smaller brain lobes, a diminished neuroblast population, and an extended VNC. In the PNS, I found that Sdc plays a key role in the perineurial glial ensheathment of the peripheral nerve. Overall, I found two novel aspects of Sdc function in glia, where Sdc is required for optic lobe neuroblast proliferation and is necessary for glial cell ensheathment in PNS, thus expanding the understanding of Sdc's influence on neural development.

2.3 Results

2.3.1 Syndecan is expressed in a range of glia in the larval nervous system

To determine the expression pattern and protein localization of Sdc among the cell populations within *Drosophila* CNS and PNS, I used Sdc endogenously tagged with GFP (Sdc::GFP.PTT) to view its endogenous expression (Buszczak et al., 2007). Animals homozygous for the *Sdc::GFP.PTT* allele displayed no gross structural defects and were viable. This suggests that the GFP insertion does not significantly impact Sdc function and localization and thereby allowing for an accurate representation of Sdc expression. The localization of Sdc was further confirmed using a second independent GFP insertion in the *Sdc* gene (Sdc::GFP.MI), which revealed no change in Sdc expression patterns (**Supp. Fig 1, see appendix**).

Within the 3rd instar larvae, Sdc is expressed throughout the nervous system, including the brain lobe, the ventral nerve cord, and the peripheral nerves. Using super-resolution imaging, I revealed that Sdc is expressed in a linear punctate pattern that often outlines the appearance of the glial membranes (all glial membrane labeled with *repo-GAL4>mCD8::RFP*) in the CNS and PNS (**Fig 2.1 A-C**). Additionally, I observed robust Sdc::GFP.PTT outlining cell boundaries within the brain lobe that did not colocalize with any glial cells (**Fig. 2.1** yellow arrow). I believe Sdc::GFP.PTT is also expressed by neurons, consistent with previous studies (Johnson et al., 2004; Steigemann et al., 2004). Moreover, Sdc puncta localized to the superficial glial layers, suggesting that Sdc is expressed in the perineurial glia population (**Fig 2.1** white arrow).
To confirm Sdc's expression in perineurial glia, I looked for GFP tagged Sdc (Sdc::GFP.PTT) localization specifically within the perineurial glia, which were labelled with membrane-bound

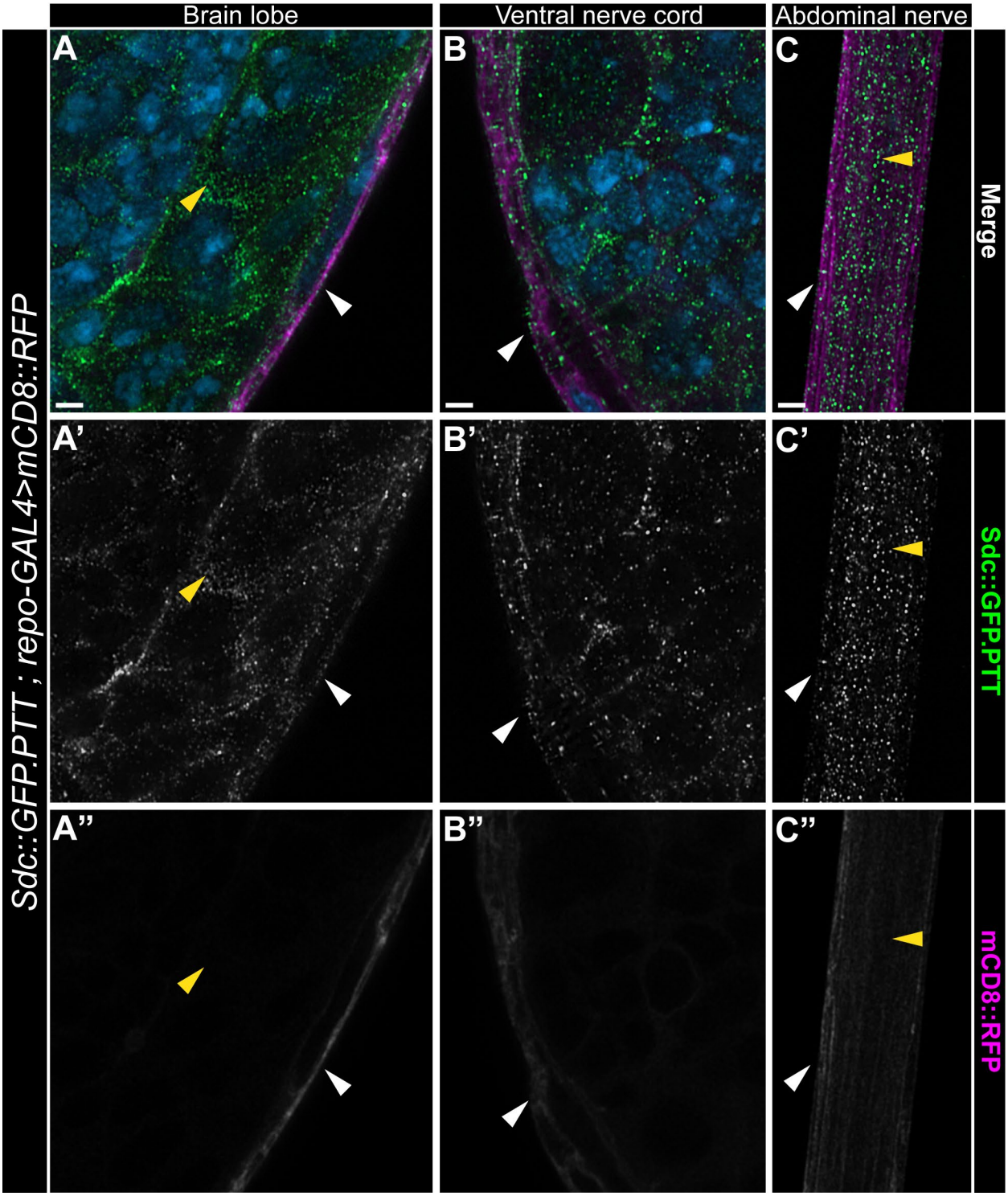
Brain lobe
Ventral nerve cord
Abdominal nerve
Sdc::GFP.PTT ; repo-GAL4>mCD8::RFP
A
B
C
Merge
A'
B'
C'
Sdc::GFP.PTT
A''
B''
C''
mCD8::RFP

Figure 2.1: Syndecan is present in the central and peripheral nervous system and expressed in neurons and glia

(**A-C**) Cross-section of 3rd instar larval nervous system in which all glial membranes are labeled with membrane-bound mRFP (mCD8::RFP, magenta) driven by *repo-GAL4*. Sdc::GFP.PTT (green) localization is visualized using an anti-GFP antibody in the brain lobe (A-A"), the ventral nerve cord (B-B"), and the abdominal segmental nerve (C-C"). I detect Sdc::GFP.PTT puncta in the glial membranes (white arrow), as well as instances where the glial membrane cannot be observed (yellow arrow). All nuclei are marked with DAPI (blue). Scale bar, 2 μm.

RFP (mCD8::RFP) using *46F-GAL4* (a confirmed perineurial glial driver (Xie and Auld, 2011)). I found that Sdc is expressed by perineurial glia and that Sdc::GFP.PTT puncta are closely associated with the perineurial glial membrane at the glial-ECM interface (**Fig 2.2 A-C**). There were also instances where Sdc puncta localized to the perineurial-subperineurial cell-cell interface (**Fig 2.2** yellow arrow). Next, I sought to see if Sdc is found within subperineurial glia. The subperineurial glia were labeled with membrane-bound RFP (mCD8::RFP) driven by the *moody-GAL4,* and I observed patches of Sdc puncta localized to the subperineurial glial membrane (**Fig. 2.3 A-C**). Interestingly, within the peripheral nerve, the localization of Sdc to the subperineurial glia membrane was more consistent and covered longer regions compared to the CNS. The observation with subperineurial glia also confirmed the distribution of Sdc in the perineurial glia as I observed lines of Sdc puncta exterior to the subperineurial glia. To distinguish whether the strings of Sdc puncta I observed in the cores of the peripheral nerves were expressed by axons or wrapping glia, I used *nrv2-GAL4* to drive mCD8::RFP to label wrapping glial membranes. In the peripheral nerves, I saw consistent Sdc puncta corresponding to wrapping glia membranes (**Fig. 2.4**, white arrow), suggesting wrapping glia express Sdc. However, it is likely that Sdc is also expressed in the peripheral axons (Smart et al., 2011).

Given the widespread expression of Sdc lining the cell-ECM interface, I tested whether Sdc co-localizes with integrins within the peripheral nerve. To gain a more comprehensive picture of Sdc expression, I analyzed the distribution of Sdc::GFP.PTT in homozygotes of the allele compared to the β-subunit of the integrin heterodimer, myospheroid (aka βPS). Within the PNS, Sdc puncta do not co-localize with the integrin-belts. Though not quantified, I often observed Sdc and integrin localized in a mutually exclusive manner (**Fig. 2.5**; white arrows).

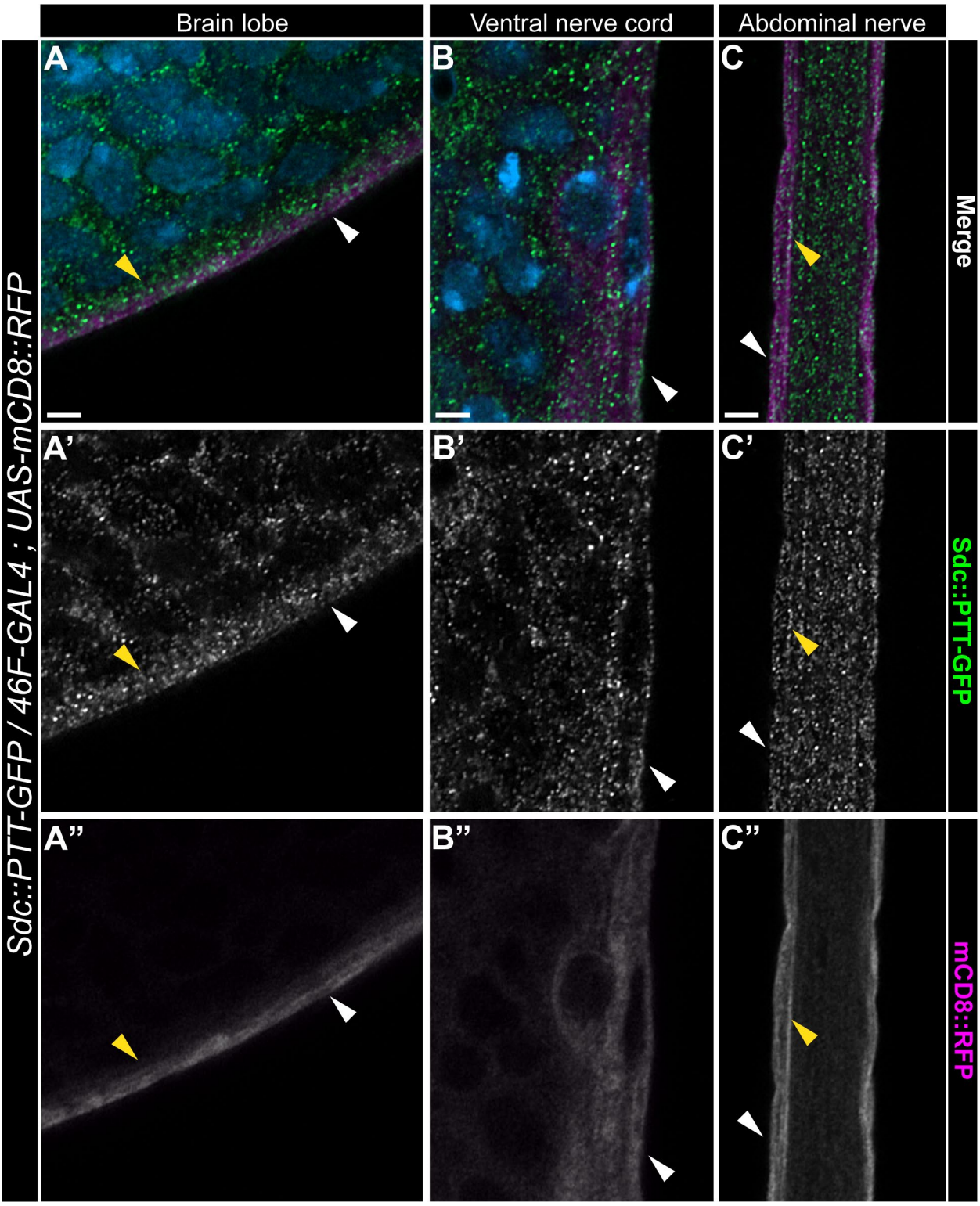
Brain lobe
Ventral nerve cord
Abdominal nerve
Sdc::PTT-GFP / 46F-GAL4 ; UAS-mCD8::RFP
A
B
C
Merge
A'
B'
C'
Sdc::PTT-GFP
A''
B''
C''
mCD8::RFP

Figure 2.2: Syndecan is expressed by perineurial glia and localized to the glial-ECM interface

(**A-C**) Cross-section of 3rd instar larval brain (A-A"), ventral nerve cord (B-B"), peripheral nerve (C-C") in which all perineurial glia are labeled with membrane-bound mRFP (mCD8::RFP, magenta) driven by *46F-GAL4*. Sdc::PTT.PTT (green) localization is visualized using an anti-GFP antibody. Note the consistent localization of Sdc::GFP.PTT puncta along the outer perineurial glial membrane facing the ECM (white arrow) throughout the nervous system. Sdc:: GFP.PTT puncta can also be detected along the perineurial glial membrane facing the subperineurial glia (yellow arrow). All nuclei are marked with DAPI (blue). Scale bar, 2 μm.

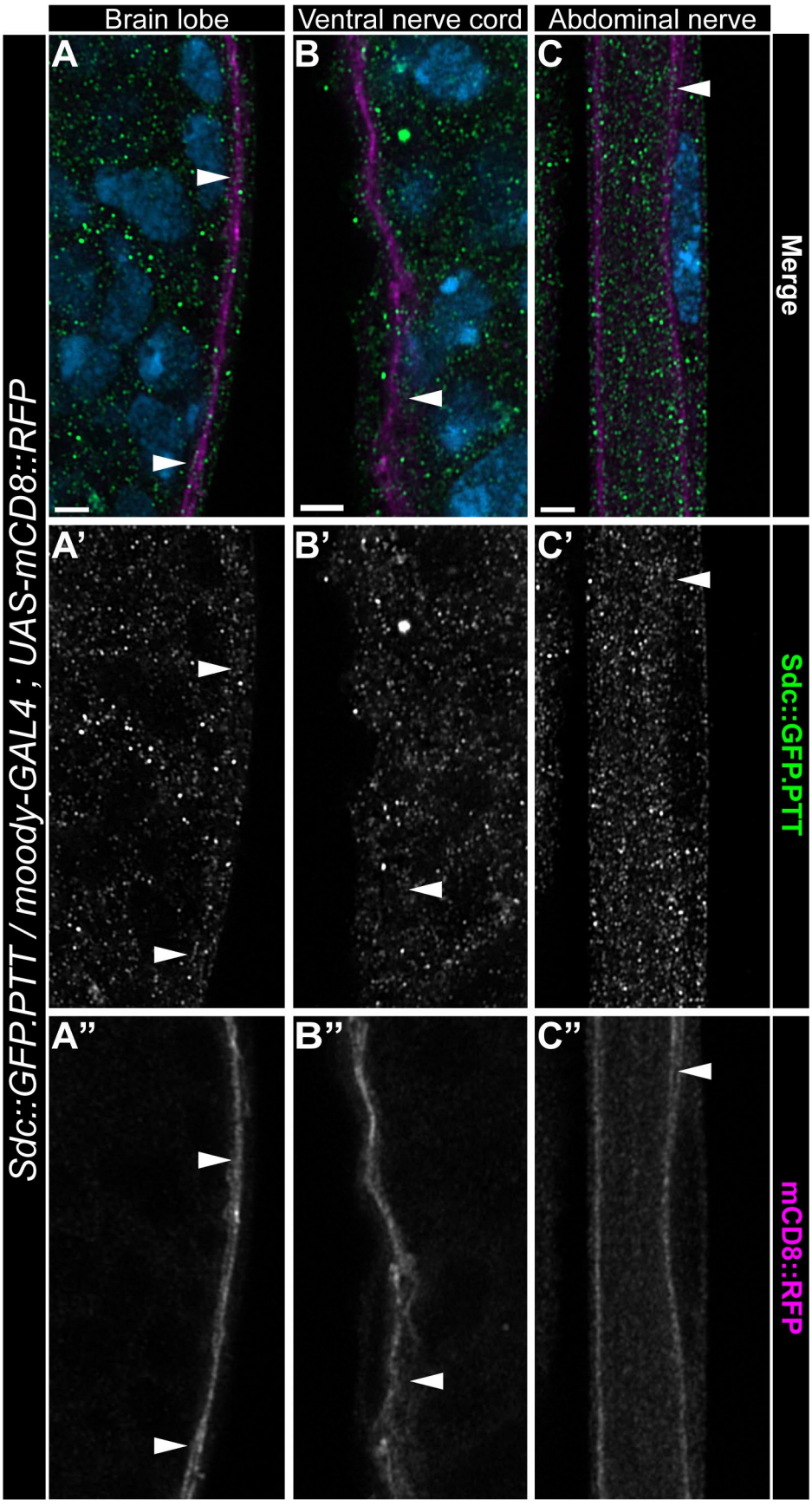
Brain lobe
Ventral nerve cord
Abdominal nerve
Sdc::GFP.PTT / moody-GAL4 ; UAS-mCD8::RFP
A
B
C
Merge
A'
B'
C'
Sdc::GFP.PTT
A''
B''
C''
mCD8::RFP

Figure 2.3: Syndecan localization coincides with the subperineurial glial membrane

(**A-C**) Cross-section of 3rd instar larval brain (A-A”), ventral nerve cord (B-B”), peripheral nerve (C-C”) in which subperineurial glia are labeled with membrane-bound mRFP (mCD8::RFP, magenta) driven by *moody-GAL4*. Sdc:: GFP.PTT (green) localization is visualized using an anti-GFP antibody. I observed patches of Sdc:: GFP.PTT puncta along the subperineurial glial membrane and perineurial glia throughout the nervous system (white arrow). Note the Sdc:: GFP.PTT puncta localize to the exterior of the subperineurial glial layer. All nuclei are marked with DAPI (blue). Scale bar, 2 μm.

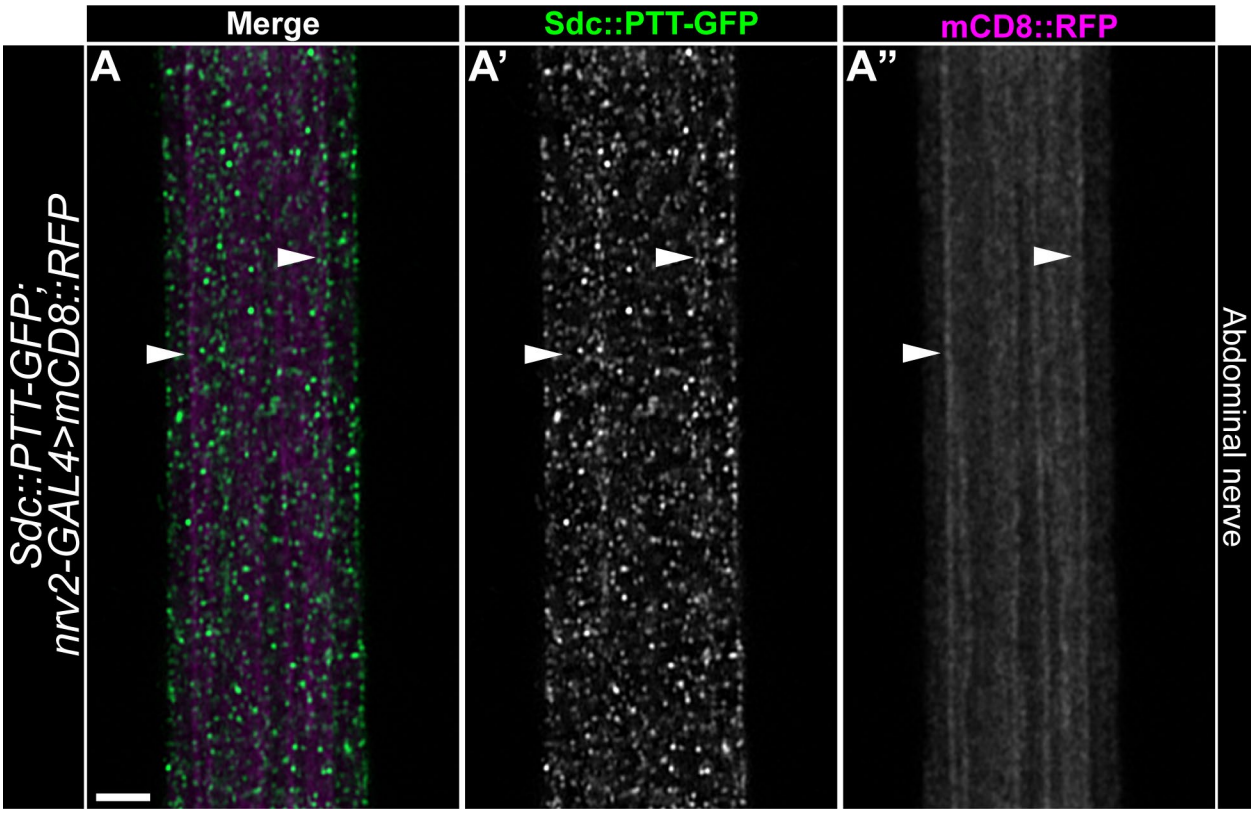

Figure 2.4: Syndecan is expressed by wrapping glia in the PNS

(**A**) Longitudinal cross-section of a 3rd instar larval peripheral nerve in which the wrapping glia are labeled with membrane-bound mRFP (mCD8::RFP, magenta) driven by *nrv2-GAL4*. Sdc:: GFP.PTT (green) localization is visualized using an anti-GFP antibody. I observed a linear distribution of Sdc:: GFP puncta along the strands of wrapping glial membranes (white arrow). Scale bar, 2 μm.

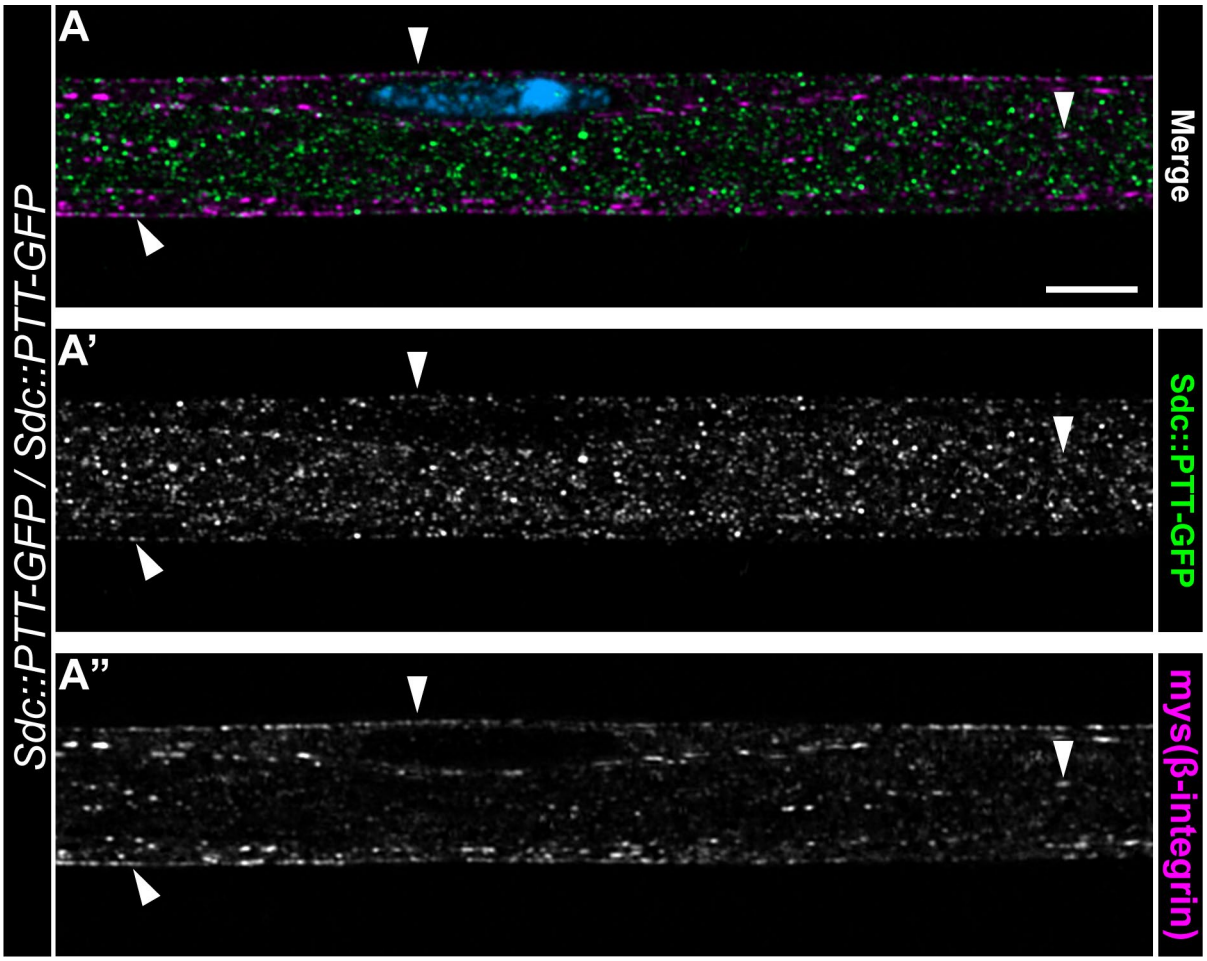

Figure 2.5: Syndecan does not co-localize with integrin in the peripheral nerve

(**A**) Longitudinal cross-section of a 3rd instar larval peripheral nerve. Sdc::GFP.PTT (green) expression is visualized using an anti-GFP antibody in comparison with integrin β-subunit, myospheroid (mys, magenta) visualized with the βPS mAb. I observed Sdc and integrin localization was in a juxtaposed relationship throughout the nerve (white arrow). All nuclei were marked with DAPI (blue). Scale bar, 5 μm.

2.3.2 Syndecan is required for the functioning of the nervous system

To establish the overall requirement of Sdc in *Drosophila* glia, I reduced Sdc expression using multiple RNAi lines targeting different regions of the *Sdc* transcript (**Fig. 2.6**) using a pan glial driver, *repo-GAL4, and UAS-Dicer2 (Dcr2)*. To visualize and assess changes to

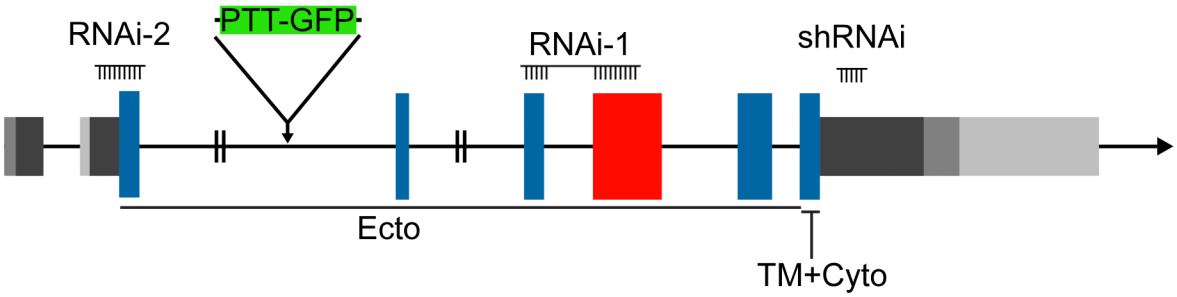

Figure 2.6: Schematic of the *Drosophila Sdc* gene map

The *Sdc* gene genomic region consists of seven exons and six introns. Blue marks the protein-encoding regions, and grey is indicative of untranslated regions (UTR). Red marks the only region of alternative splicing within the protein-encoding region. The function of this region in *Drosophila* is unknown. Note the majority of the exons for the protein-encoding regions encompassing the ectodomain (Ecto) of the protein, both the transmembrane domain (TM) and the cytoplasmic tail (Cyto) are encoded by exon 7. The different shades of grey within the UTRs represent the prevalence within the isoforms, increased darkness indicates more commonly found on different isoforms. The GFP exon tag is inserted in the second intron. To reduce Sdc expression I used different RNAi lines to target different regions of the sequence with *RNAi-1*, *RNAi-2*, and *shRNAi* targeting all confirmed isoforms and indicated on the diagram.

the glia morphology, I expressed a membrane marker (mCD8::GFP or RFP) in conjunction with the RNAi. In comparison to control animals (*repo-GAL4>Dcr-2, mCD8::GFP*) (**Fig. 2.7 A**), I found various morphological defects spanning the CNS and PNS upon Sdc knockdown. The VNC appeared elongated (**Fig 2.7 B-C**, yellow arrow), and the brain lobes were noticeably smaller (**Fig. 2.7 B-C**, white arrow). We quantified the effects with knockdown using *repo-GAL4>mCD8::RFP* and *Dicer2* and found a statistically significant increase in the ratio of VNC to body length with *RNAi-1* and *RNAi-2* (**Fig 2.7 E**). Compared to control, where the VNC is on average 9.8% of the body length, we saw an increase where the VNC extends to 11% and 10.8% of the body length on average in *RNAi-1* and *RNAi-2*, respectively. Also, we observed the VNC length ratio covered a wider distribution with *RNAi-1*, ranging from 8.2% to 14.2% of the body

length (**Fig. 2.7 E**), but this was not observed in *RNAi-2*. The *shRNAi* line was not significantly different from the control, suggesting shRNAi did not generate a sufficient knockdown. The elongation of VNC seen with Sdc RNAi knockdown indicates Sdc's possible contribution to cell-ECM adhesion as elongation to the VNC is often observed with disruption in glial-ECM contact (Meyer et al., 2014; Skeath et al., 2017). Next, we quantified the severity of the brain lobe size decrease with pan glial Sdc-RNAi (**Fig. 2.7 F**). By measuring the brain lobe at the widest point (from outer edge to center), we saw a 27.8% decrease in brain lobe width with *RNAi-1* and a 13.4% reduction in *RNAi-2* compared to control. However, we did not observe a significant change in VNC length and brain lobe size associated with the *shRNAi* line (**Fig. 2.7 E-F**). Our results also suggested that *RNAi-1* is more effective in knocking down Sdc compared to *RNAi-2* or the *shRNAi*. While not quantified, I saw a clear down regulation of Sdc::GFP in RNAi-1, which shows it is an effectively tool in reducing Sdc expression (**Supp. Fig 2, see appendix**).

The peripheral axons are encapsulated by multiple glial layers that often appear compact and smooth as seen in control (*repo-GAL4>Dcr2, mCD8::GFP)* (**Fig. 2.7 G**). After pan-glial expression of *RNAi-1,* peripheral nerves frequently displayed swelling and glial membrane fragmentation (100% of all nerves counted, number of animals = 6) (**Fig. 2.7 H**, white arrow). I observed similar phenotypes with *RNAi-2* and *shRNAi*, albeit with much lower penetrance (RNAi-2 = 14% of all nerves counted, number of animals = 6; shRNAi = 6% of all nerves counted, number of animals = 6), and many nerves appeared smooth and continuous like that of control.

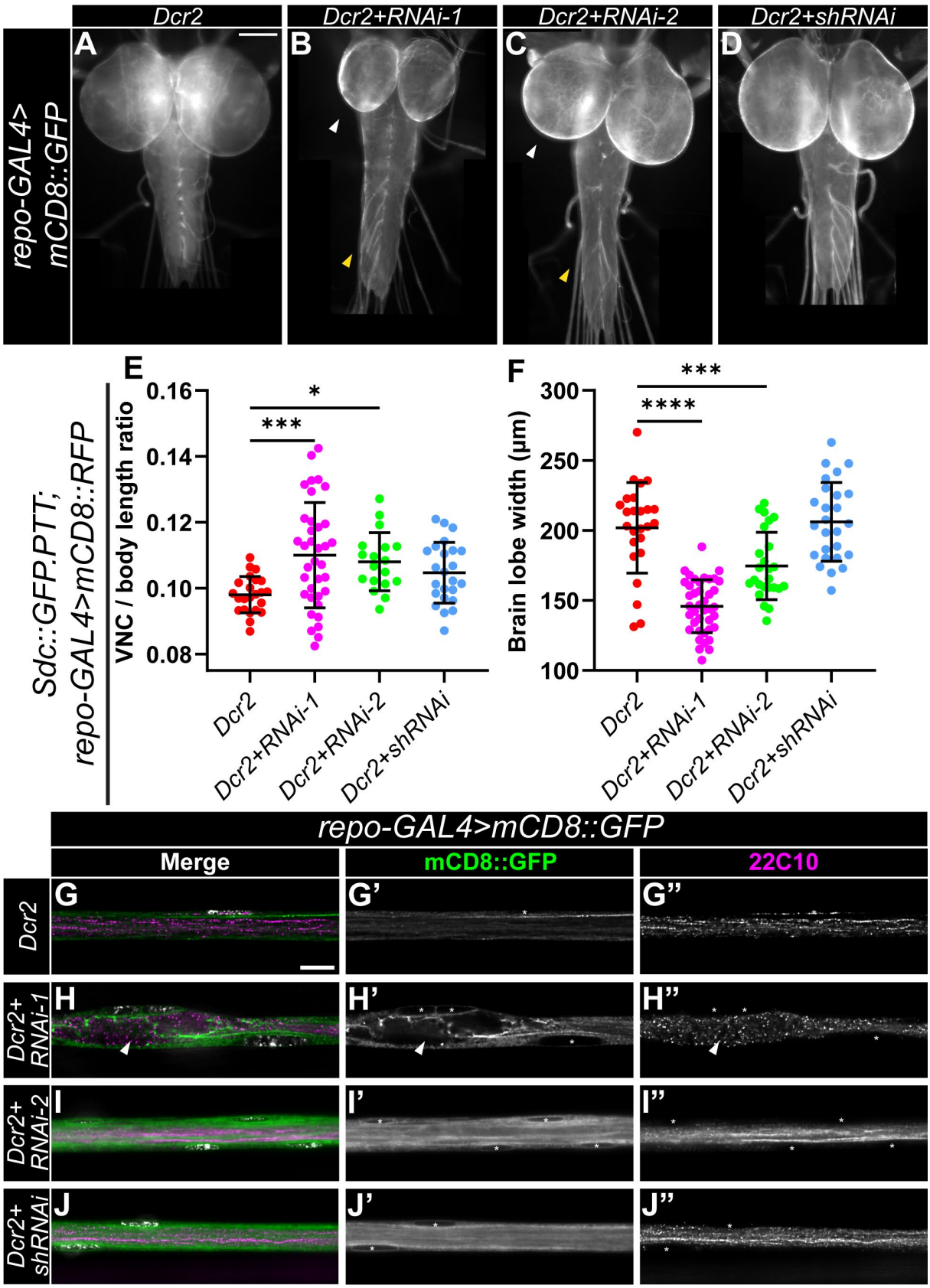
Dcr2
Dcr2+RNAi-1
Dcr2+RNAi-2
Dcr2+shRNAi
repo-GAL4>
mCD8::GFP
A
B
C
D
Sdc::GFP.PTT;
repo-GAL4>mCD8::RFP
E
VNC / body length ratio
0.16
0.14
0.12
0.10
0.08
*
***
F
Brain lobe width (µm)
300
250
200
150
100
***
****
repo-GAL4>mCD8::GFP
Merge
mCD8::GFP
22C10
G
G'
G''
H
H'
H''
I
I'
I''
J
J'
J''

Figure 2.7: Glial Syndecan is necessary to ensure the structural integrity of the larval nervous system

(**A-D**) Representative stacked images of larval CNS with *repo-GAL4* and expressing only *Dcr2* as control (A), *Dcr2+RNAi-1* (B), *Dcr2+RNAi-2* (C), and *Dcr2+shRNAi* (D). Membrane-bound GFP (mCD8::GFP) expressed by *repo-GAL4* was used to visualize all glia membranes. Note the misshaped ventral nerve cord (yellow arrow) and shrinkage of the brain lobe (white arrow) upon expression of Sdc RNAi in all glia.
(**E-F**) Quantification of ventral nerve cord (VNC) elongation (E) and brain lobe shrinkage (F). Black brackets show the mean ± SD. Intact VNC and brain lobes were measured in the *repo-GAL4>mCD8::RFP* background with VNC length measured as the distance between the head nerve exit point to theA8 abdominal nerve exit point. In (F), one brain lobe from each animal was sampled. The mean prevalence were analyzed using one-way ANOVA (*P<0.0001*) with a Dunnett's multiple *post-hoc* comparison test of *Dcr2+RNAi-1* (E; n = 36), (F; n = 40), *Dcr2+RNAi-2* (E; n = 18), (F; n = 25) and *Dcr2+shRNAi* (E; n = 24, F; n = 26) compared to control, *Dcr2* (E; n = 23), (F; n =25) (n = number of animals pooled from four replicates). * $p \leq 0.5$, *** $p \leq 0.001$, **** $p \leq 0.0001$.
(**G-J**) Representative longitudinal cross-section images of peripheral nerve in control (*repo-GAL4>Dcr2*) (G-G"), *Dcr2+RNAi-1* (H-H"), *Dcr2+RNAi-2* (I-I"), and *Dcr2+shRNAi* (J-J"). Glial membranes are marked with mCD8::GFP (green) and axons with anti-Futsch (mAb 22C10; magenta). Nuclei were labelled using DAPI (white; G-J) and an asterisk (G'-J', G"-J"). I observed swelling (white arrow) and defasciculation of axons (H") when expressing *Dcr2+RNAi-1* using *repo-GAL4*.

Next, I analyzed the animal's locomotion output to determine if the morphological defects observed with pan glial Sdc knockdown have any functional consequences. Using a larval tracking assay, I observed a significant reduction in overall movement over one minute and comparing the Sdc knockdown groups to control (*repo-GAL4>Dcr2,)* (**Fig. 2.8 A-D**). Further quantification of maximum speed (**Fig. 2.8 E**), average speed (**Fig. 2.8 F**), and total distance travelled (**Fig. 2.8 G**) revealed the impaired locomotion associated with *RNAi-1* was the most severe, showing a more than 50% reduction in average traveling speed and distance, which is reflected in the movement trajectory (**Fig. 2.7 A-B**). A significant decrease in movement output was observed with the other RNAi lines, though the degree of severity was less and the decreases in *RNAi-1* was significantly greater in comparison with both *RNAi-2* and *shRNAi* lines. These data show that glial Sdc is necessary for proper animal locomotion.

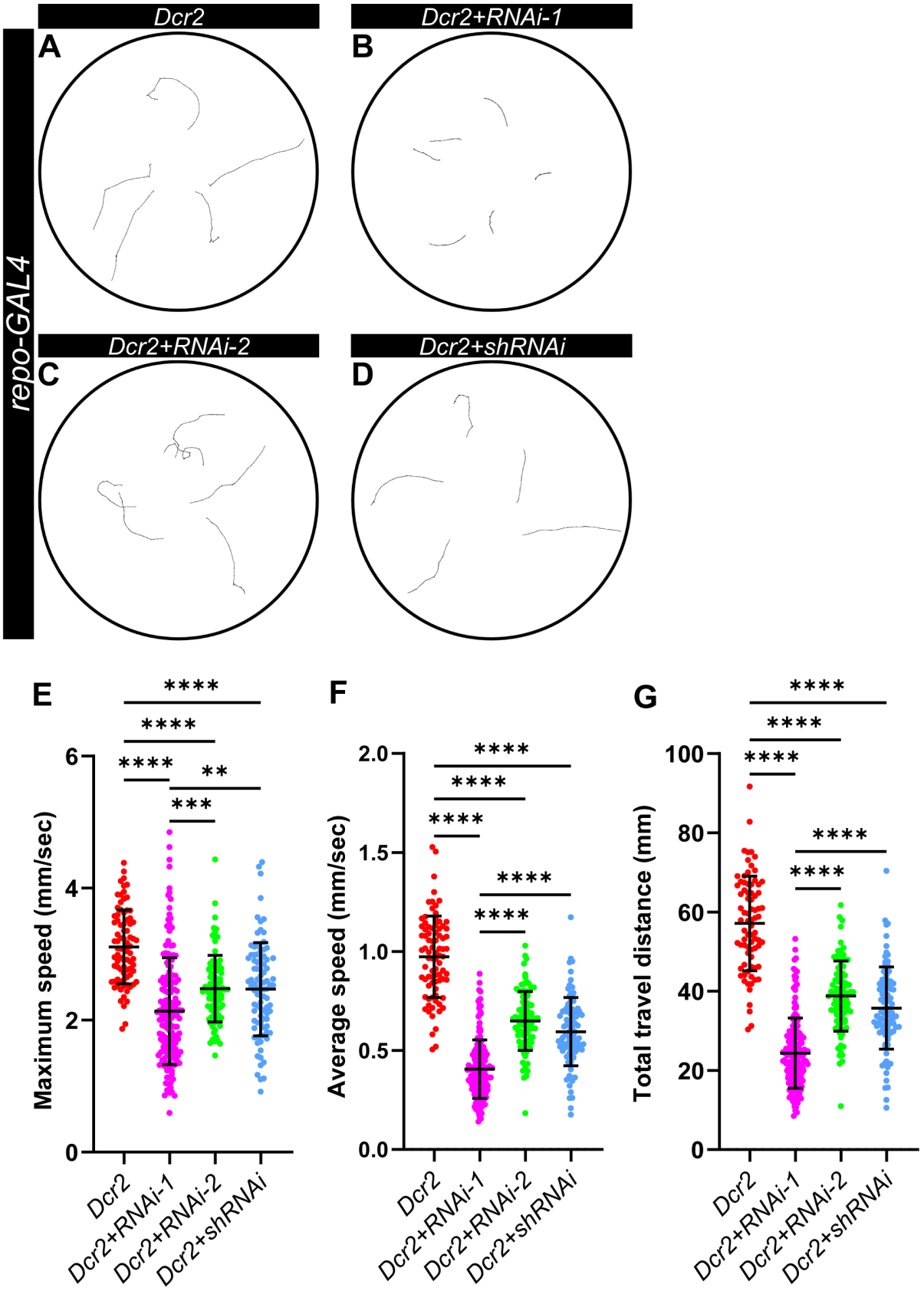
repo-GAL4
Dcr2
Dcr2+RNAi-1
Dcr2+RNAi-2
Dcr2+shRNAi
A
B
C
D
E
F
G
Maximum speed (mm/sec)
Average speed (mm/sec)
Total travel distance (mm)
****
**
***
Dcr2
Dcr2+RNAi-1
Dcr2+RNAi-2
Dcr2+shRNAi

Figure 2.8: Impaired larval locomotion is associated with pan-glial Syndecan reduction

(**A-D**) Representative 3rd instar larval movement trajectory of *repo-GAL4* driving *Dcr2* as control (A), *Dcr2+RNAi-1* (B), *Dcr2+RNAi-2* (C), and *Dcr2+shRNAi* (D). Each line is representative of one larvae's movement in 60s with a starting point near the center.
(**E-G**) Quantification of the mean maximum crawl speed (E), mean average crawling speed (F), and mean total travel distance (G). *repo-GAL4* driving: *Dcr2* (E; n = 83), (F; n = 84), (G; n = 78), *Dcr2+RNAi-1* (E-G; n = 166), *Dcr2+RNAi-2* (E-F; n = 92), (G; n = 91), *Dcr2+ shRNAi* (E-G; n = 91) (n = number of animals analyzed pooled from two replicates). Black brackets show mean ± SD, with difference of mean between each group analyzed using one-way ANOVA (*P<0.0001*) with Tukey's multiple comparison test. $^{**}p \leq 0.01$, $^{***}p \leq 0.001$, $^{****}p \leq 0.0001$, comparison not shown = ns, not significant.

2.3.3 Glial Syndecan is needed for neuroblast population expansion in the CNS

In 3rd instar larval brain lobes, neurons account for the majority of the tissue volume, with discrete regions of neuroblast proliferation that undergo cell division to generate new neurons (Egger et al., 2008)**.** The brain lobe shrinkage I identified with pan-glial expression of the Sdc-RNAi lines could be associated with decreased proliferation or an increase in programmed cell death. I used phosphohistone-3 (pHis-3) as a marker for mitotic events in the brain lobe. In the control (*repo-GAL4>Dcr2, mCD8::GFP)*, I observed a belt with active proliferation events, as marked by the robust signal of pHis-3 surrounding by dense-area of nuclei marked by DAPI (**Fig 2.9 A**) that likely corresponds to the optic lobe outer proliferation zone (Egger et al., 2007). By reducing Sdc expression in all glia, I observed a reduction of active cell division where the degree of brain lobe shrinkage with *RNAi-1* was the greatest. *RNAi-2* showed a lesser reduction, and *shRNAi* had no effect. To test our hypothesis that increased apoptosis is not associated with the Sdc knockdown dependent phenotype, I examined the activity of cleaved Death caspase-1 (cDCP-1), an effector protein in the apoptosis pathway and a homolog of mammalian caspase-7 (Song et al., 1997). Across all RNAi groups, I did not observe a noticeable increase in the amount of cDCP-1 activity comparing to the control, despite the recapitulation of the brain lobe shrinkage phenotype (**Fig. 2.9 E-G**). This result suggests that the decrease in brain lobe size is due to a lack of proliferation and not an increase in cell death.

I then sought to further examine the impact on the neuroblast (NB) population upon Sdc reduction. To visualize neuroblasts, I used Deadpan (Dpn) (San-Juán and Baonza, 2011) , and focused on the impact of Sdc knockdown in the optic lobe outer proliferation zone, due to its reduction in size relative to control (**Fig. 2.9 A-C**). The neuroblast region within the optic lobe displayed dramatic loss in size with the Sdc knockdowns compared to control (**Fig. 2.9 I-L**).

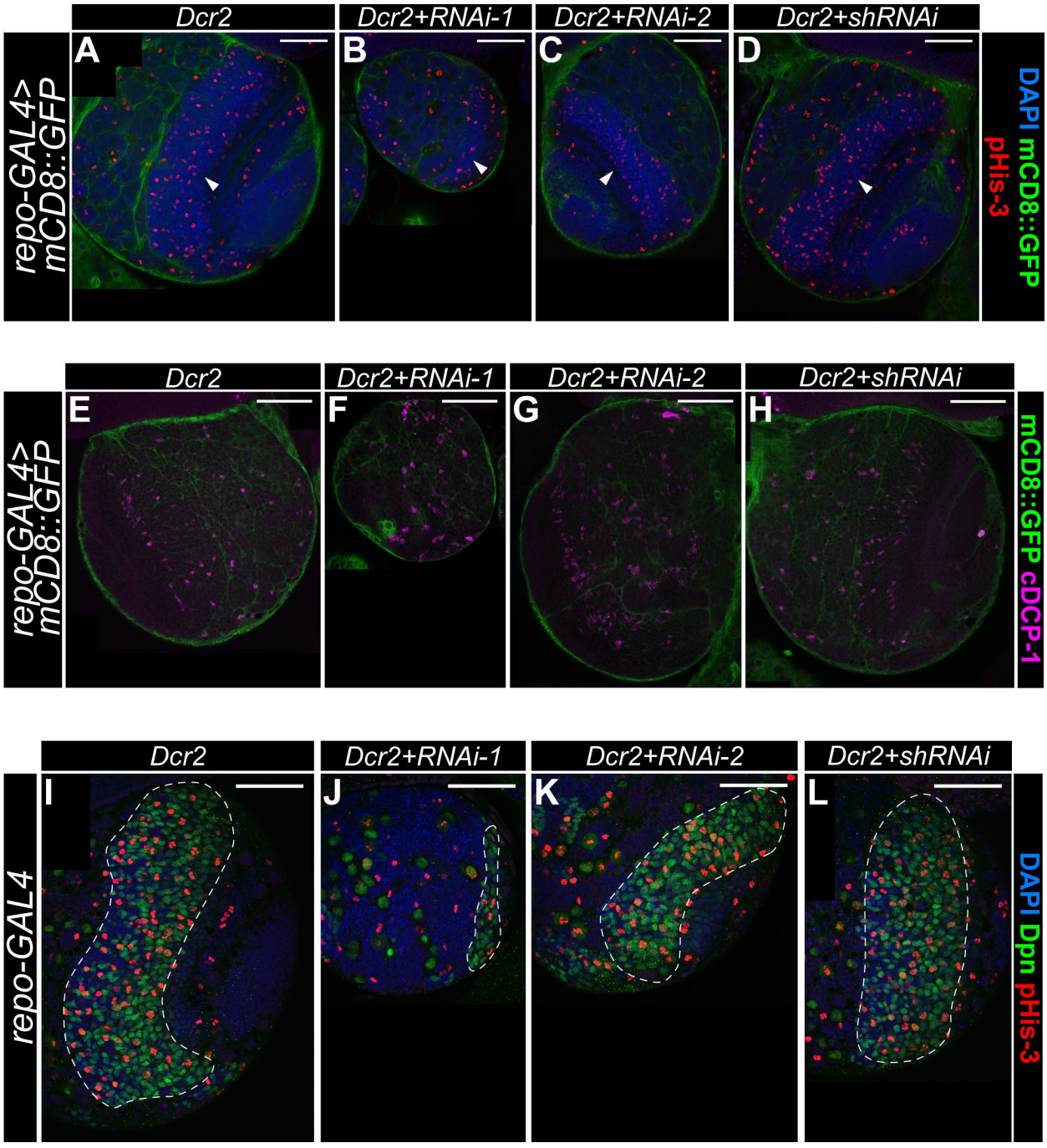
Dcr2
Dcr2+RNAi-1
Dcr2+RNAi-2
Dcr2+shRNAi
repo-GAL4>
mCD8::GFP
A
B
C
D
DAPI mCD8::GFP
pHis-3
Dcr2
Dcr2+RNAi-1
Dcr2+RNAi-2
Dcr2+shRNAi
repo-GAL4>
mCD8::GFP
E
F
G
H
mCD8::GFP cDCP-1
Dcr2
Dcr2+RNAi-1
Dcr2+RNAi-2
Dcr2+shRNAi
repo-GAL4
I
J
K
L
DAPI Dpn pHis-3

Figure 2.9: Neuroblast numbers and proliferation requires glial Syndecan

(**A-D**) Representative images of the cross-sections of 3rd instar larval brain lobes. All glial membranes were labelled with membrane-bound GFP (mCD8::GFP, green) expressed by *repo-GAL4*. Mitotic cells were labeled with antibodies to phosphohistone-3 (pHis-3, red) within the brain lobe. DAPI (blue) is used to mark nuclei and the cell-dense outer proliferation belt within the optic lobe. Notice the changes within brain lobe size and reduced pHis-3 staining within *Dcr2+RNAi-1*(B) and *Dcr2+RNAi-2* (C) compared to control *Dcr2* (A). Number of brain lobes analyzed (A; n = 4, B; n = 7, C; n = 7, D; n = 8)
(**E-H**) Representative images of the cross-sections of the 3rd instar larval brain lobe revealing pan glial Sdc knockdown did not increase apoptosis. Under the control of *repo-GAL4*, all glial membranes were visualized by mCD8::GFP (green). An anti-cleaved *Drosophila* caspase-3 (cDCP-1, magenta) antibody was used to detect cell apoptosis. There was no observed increase in cDCP-1 within *Dcr2+RNAi-1*(F) and *Dcr2+RNAi-2* (G) compared to control *Dcr2* (E). Number of brain lobes analyzed, (E; n = 6, F; n = 2, G; n = 7, H; n = 8).
(**I-L**) Representative crossing section image showing the proliferation belt within 3rd instar *Drosophila* brain lobes. The neuroblast population was revealed using an anti-deadpan (Dpn, green) antibody with pHis-3 (red) marking the mitotic events and DAPI (blue) labeling all nuclei. Note the less abundant neuroblast and miotic events with *repo-GAL4* driving *Dcr-2+RNAi-1* (J) and *Dcr-2+RNAi-2* (K) compared to control *Dcr2* (I). Number of brain lobes analyzed (I; n = 11, J; n = 8, K; n = 12, L; n = 10). Scale bars, 50 μm (A-L).

RNAi-1 demonstrated the most severe phenotype (**Fig. 2.9 J**), where a large portion of the outer proliferation belt (white dash line) was greatly reduced or completely absent. In the *RNAi-2* group, I observed a decrease in the neuroblast region, though it was not as dramatic as *RNAi-1*. The penetrance and severity of these phenotypes further suggests that *RNAi-1* is the most effective at reducing Sdc expression, followed by *RNAi-2*, and lastly, *shRNAi*. These results indicated that glial Sdc is necessary for neuroblast population expansion or maintenance.

2.3.4 Loss of Syndecan disrupts ensheathment by wrapping glia

Based on the expression pattern in the PNS of Sdc::GFP.PTT, Sdc appears to be expressed by wrapping glia. Thus, I sought to determine the possible function of Sdc in this glial layer. Normally, wrapping glia expand membrane projections to encase the axon bundles (**Fig. 2.10 A-A"**). Using a wrapping glia driver (*nrv2-GAL4*) for Sdc knockdown, I observed prominent wrapping glia ensheathment defects in all RNAi groups compared to control (*nrv2-GAL4>Dcr2, mCD8::RFP*). Specifically, I observed a loss of the complex glial processes (**Fig. 2.10 B-B', C-C'**) or breakage of the wrapping glia processes along the length of the nerve (**Fig. 2.10 D-D'**). Often small and thin cell processes can be seen projecting out of the central bundle (**Fig. 2.10 B'-C'**), however, the lack of wrapping did not impact axonal morphology (**Fig. 2.10 A"-C"**). Interestingly, the migratory ability of wrapping glia remain intact with Sdc knockdown as the wrapping glia were distributed normally along the nerve (n = 29). In *RNAi-1,* 95.7% of the peripheral nerves showed a lack of ensheathment compared to 46% in *RNAi-2* , 34.1% in *shRNAi*, and 13% in control (**Fig. 2.10 E**).

I was curious to see whether the lack of ensheathment by Sdc knockdown in the wrapping glia would affect animal locomotion. In comparison to the control (*nrv2-GAL4>Dcr2*), *RNAi-1* showed a significant decrease in all analyzed metrics (**Fig. 2.11 A-C**). *ShRNAi* also showed significant decrease in total travel distance and average speed, though not in maximum speed, compared to control. The locomotion defect pattern is likely due to changes in the CNS, as lack of ensheathment by wrapping glia in the PNS does not alter animal movement significantly. Indeed only in the complete absence of wrapping glia do larvae show decreases in locomotion performance (Kottmeier et al., 2020).

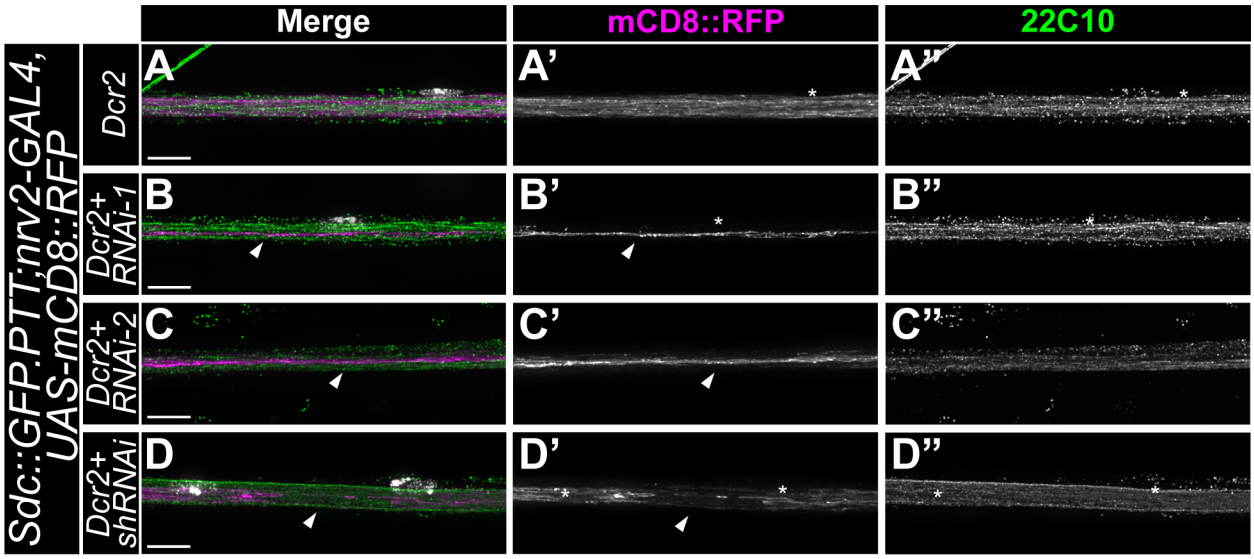
Merge
mCD8::RFP
22C10
Sdc::GFP.PTT;nrv2-GAL4, UAS-mCD8::RFP
Dcr2
Dcr2+ RNAi-1
Dcr2+ RNAi-2
Dcr2+ shRNAi
A
A'
A''
B
B'
B''
C
C'
C''
D
D'
D''

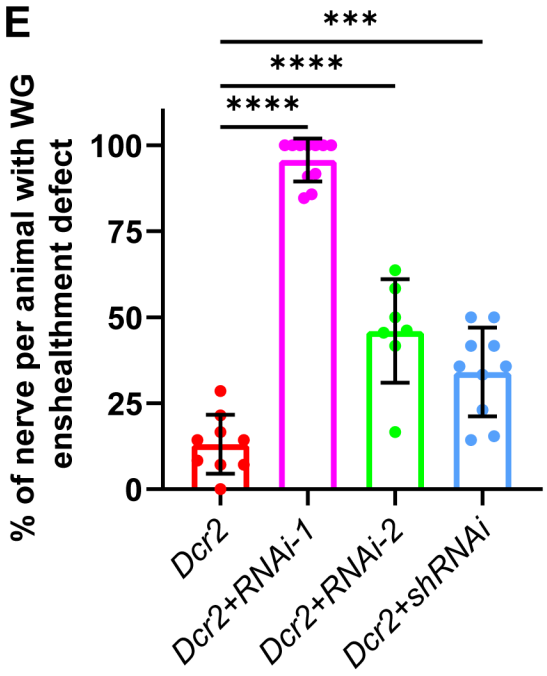
E
***
****
****
% of nerve per animal with WG enshealthment defect
100
75
50
25
0
Dcr2
Dcr2+RNAi-1
Dcr2+RNAi-2
Dcr2+shRNAi

Figure 2.10: Wrapping glia require Syndecan for axonal ensheathment

(**A-D**) Representative stacked images of wrapping glia in the peripheral nerves labelled with membrane-bound RFP (mCD8::RFP, magenta) under the control of *nrv2-GAL4*, with anti-Futsch (mAb 22C10) antibody immunolabeling axons (green). DAPI marked all nuclei colored in grey (A-D) and with an asterisk (A'-D', A"-D"). *Nrv2-GAL4* drove the expression of *Dcr2* (A), *Dcr2+RNAi* (B), and *Dcr2+RNAi-2* (C). Note the absence of wrapping glia ensheathment (B'-C') and membrane breakage (D') with RNAi knockdown (white arrows). Scale bar, 10 µm (**E**) Quantification of prevalence of wrapping glia with ensheathment defects. Data showing the mean ± SD, with the defect percentage calculated by the number of defective nerves divided by the number of intact peripheral nerves. I defined a defective nerve as containing at least one wrapping glia showing defects in ensheathment within the nerve extension region. Quantification was with a one-way ANOVA (*P<0.0001*) and a Dunnett's multiple *post-hoc* comparison test. *Dcr2+RNAi-1* (n = 11), *Dcr2+RNAi-2* (n = 7) and *Dcr2+shRNAi* (n = 10) compared to control, *Dcr2* (n = 9) (n = number of animals pooled from two replicates). ***$p \leq 0.001$, ****$p \leq 0.0001$.

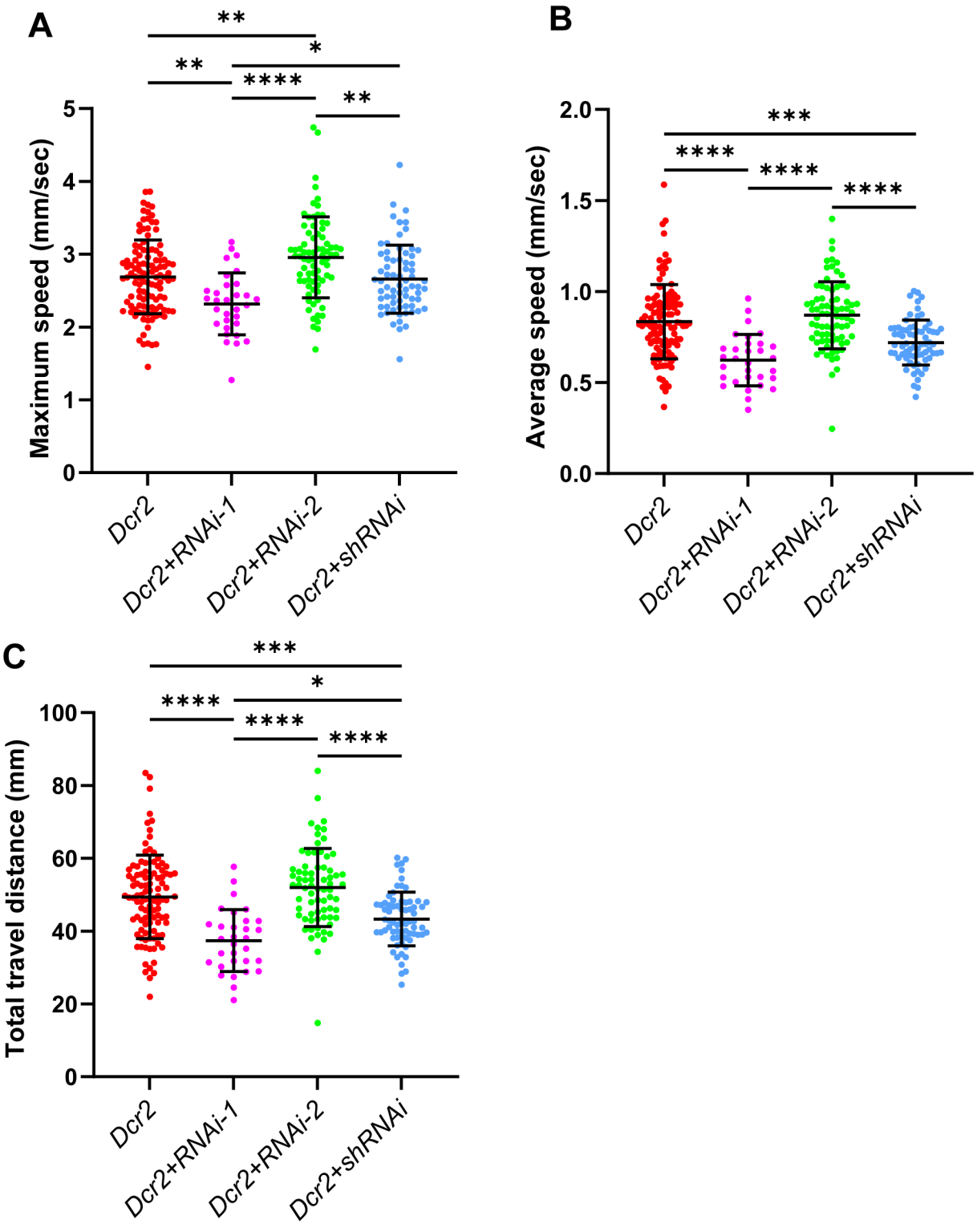
A
Maximum speed (mm/sec)
0
1
2
3
4
5
**
*
**
****
**
Dcr2
Dcr2+RNAi-1
Dcr2+RNAi-2
Dcr2+shRNAi
B
Average speed (mm/sec)
0.0
0.5
1.0
1.5
2.0
***
****
****
****
Dcr2
Dcr2+RNAi-1
Dcr2+RNAi-2
Dcr2+shRNAi
C
Total travel distance (mm)
0
20
40
60
80
100
***
*
****
****
****
Dcr2
Dcr2+RNAi-1
Dcr2+RNAi-2
Dcr2+shRNAi

Figure 2.11: Wrapping glial knockdown of Syndecan alters animal locomotion

(**A-C**) Quantification of mean maximum crawl speed (A), mean average crawling speed (B), and mean total travel distance (C) from recordings of *Nrv2-GAL4* driven *Dcr2* (A-B; n = 113, C; n = 103), *Dcr2+RNAi-1* (A-C; n = 31), *Dcr2+RNAi-2* (A; n = 77, B; n = 71, C; n = 78), *Dcr2+shRNAi* (A, C; n = 70, B; n = 69) (n = number of animals analyzed pooled from two replicates). Scatter plots show the mean ± SD with black brackets using a one-way ANOVA (*P<0.0001*) and Tukey's multiple comparison test. **p*≤0.05, ***p* ≤0.01, ****p* ≤0.001, *****p* ≤0.0001, comparison not shown = ns, not significant.

2.3.5 Syndecan is necessary for subperineurial glia morphology and septate junction integrity

As Sdc::GFP.PTT appeared to localize to the subperineurial glial membrane, I sought to assess whether the morphology of subperineurial glia can be affected by the loss of Sdc. In the subperineurial glia, septate junctions are formed between two facing subperineurial membranes and appear as a single continuous line along the length of the nerve (**Fig. 2.12 A-A'**). I visualized the septate junctions using Neurexin-IV (NrxIV), a core septate junction component endogenously tagged with GFP, and to mark the subperineurial membranes I used mCD8::RFP under the control of *moody-GAL4*, a subperineurial driver. With Sdc knocked down in the subperineurial glia, nerves appeared to be larger in diameter in discreet areas along the nerve. The distribution of those subperineurial glial enlargements appeared to be random with no apparent proximity preference near the MFA or VNC. Within the regions of enlargement, the subperineurial glia membranes exhibit lateral expansion and becomes irregular and disorganized, in contrast to the thin and smooth membranes seen in control (**Fig. 2.12 A-D, A"-D"**, white arrows). I observed that septate junction strands became destabilized from a single continuous line to form multiple interconnected webs diffused but these changes were only observed within

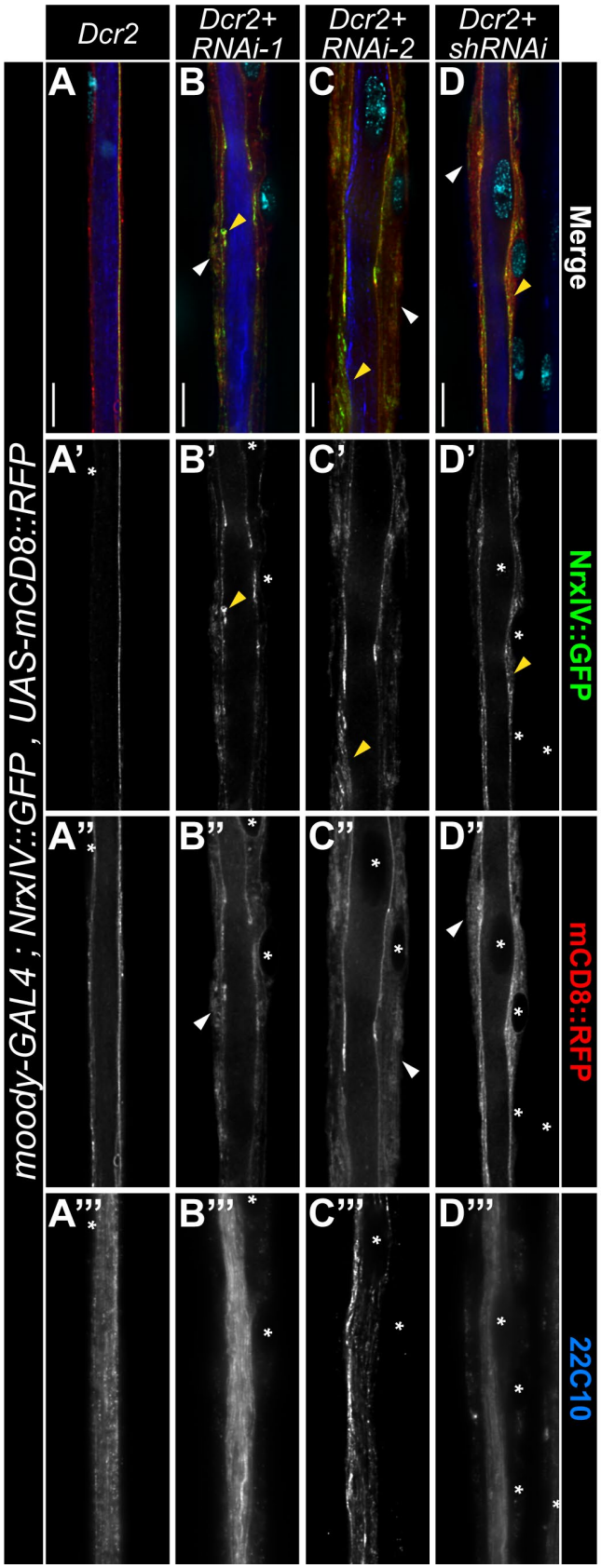
Dcr2
Dcr2+ RNAi-1
Dcr2+ RNAi-2
Dcr2+ shRNAi
moody-GAL4 ; NrxIV::GFP , UAS-mCD8::RFP
Merge
NrxIV::GFP
mCD8::RFP
22C10

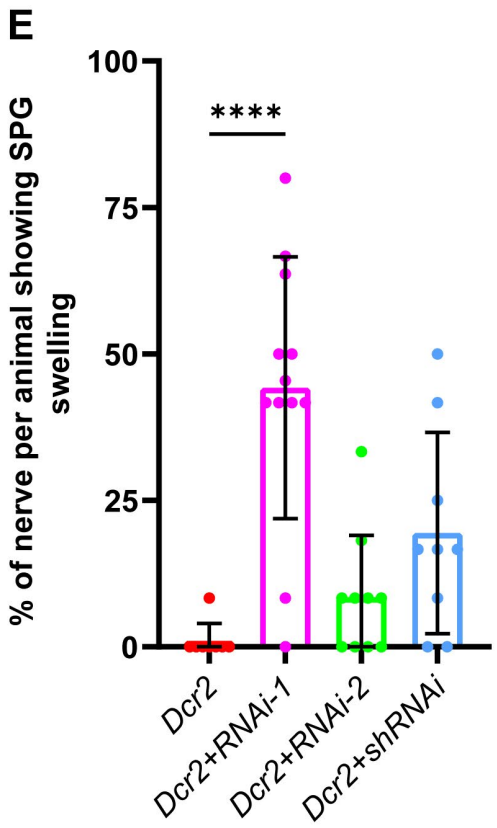
E
% of nerve per animal showing SPG swelling
100
75
50
25
0
****
Dcr2
Dcr2+RNAi-1
Dcr2+RNAi-2
Dcr2+shRNAi

Figure 2.12: Knockdown of Syndecan disrupted subperineurial glia morphology

(**A-D**) Representative longitudinal cross-sectional images of peripheral nerves. The septate junctions were visualized using Neurexin-IV::GFP (NrxIV-GFP, green) with the GFP signal enhanced using an anti-GFP antibody. Axons were immunolabeled with anti-Futsch (mAb 22C10; blue). The morphology of subperineurial glia was marked with membrane-bound RFP (mCD8::RFP, red) controlled under *moody-GAL4*. DAPI marked all nuclei (cyan; A-D) and asterisks (A'-D', A''-D'', A'''-D'''). *Moody-GAL4* drove the expression of *Dcr2* (control A), *Dcr2+RNAi-1* (C), *Dcr2-RNAi-2* (D). NrxIV spread within the glia (yellow arrow, B-D, B'-D') and localized glial sheath enlargement (white arrow, B-D, B"-D") was observed in all RNAi groups. Scale bar, 10 μm.
(**E**) Quantification of enlargement frequency. Data showing the mean ± SD in black brackets, with the percentage of the phenotype calculated by the number of nerves with the phenotype divided by the number of intact peripheral nerves. A defective nerve is defined as at least one subperineurial glia showing cell swelling within the nerve extension region. Quantified through a one-way ANOVA (*P<0.0001*) with Dunnett's multiple *post-hoc* comparison test *Dcr2+RNAi-1* (n = 12), *Dcr2+RNAi-2* (n = 10) and *Dcr2+shRNAi* (n = 9) compared to control, *Dcr2* (n = 8) (n = number of animals pooled from two replicates). ****$p \leq 0.0001$, comparison not shown = ns, not significant.

the enlarged regions (**Fig. 2.12 B'-D'**, yellow arrow) and the septate junctions appeared normal outside these regions. Of interest was the enlargement of the subperineurial glia did not resemble a typical swelling phenotype seen with other mutants such as transporter mutants or ER stress, which cause bulges, fluid accumulation, or visible vacuoles (Leiserson et al., 2011), instead the phenotype is more comparable to that of a baked puff pastry. Additionally, the enlargement of the glia did not appear to trigger cell death, as I did not notice any glial membrane fragmentation or pyknotic nuclei. Moreover, the disruption within subperineurial glia did not alter axon bundle morphology (**Fig. 2.12 B'''-D'''**). When quantified, the prevalence of such an enlargement phenotype was significantly higher with *RNAi-1* compared to control (*moody-GAL4>Dcr2,*

mCD8::RFP) (**Fig. 2.12 E**). While there was not a statically significant increase in the phenotypes with *RNAi-2* and *shRNAi*, I observed an increased trend in the penetrance of the subperineurial glia enlargement (**Fig. 2.12 E**). It should be noted that the subperineurial glia disruption did not impact the animals' survivability as Sdc knockdowns and controls produced viable adults.

I further characterized the functional impact of the subperineurial glia phenotype by conducting larval locomotion assays. I saw a reduction in animal movement across all RNAi groups compared to control (*moody-GAL4>Dcr2*) (**Fig. 2.13 A-C**). However, among the RNAi-groups, there was no difference between the RNAi lines in terms of maximum speed (**Fig. 2.13 A**) and, in contrast to previous experiments, *shRNAi* displayed the greatest decrease in average velocity and travel distances. Given moody-GAL4 is also labels subperineurial glia in the CNS, the locomotion defect pattern could be due to changes in the CNS, independent of the glial sheath enlargement I observed in the PNS.

Subperineurial glia are close to perineurial glia, suggesting that subperineurial glia may alter perineurial glial development and behaviour (Lavery et al., 2007). I sought to investigate whether the localized enlargements in subperineurial glia impacts perineurial glia ensheathment and migration. To track the perineurial glia, I used an antibody against Zipper, a myosin II heavy chain shown to preferentially label perineurial glia in the PNS (Hunter et al., 2020) (**Fig. 2.14 A-A'**). Within the regions of enlargement, I noticed that Zipper was diffuse throughout the nerve; this is in contrast to the control, where Zipper labeling formed distinctive belts and puncta (**Fig. 2.14 B'-C'**). The Zipper staining outlining the glial-ECM interface suggests perineurial glia ensheathment was not affected. Moreover, Zipper had a normal distribution and pattern in

regions distant to the enlargement suggesting that the abnormal subperineurial membrane landscape likely did not affect perineurial glial migration.

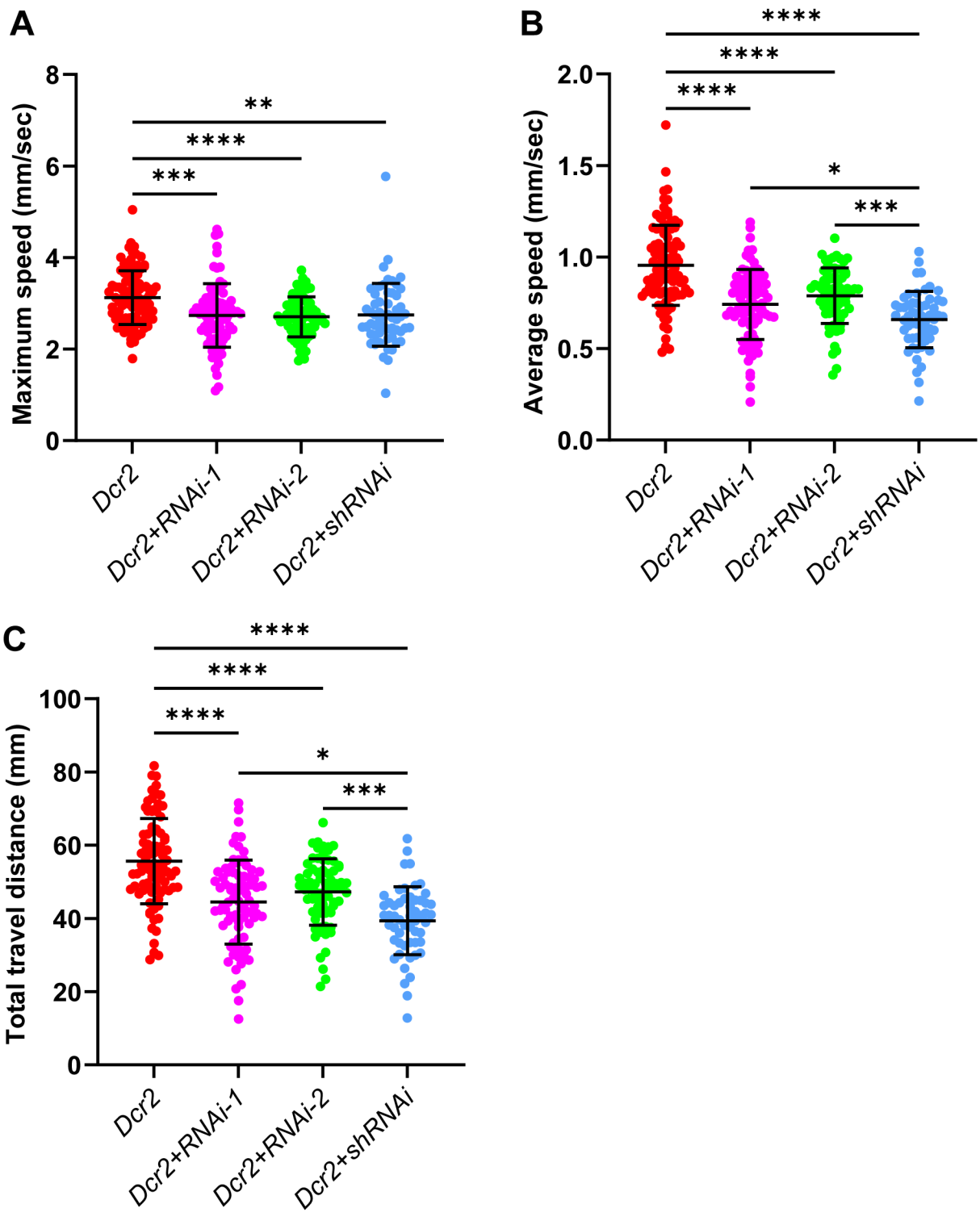
A
Maximum speed (mm/sec)
0
2
4
6
8
**
****
***
Dcr2
Dcr2+RNAi-1
Dcr2+RNAi-2
Dcr2+shRNAi
B
Average speed (mm/sec)
0.0
0.5
1.0
1.5
2.0
****
****
****
*
***
Dcr2
Dcr2+RNAi-1
Dcr2+RNAi-2
Dcr2+shRNAi
C
Total travel distance (mm)
0
20
40
60
80
100
****
****
****
*
***
Dcr2
Dcr2+RNAi-1
Dcr2+RNAi-2
Dcr2+shRNAi

Figure 2.13: Subperineurial glial Syndecan downregulation is associated with impaired larval locomotion

(**A-C**) Quantification of mean maximum crawl speed (A), mean average crawling speed (B), and mean total travel distance (C) from recordings of *moody-GAL4* driven *Dcr2* (A-B; n=98, C; n=90), *Dcr2+RNAi-1* (A; n = 82, B-C; n=83), *Dcr2+RNAi-2* (A-C; n = 72), *Dcr2+shRNAi* (A-B; n = 57, C; n=55) (n = number of animals analyzed pooled from two replicates). Data shows the mean ± SD, using a one-way ANOVA (*P<0.0001*) with Tukey's *post-hoc* multiple comparison test. **p*≤0.05, ***p* ≤0.01, ****p* ≤0.001, *****p* ≤0.0001, comparison not shown = ns, not significant.

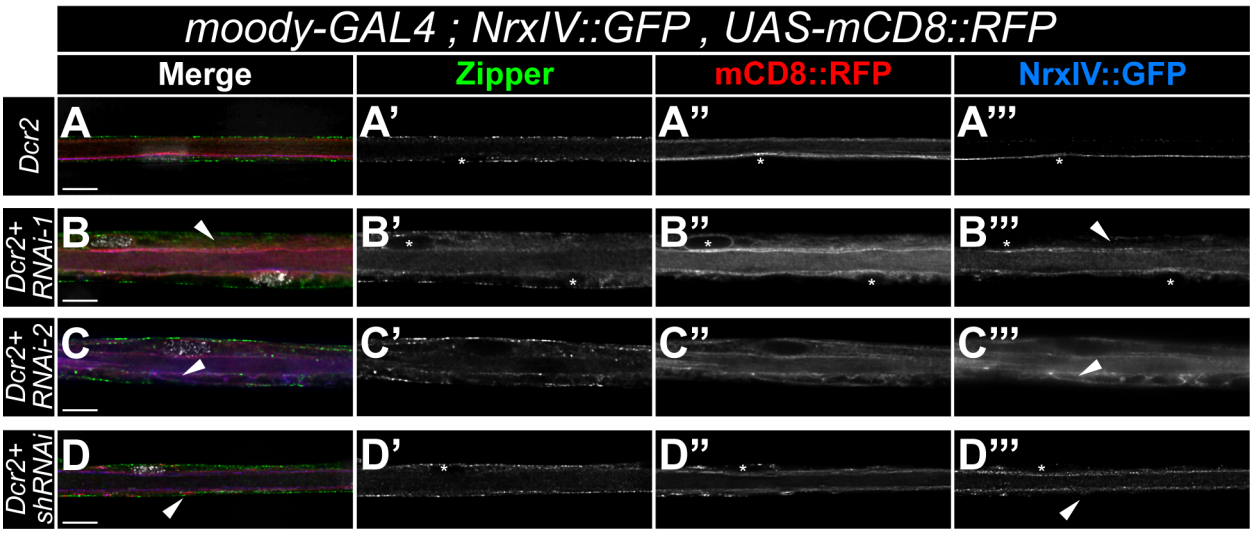

Figure 2.14: Loss of Syndecan in subperineurial glia does not affect perineurial glia ensheathment

(**A-D**) Representative longitudinal cross-section of peripheral nerves with subperineurial glial visualized using membrane-bound RFP (mCD8::RFP, red) expressed by *moody-GAL4*, immunostaining using an anti-GFP antibody to enhance the SJ marker NrxIV::GFP (blue), anti-Zipper (green) antibody to immunolabeled perineurial glia. All nuclei are marked with DAPI grey (A-D) and asterisks (A'-D', A"-D", A"'-D"'). *moody-GAL4* drove the expression of *Dcr2* (A), *Dcr2+RNAi-1* (B), *Dcr2+RNAi-2* (C), *Dcr2+shRNAi* (D). Note the dispersed pattern of NrxIV (white arrow) in the RNAi groups. Scale bar, 10 µm.

2.3.6 Syndecan is required for perineurial glial ensheathment

As outlined above, Sdc has a clear presence in the perineurial glia. To determine the role of Sdc in perineurial glia, I expressed Sdc-RNAis along with Dcr2 and a fluorescently tagged cytoskeleton marker (Lifeact::GFP) using the perineurial glial driver, *46F-GAL4*. Compared to control nerves (*46F-GAL4>Dcr2, Lifeact::GFP*) (**Fig. 2.15 A**), I detected sections of peripheral nerves with scattered rather than continuous perineurial glial ensheathment and

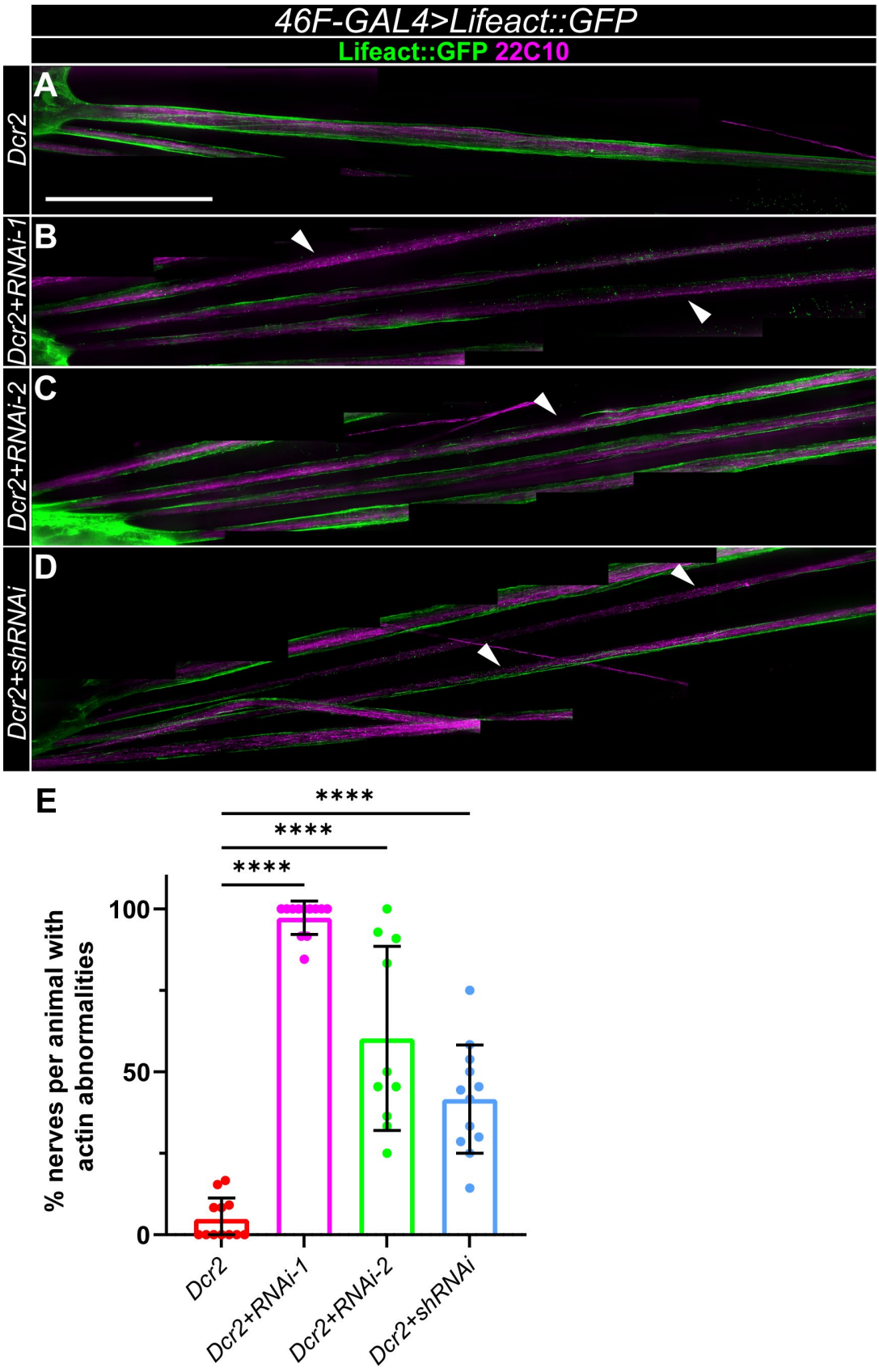
46F-GAL4>Lifeact::GFP
Lifeact::GFP 22C10
A
Dcr2
B
Dcr2+RNAi-1
C
Dcr2+RNAi-2
D
Dcr2+shRNAi
E
****
****
****
% nerves per animal with actin abnormalities
100
50
0
Dcr2
Dcr2+RNAi-1
Dcr2+RNAi-2
Dcr2+shRNAi

Figure 2.15: Perineurial glial ensheathment defects observed with Syndecan knockdown

(**A-D**) Representative stacked fluorescent image of the abdominal peripheral nerves. Using *46F-GAL4*, I ectopically expressed Lifeact::GFP (green) to label the actin-cytoskeleton network in the perineurial layer. Axons are visualized using anti-Futsch (mAb 22C10; magenta). 46F-GAL4 drove the expression of *Dcr2* (A), *Dcr2+RNAi-1* (B), *Dcr2+RNAi-2* (C), *Dcr2+shRNAi* (D). Note the segments of the peripheral nerve lacking coverage of perineurial glia (white arrow) in all RNAis knockdown groups (B-D).
(**E**) Quantification of ensheathment disruption in perineurial glia. Data showing mean ± SD, with the defect percentage is calculated by the number of nerves with the phenotype divided by the number of intact peripheral nerves. A defective nerve is defined as a segment of the nerve within the nerve extension region showing unilateral distribution, absence, or breakage of actin coverage in perineurial glia. Statistical analysis used a one-way ANOVA ($P<0.0001$) with Dunnett's multiple *post-hoc* comparison test for *Dcr2+RNAi-1* (n = 12), *Dcr2+RNAi-2* (n = 10) and *Dcr2+shRNAi* (n = 12) compared to control, *Dcr2* (n = 12) (n = number of animals analyzed pooled from two replicates). ****$p \leq 0.0001$. Scale bar, 100 μm.

segments of nerve lacking perineurial glial all together (**Fig. 2.15 B-D**, white arrow). With *RNAi-1*, 97% of the peripheral nerves had a non-uniform coverage by perineurial glia compared to 5% of nerves in control larvae (**Fig. 2.15 E**). The effectiveness of the different RNAi groups was consistent here where *RNAi-2* and *shRNAi* had more significant numbers of affected nerves compared to control but the penetrance of the phenotype was reduced.

I then wanted to determine if whether the lack of perineurial glial ensheathment in the PNS impacted animal locomotion. Surprisingly, the loss of Sdc in the perineurial glia with the stronger *RNAi-1* line did not disrupt animal locomotion (**Fig. 2.16 A-C**). Specifically, *RNAi-1* and *shRNAi* were not different from control (*46F-GAL4>Dcr2*) in all aspects. There was a notable and significant increase in both movement and speed with *RNAi-2* after the perineurial glial knockdown. All the RNAi groups survived to the adult stage further suggesting that the disruption of the perineurial glia by loss of Sdc is not deleterious.

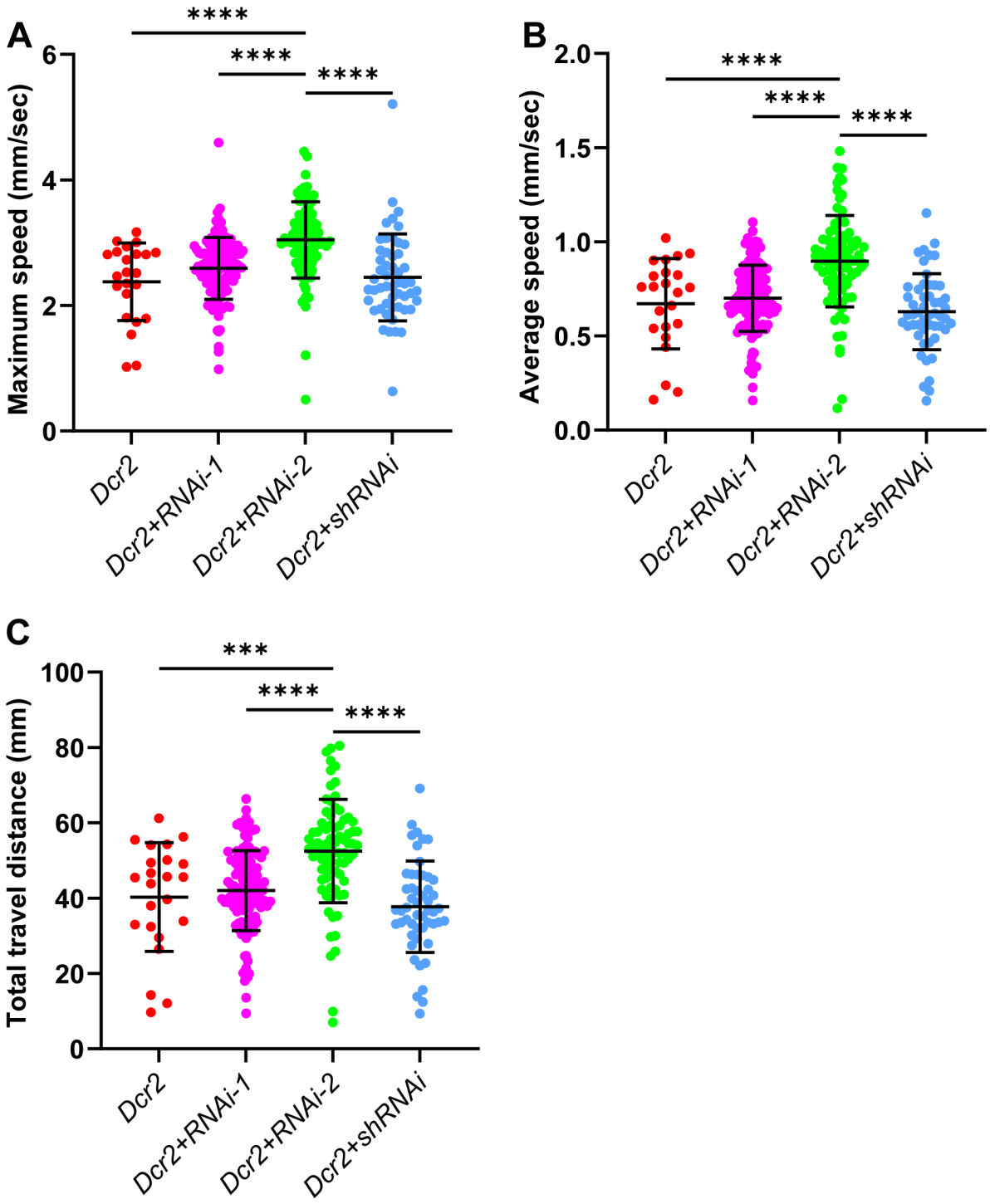
A
Maximum speed (mm/sec)
0
2
4
6
****
****
****
Dcr2
Dcr2+RNAi-1
Dcr2+RNAi-2
Dcr2+shRNAi
B
Average speed (mm/sec)
0.0
0.5
1.0
1.5
2.0
****
****
****
Dcr2
Dcr2+RNAi-1
Dcr2+RNAi-2
Dcr2+shRNAi
C
Total travel distance (mm)
0
20
40
60
80
100
***
****
****
Dcr2
Dcr2+RNAi-1
Dcr2+RNAi-2
Dcr2+shRNAi

Figure 2.16: Reducing Syndecan expression in perineurial glia did not negatively impact animal locomotion

(**A-C**) Quantification of mean maximum crawl speed (A), mean average crawling speed (B), and mean total travel distance (C) from recordings of *46F-GAL4* driving *Dcr2* (A-C; n=23), *Dcr2+RNAi-1* (A, C; n = 118, B; n=120), *Dcr2+RNAi-2* (A; n = 85, B; n=86, C; n=78), *Dcr2+shRNAi* (A-C; n = 52) (n = number of animals analyzed pooled from two replicates). Bars indicate the mean ± SD with significance calculated using a one-way ANOVA (*P<0.0001*) with Tukey's *post-hoc* multiple comparison test. ***$p \leq 0.001$, ****$p \leq 0.0001$, comparison not shown = ns, not significant.

2.3.7 Loss of Syndecan affects laminin deposition in the PNS through alteration in perineurial glial populations

In vitro, syndecan deficiency is often observed with disorganized ECM fibers (Klass et al., 2000; Yang and Friedl, 2016). With the defects in radial ensheathment by the perineurial glia, I was curious to investigate the impact loss of Sdc would have on the ECM. I primarily focused on three common ECM components that were previously identified and analyzed in the *Drosophila* neural lamella (Xie and Auld, 2011): perlecan (Trol), collagen-IV (Viking), and laminin (LanA), all endogenously tagged with GFP. Normally, the ECM appears as a continuous uniform sheath surrounding the surface of the nervous system as demonstrated by a single line of Perlecan and Collagen in nerve longitudinal sections (**Fig. 2.17 A-A', D-D'**). Perlecan and Collagen distribution within the nervous system was not different between control and Sdc knockdowns. Continuous, uninterrupted ensheathment was observed in all groups (**Fig. 2.17 A-F', A'-F'**), despite the presence of the perineurial ensheathment defect (**Fig. 2.17** white arrow). I next assayed laminin deposition using LanA::GFP in the PNS and CNS (**Fig. 2.18**). Laminin normally forms a uniform sheath around the exterior of the nervous system and is also often

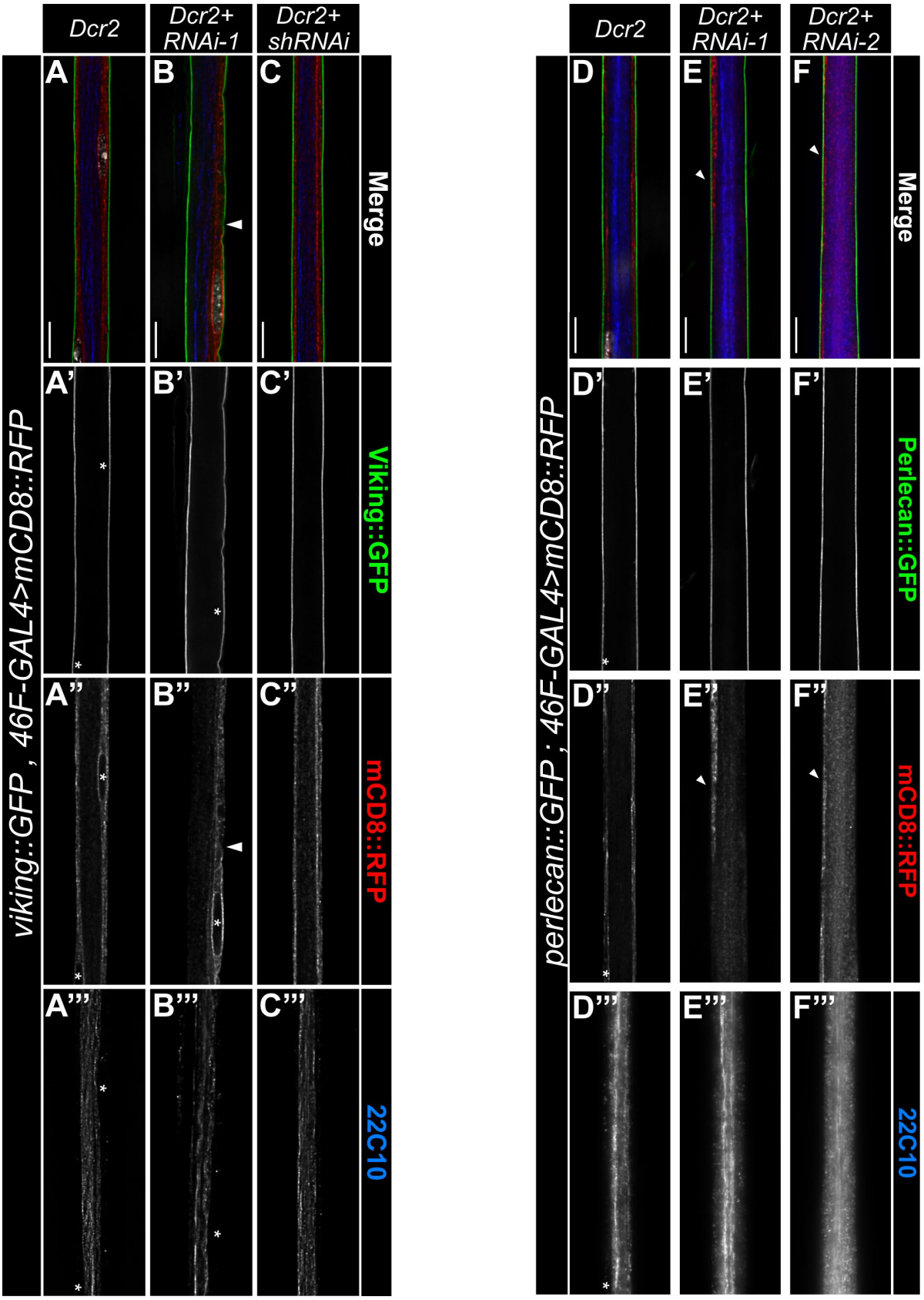
Dcr2
Dcr2+ RNAi-1
Dcr2+ shRNAi
Dcr2+ RNAi-2
viking::GFP ; 46F-GAL4>mCD8::RFP
perlecan::GFP ; 46F-GAL4>mCD8::RFP
A
B
C
D
E
F
Merge
A'
B'
C'
D'
E'
F'
Viking::GFP
Perlecan::GFP
A''
B''
C''
D''
E''
F''
mCD8::RFP
A'''
B'''
C'''
D'''
E'''
F'''
22C10

Figure 2.17: Impaired perineurial glial ensheathment did not impact Viking and Perlecan deposition in the neural lamella

(**A-F**) Representative longitudinal section of peripheral nerve. ECM proteins, Viking, a collagen subunit (green, A-C), and Perlecan (green, D-F) endogenously tagged GFP. Membrane-bound RFP (mCD8::RFP, red) under the control of *46F-GAL4* is used to visualized perineurial glia. Axons were immunolabeled with anti-Futsch (mAb 22C10; blue) and nuclei with DAPI (white (A, B, D), asterisks (A'-A"', B'-B"', D'-D"')). *46F-GAL4* drove the expression of *Dcr2* (A, D), *Dcr2+RNAi-1* (B, E), *Dcr2+RNAi-2* (F), *Dcr2+shRNAi* (C). White arrows denote perineurial glia ensheathment defects. Note the continuously Viking and Perlecan pattern in all groups. Scale bar, 10 μm.

found concentrated within the center of each peripheral nerve (**Fig. 2.18 A**). Of note with Sdc *RNAi-1*, I detected segments of the nerve that had reduced or lacked laminin distribution along the exterior of the nerve (**Fig. 2.18 D**, yellow arrow). However, with *RNAi-1* there were no changes to laminin distribution in the CNS (**Fig. 2.18 C**) and with *RNAi-2,* laminin remained unaffected in both the CNS and PNS (**Fig. 2.18 E-F**, hollow arrow). To verify our observation, I quantified the instances of laminin abnormality in the PNS and only *RNAi-1* showed a significant increase in the percentage of nerves with laminin defects compared to control (*LanA::GFP, 46F-GAL4>Dcr2, mCD8::RFP*) (**Fig. 2.19**).

The assembly of the ECM is disrupted in syndecan deficient cells with reduced levels of ECM proteins and disruption of the matrix fibrillar arrangement (Klass et al., 2000; Yang and Friedl, 2016). Perineurial glia in *Drosophila* express and secrete laminin (Petley-Ragan et al., 2016) and I hypothesized changing the distribution of the perineurial glia or the number of PG's present could result in a change in the laminin deposition along each nerve. To test whether loss of Sdc affects the number of perineurial glia, I quantified the number of perineurial nuclei on the A8 abdominal segmental nerve using NLS::GFP driven by *46F-GAL4* to label the

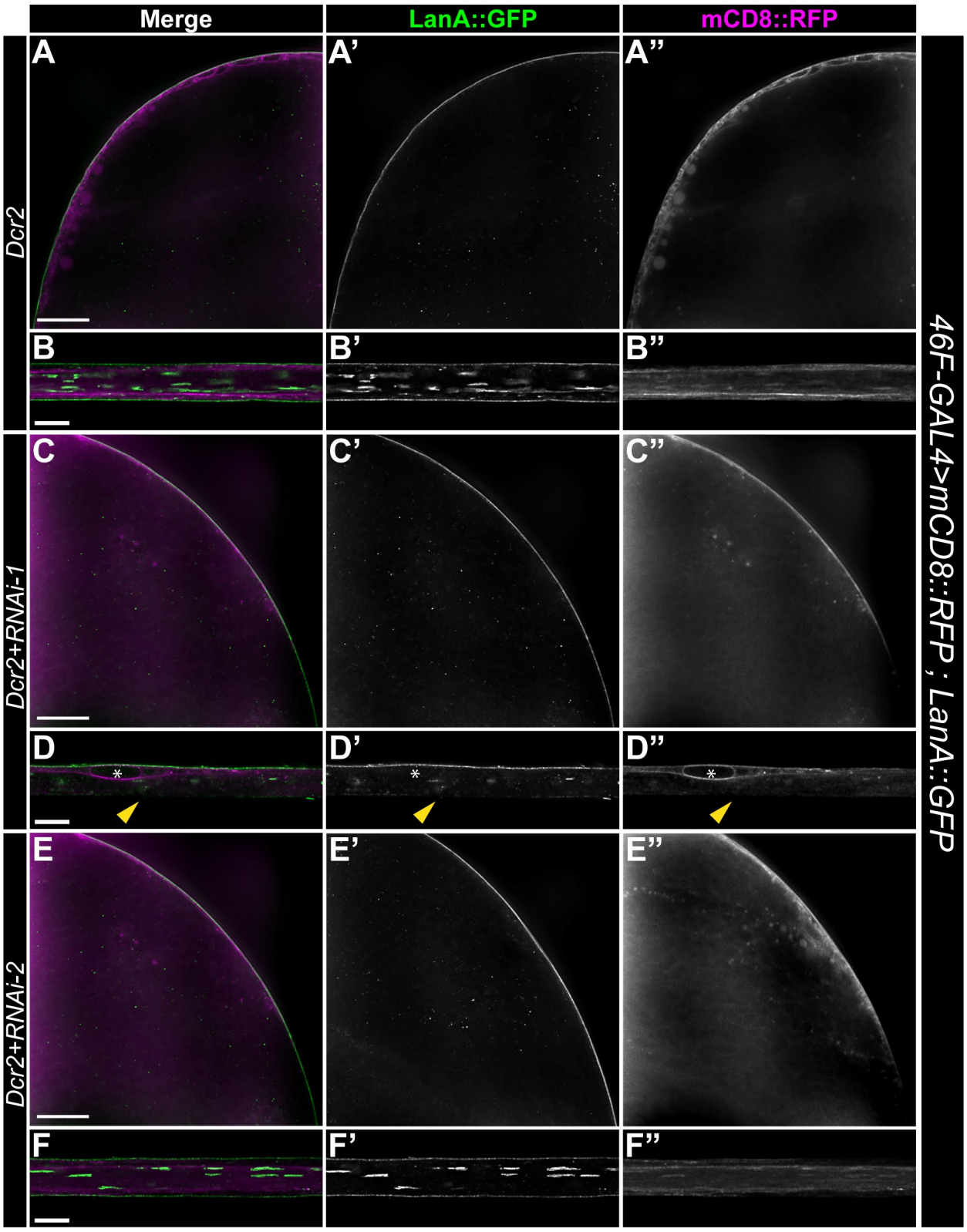
Merge
LanA::GFP
mCD8::RFP
A
A'
A''
B
B'
B''
C
C'
C''
D
D'
D''
E
E'
E''
F
F'
F''
Dcr2
Dcr2+RNAi-1
Dcr2+RNAi-2
46F-GAL4>mCD8::RFP ; LanA::GFP

Figure 2.18: Reduction in Syndecan expression in perineurial glia only disrupted laminin deposition in the PNS

(**A-F**) Representative cross-section images of larval brain lobe (A, C, E) and peripheral nerve (B, D, F). Using *46F-GAL4* perineurial glial membranes were labeled with membrane-bound RFP (mCD8::RFP, magenta). The GFP signal for LanA::GFP was enhanced using an anti-GFP antibody (green). *46F-GAL4* drove the expression of *Dcr2* (A), *Dcr2+RNAi-1* (B), *Dcr2+RNAi-2* (C). Note the non-symmetric distribution of laminin (yellow arrow) to one side of the peripheral nerve with *Dcr2+RNAi-1* (D-D") in contrast to the uniform distribution of laminin in *Dcr2+RNAi-2* (hollow arrow) and *Dcr-2*. The asterisk marks a glial nucleus. Scale bar, 20 μm (A, C, E), 10 μm (B, D, F).

nucleus. With Sdc knockdown using *RNAi-1*, I observed the perineurial glia population reduced by more than 50% compared to control (*46F-GAL4>Dcr2, nls::GFP*) (**Fig. 2.20 A-B, E**). Oddly, I found a significant increase in the perineurial glia population with *RNAi-2* (**Fig. 2.20 A, C, E**), matching our prior observations with *repo-GAL4* (**Fig. 2.7 I**). Thus, the lack of defects in laminin deposition with *RNAi-2* compared to RNAi-1 could be a function of the reduced glial presence with *RNAi-1* while *RNAi-2* has an increased number of glial cells. To further test our hypothesis, I analyzed the perineurial glia population in the CNS given that laminin deposition within the CNS is unaltered by expression of any of the Sdc RNAi lines. Using *46F-GAL4* to express GFP and label the perineurial glial cells, I found the CNS ensheathment by the perineurial glia is not disrupted of expression of either the *RNAi-1* or *RNAi-2* lines and matched control (**Fig. 2.21 A-C**). These results suggest that the changes in laminin radial deposition in PNS with respect to Sdc deficiency are due to the diminished presence of perineurial glial cells and that loss of Sdc preferentially affects the distribution of peripheral but not central perineurial glia.

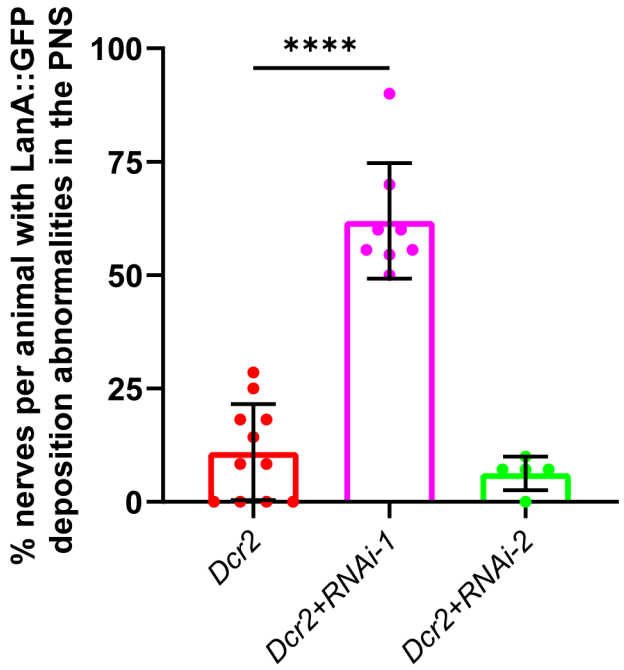

Figure 2.19: Quantification of the laminin deposition defect in the PNS

Quantification showing the mean ± SD, the defect percentage is calculated by the number of nerves with the phenotype divided by the number of intact peripheral nerves. Laminin abnormality in the PNS is defined as a segment of the nerve within the nerve extension region showing breakage or absence in the LanA distribution. A one-way ANOVA (*P<0.0001*) followed up with Dunnett's multiple *post-hoc* comparison test of *46F-GAL4* driven *Dcr2+RNAi-1* (n = 8), *Dcr2+RNAi-2* (n = 5) compared to control, *Dcr2* (n = 11) (n = number of animals analyzed pooled from two replicates). ****$p \leq 0.0001$.

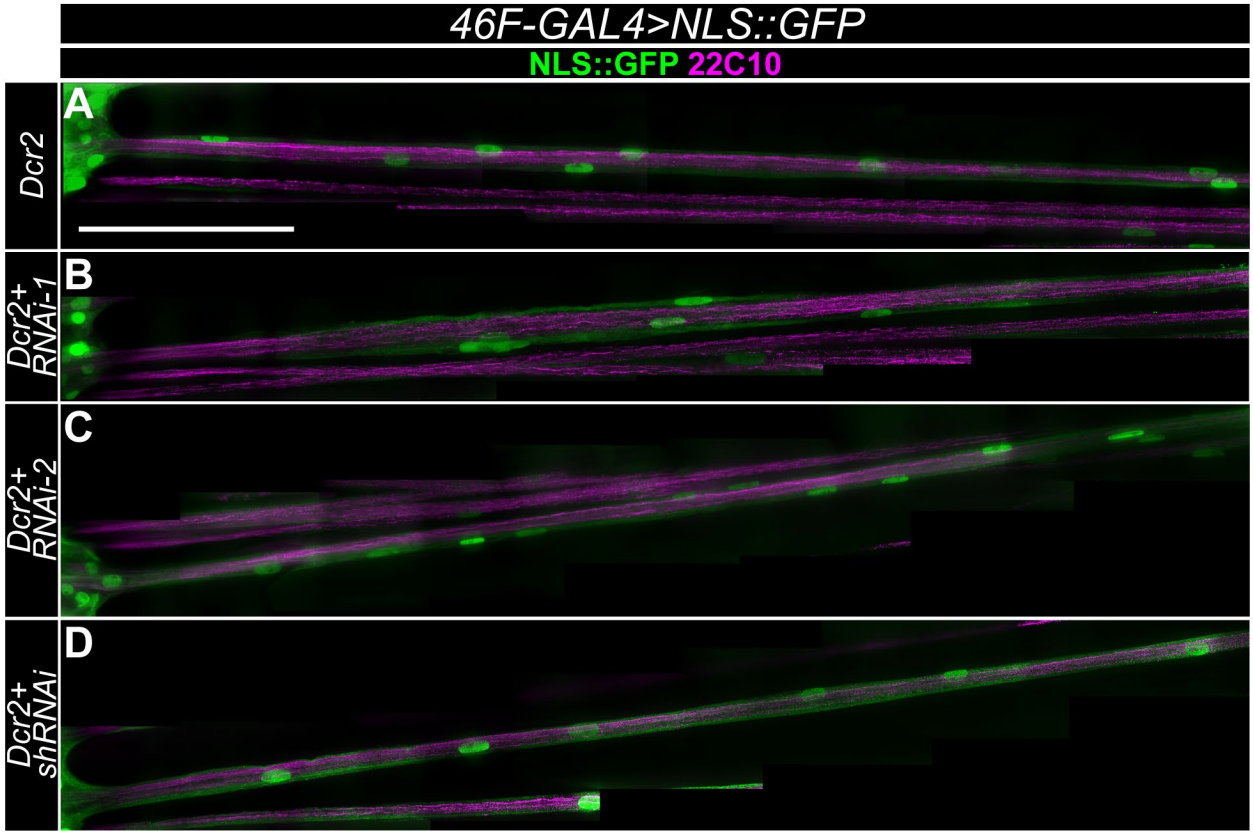
46F-GAL4>NLS::GFP
NLS::GFP 22C10
A
Dcr2
B
Dcr2+ RNAi-1
C
Dcr2+ RNAi-2
D
Dcr2+ shRNAi

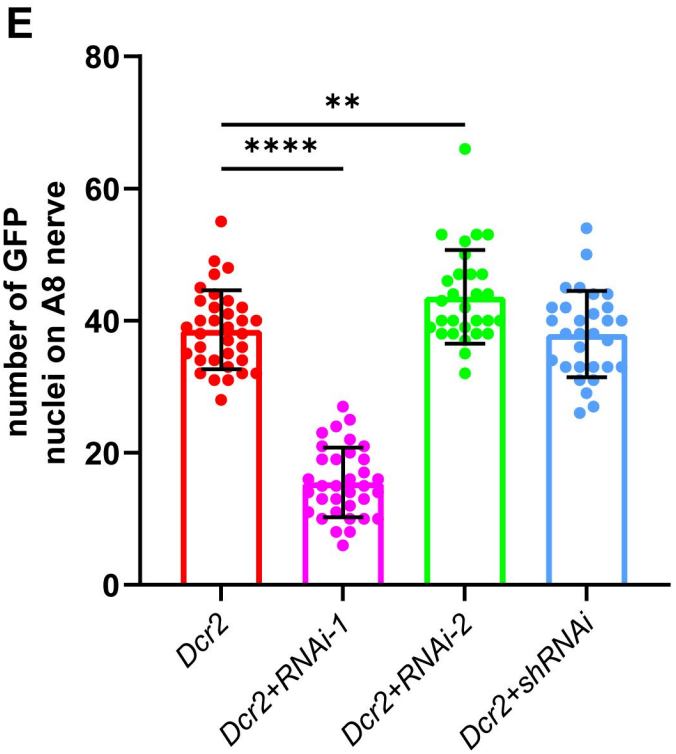
E
number of GFP nuclei on A8 nerve
80
60
40
20
0
**
****
Dcr2
Dcr2+RNAi-1
Dcr2+RNAi-2
Dcr2+shRNAi

Figure 2.20: Alteration in the PNS perineurial glial populations upon Syndecan knockdown

(**A-D**) Representative stacked fluorescent image of the A8 abdominal peripheral nerves. *46F-GAL4* drove the expression of a nuclear-localized GFP (NLS::GFP, green) to label the perineurial nuclei. Axons were immunolabeled using anti-Futsch (mAb 22C10, magenta) to trace the nerve. Each of *Dcr2* (control, A), *Dcr2+RNAi-1* (B), *Dcr2+RNAi-2* (C) and *Dcr2+shRNAi* (D) are co-expressed with NLS::GFP under the control of *46F-GAL4*. Of interest to note, the relative increase in perineurial nuclei in *Dcr2+RNAi-2* (C), and the non-uniform distribution of perineurial nuclei in *Dcr2+RNAi-1* (B). I did not observe perineurial nuclei fragmentation. Scale bar, 100 μm.
(**E**) Quantification of GFP+ nuclei count. Bars indicate the mean ± SD, with the mean nuclei count analyzed using a one-way ANOVA (*P<0.0001*) with Dunnett's multiple *post-hoc* comparison test. *Dcr2+RNAi-1* (n = 34), *Dcr2+RNAi-2* (n = 29) and *Dcr2+shRNAi* (n = 30) compared to control, *Dcr2* (n = 34) (n = number of intact A8 nerve analyzed pooled from three replicates, each animal contains a pair of A8 nerves). ***p* ≤0.01, *****p* ≤0.0001.

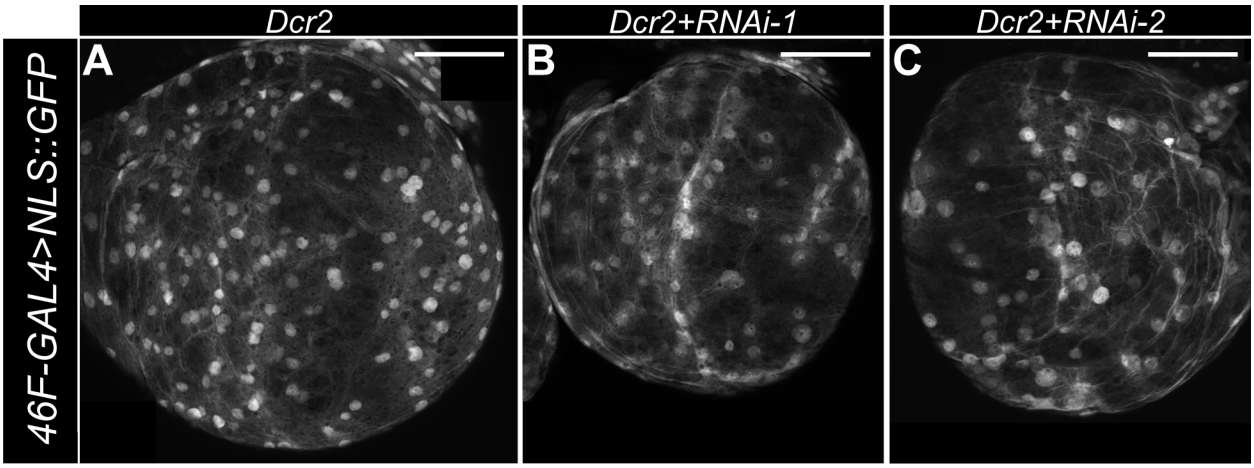

Figure 2.21: Syndecan knockdown in perineurial glia did not affect CNS ensheathment

(**A-C**) Representative stacked image of 3rd instar larval brain lobe, in which perineurial glia express nuclear-localized GFP (NLS::GFP) to label perineurial nucleus under the control of *46F-GAL4*. The perineurial glia coverage is visualized by the cytosolic portion of the NLS::GFP. *Dcr2* (A; n = 16), *Dcr2+RNAi-1* (B; n = 15), *Dcr2+RNAi-2* (C; n = 16) (n = number of brain lobes analyzed pooled from two replicate). Scale bar, 50 μm.

2.4 Discussion

Syndecan, a transmembrane heparan-sulfate proteoglycan, has long been postulated as a key player in intercellular communication since its identification, yet its *in vivo* impact in nervous system function remains largely untested. In this thesis, I have delineated two aspects of Sdc function in neural development: Sdc regulates neuroblast proliferation in a cell non-autonomous manner; Sdc regulates the ensheathment processes of multiple glial types. Overall, this thesis suggests Sdc acts as a fundamental regulator of key cellular processes in *Drosophila* glia. This highlights the nature of Sdc's function, in which Sdc functions to sequester trophic factors, thereby increasing the local concentration of ligands, and interact with ECM proteins directly to promote cell adhesion and motility.

2.4.1 Syndecan as a non-cell autonomous regulator of neuroblast niche

The diminished neurogenesis observed in pan glial Sdc knockdown may have several causes. From our observations in the optic lobe of cell death and mitosis, one possibility could be that Sdc functions in the cortex glia or the subperineurial glia that are associated with the neuroepithelium. A sub-population of cortex glia are in direct contact with the neuroblasts, transition zone, and neuroepithelium of the optic lobe (Morante et al., 2013). These cortex glia are capable of regulating the proneural wave progression that pushes the neuroepithelium to neuroblast transition (Morante et al., 2013). Disruption of Sdc in the cortex glia may interfere with components of this transition zone resulting in the incomplete expansion of the neuroepithelium and the subsequent reduction in the outer proliferation zone neuroblast population. Another possibility arising from the absence of glial Sdc may be due to direct glial communication that impacts the neuroepithelium expansion directly. A third alternative for the diminishing outer proliferation zone neuroblast population is due to the glia ensheathing the outer proliferation zone influencing both direct and indirect processes (Morante et al., 2013; Pérez-Gómez et al., 2013). The subperineurial glia can also make direct contact with the neuroepithelium and control the neuroepithelium through Notch signaling (Pérez-Gómez et al., 2013). The loss of Notch ligand in glia affects the spatial activation of the proneural wave, triggering a premature activation of EGFR-Ras-PntP1 signaling, which pushes the neuroepithelium to a neuroblast fate (Wang et al., 2011). Interestingly, mammalian syndecan-3 cooperates with Notch signaling to regulate adult myogenesis through interaction with Notch ligands (Pisconti et al., 2010). This suggests a potential role for Sdc with Notch ligands to regulate the spatial boundary of the proneural wave in the *Drosophila* brain lobe.

However, it is unlikely that the subperineurial glia are solely responsible for the effects observed with the loss of Sdc. I did not observe a noticeable decrease in brain lobe width by downregulating Sdc in the subperineurial glia, though more quantification is needed. The cortex glia are not only intimately associated with the neuroblast population in the brain lobe (Morante et al., 2013), but also are known to regulate the neuroepithelium through a range of trophic factors. Specifically, the optic lobe-associated cortex glia can serve as a direct source of the EGFR ligand, Spitz, which triggers the neuroblast transition in the neuroepithelium (Morante et al., 2013). Additionally, the autocrine signalling of Spitz in the optic lobe-associated cortex glia regulates its cell size and subsequent Spitz secretion. Heparan-sulfate proteoglycans, such as syndecan, are necessary components in the activation of EGF-signaling cascades in multiple tissues, including myelomas and keratinocytes (Mahtouk et al., 2006; Wang et al., 2015). Thus, another potential role for Sdc in the *Drosophila* brain lobe could be in the modulation of EGFR signaling that tunes optic lobe-associated cortex glia cell growth with downstream effects on the neuroepithelium. Cortex glia also respond to other growth factors that promote its growth and proliferation, including FGF, IGF, and PDGF. In turn, this links growth factor pathways indirectly to neuroblast proliferation (Avet-Rochex et al., 2012, 2014; Read, 2018). The bioavailability and signaling of growth factors are tightly regulated through the binding of heparan sulfate proteoglycans at the cell surface (Rogers and Schier, 2011). Syndecan is capable of regulating the availability and ligand-receptor interaction of various growth factors by acting as a ligand docking site at the cell surface (Kwon et al., 2012). For example, the binding of FGF-2 to syndecan's HS-GAG chains leads to a high local concentration of FGF-2 close to the cell surface and contributes to the assembly of the ligand-receptor complex (Afratis et al., 2017). A similar relationship has been identified between VEGF and syndecan-2 with VEGF binding to

syndecan via its heparin-binding domain, enhancing the activity of VEGFR (Corti et al., 2019). Comparably, the binding of PBGF-BB and EGF to syndecan has also been shown to enhance the activity of the downstream signaling complex (Chen et al., 2004; Das et al., 2016; Mochizuki et al., 2020).

Loss of Sdc in the cortex and/or subperineurial glia could also lead to changes in neuroblast population size due to changes in nutrient delivery. In *Drosophila*, the regulation of nutrition intake is directly linked to neuroblast population expansion where CNS insulin-like peptide-2/6 (dilp-2/6) surge can lead to reactivation of type 1 and type 2 neuroblasts in the larval CNS (Chell and Brand, 2010; Yuan et al., 2020). Subperineurial glia are able to convert fat-body derived mitogen peptides and signal to the neuroblasts using Dilp-2/6 (Chell and Brand, 2010; Spéder and Brand, 2014). Along the same lines, cortex glia express Dilp-6 to regulate neuro-proliferation, however, it also requires Dilps to form extensive networks of contact with neuroblasts and establish a stem cell niche (Read, 2018; Harrison et al., 2021). Sdc has been shown to directly affect IGF signaling by altering Dilp availability in the body as a *Sdc* hypomorphic mutation shows a lower expression of Dilp-2 in the brain (De Luca et al., 2010). Though it is unclear how Sdc affects Dilp levels, vertebrate syndecan has been implicated in IGF signaling by mediating crosstalk between insulin-like growth factor-1 receptors and integrin complexes in human umbilical vein endothelial cells (HUVEC) and MDA-MB-231 cells to direct cell migration and invasion (Beauvais and Rapraeger, 2010; Rapraeger et al., 2013).

Syndecan family members in vertebrates are necessary for enhancing or transducing growth factor complex signaling cascades, including EGF, FGF, PDGF, IGF (Baron et al., 2002; Wu et al., 2003; Das et al., 2016). Thus, Sdc has a conserved role and could be central to growth factor signaling that likely drives the expansion of the cortex glial population. Thus, Sdc could

indirectly influence neuroblast population size in the brain lobe or conversely changes to glial Sdc could directly affect the disruption of growth factors available for neuroblast population maintenance and expansion.

2.4.2 Syndecan controls glial ensheathment in the PNS

I also described a role for Sdc to regulate in a cell-autonomous manner, glial ensheathment of the CNS and the PNS. Our experiments showed lack of Sdc is contributes to ensheathment defects in perineurial and wrapping glia in the PNS and to changes in the perineurial glia in the VNC. The process of glial ensheathment relies on active communication with the extracellular environment, therefore I purpose Sdc acts as an important component in the ensheathment process. In the context of perineurial glia, Sdc is highly expressed and localized to glial-ECM boundaries suggesting a role for Sdc as a mediator of cell-ECM interaction. In the CNS, the extension of the VNC length in the absence of Sdc matches observed phenotypes seen with loss of integrins and degradation of the ECM (Meyer et al., 2014; Skeath et al., 2017). In the PNS, I observed the ensheathment of the perineurial glia was disrupted in that each perineurial glia was limited to one side of the nerve or absent. These results were similar to those observed with both the loss of integrin complex components (the β-subunit of integrin and Talin) or after degradation of the ECM (Xie and Auld, 2011). Syndecan has been demonstrated to provide a mechanical linkage from the ECM to the cytoskeleton through binding to laminin via the HS-GAG chains and the actin-network through Ezrin or α-actinin (Granes et al., 2000; Yamashita et al., 2004; Carulli et al., 2012; Okina et al., 2012). Syndecan can also act synergistically with integrin to regulate ECM adhesion, focal adhesion assembly, and cytoskeletal re-arrangement (Saoncella et al., 1999; Morgan et al., 2007; Okina et al., 2012; Fiore

et al., 2014). Syndecan-4 has been identified as a cellular tension sensor whereby application of external tension on syndecan-4 drives integrin-based focal adhesion growth (Chronopoulos et al., 2020). I postulate a model in which the absence of Sdc prevents perineurial glia from interacting or binding effectively with the overlying ECM, thus resulting in the incomplete and defective ensheathment of the perineurial glia.

I do not think the polypeptide chains of Sdc and integrin function directly with each other. Using super-resolution imaging, I observed that Sdc does not co-localize with integrin in the peripheral nerves of *Drosophila*. Rather, Sdc puncta and integrin expression were often mutually exclusive. This is in contrast to reports of syndecan-4 and integrin, having direct interactions via the syndecan ectodomain and cytosolic domain (Wang et al., 2010). The spatial organization of syndecan and integrin could reflect a model of syndecan recruitment postulated by Roper et al., (2012). In this model Syndecan is present at the initial stages of integrin focal adhesion complex formation and subsequently syndecan is repelled from the focal adhesion as the focal adhesion matures. Alternatively, the long GAG chains on syndecan could influence integrin complex association with the ECM even if the protein cores do not interact (Roper et al., 2012; Stepp et al., 2015). Specifically, syndecan through its HS-GAG chains are known to interact with laminin and fibronectin in the ECM and bind directly to sequester or quench ECM components (Hoffman et al., 1998; Woods et al., 2000).

Uniquely, I saw breakages in laminin deposition upon knockdown of Sdc in the perineurial glia of the PNS. Perineurial glia secrete and can potentially be deposit laminin into the surrounding neural lamella (Petley-Ragan et al., 2016). In other cell types, syndecan knockdown doesn't impact laminin production and secretion, but rather disrupts the extracellular assembly and the arrangement of the ECM architecture for the ECM-protein producing cells

(Klass et al., 2000; Yang and Friedl, 2016). This suggests that the absence of Sdc either disrupts the perineurial glia migration into the periphery and thus the deposition of laminin, or that the loss of assembly and arrangement of laminin the ECM in the absence of Sdc changes migration of the perineurial glia and ensheathe the nerve. Our observations of the undisrupted laminin deposition in the brain lobes and the perineurial glial migration across the brain lobe suggest that laminin deposition is intimately linked to the perineurial glial cell expansion.

2.4.3 Summary

In conclusion, I have characterized two potential glial functions for Sdc *in vivo* during *Drosophila* neural development. Knockdown of Sdc reduces neuroblast proliferation within the optic lobe causing a severe reduction in brain lobe size. This phenotype is likely a result of misregulated neuroepithelial expansion and maintenance, through defective signaling within the cortex glia and the subperineurial glia associated with the optic lobe. I also found that loss of Sdc is associated with a disrupted distribution of perineurial glial processes along the length of the nerve, in combination with changes in the deposition of laminin. Our findings provide the first evidence for Sdc function in PNS glia, along with its potential implication in neural stem cell maintenance and emphasizes the advantages of using of *Drosophila* as a platform to study Sdc *in vivo* function, as there are no functional redundancy challenges to investigating as there are with vertebrates.

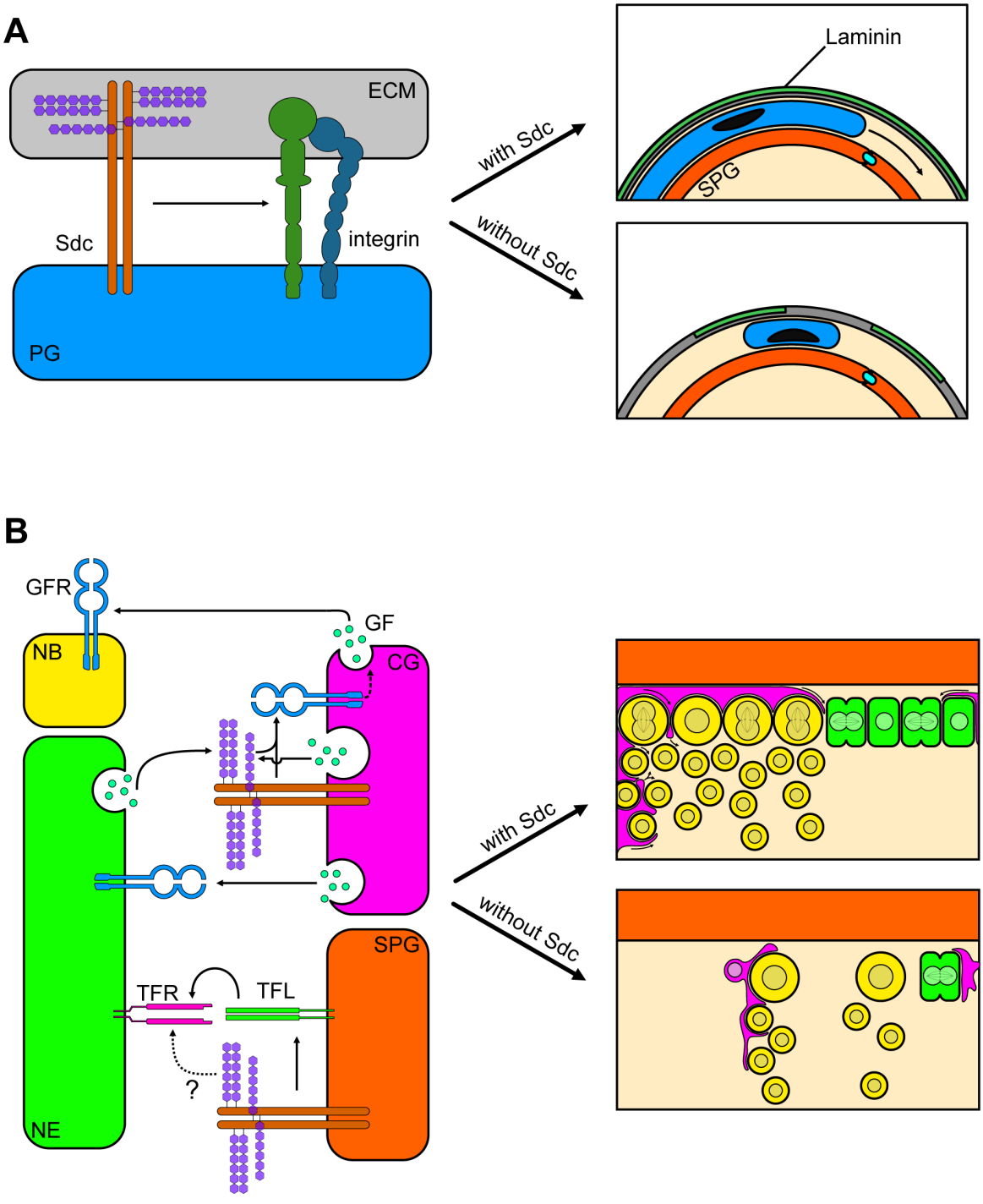
A
ECM
Sdc
integrin
PG
with Sdc
without Sdc
Laminin
SPG
B
GFR
GF
NB
CG
SPG
TFR
TFL
?
NE
with Sdc
without Sdc

Figure 2.22: Model of Syndecan function within the perineurial glia and the optic lobe

(**A**) Sdc and integrin are co-expressed by perineurial glia and interacting with the overlying ECM to mediate radial ensheathment of the peripheral nerve. Without Sdc, integrin cannot effectively adhere to the ECM protein, which causes perineurial glia unable to ensheathe the peripheral nerve. Thus, affecting laminin deposition within the PNS.
(**B**) Sdc expressed by cortex glia (CG) or subperineurial glia (SPG) is cooperating with various growth factors (GF) and growth factor receptors (GFR) in a cis- or trans-configuration to regulate neuroblast (NB) proliferation within the optic lobe. Sdc is interacting with trophic factors ligand (TFL) on the subperineurial membrane to activate trophic factor receptors (TFR), expressed by the neuroepithelium (NE). In parallel, Sdc expressed by the cortex glia acts to enhance proliferation of the cortex glia, tuning the secretion of cortex glia-derived growth factor signaling peptide that controls the neuroepithelium-to-neuroblast transition, as well as maintaining the niche established by cortex glia. Without Sdc, the growth factor signaling network is disrupted leading to defective neuroblast transition and reduced of neuroblast population.

2.5 Materials and Methods

2.5.1 Fly strains and genetics

Standard *Drosophila* husbandry techniques and genetic methodologies were used to obtain files of the required genotypes for each experiment from the original transgenes. For the original fly strains used in this study see **Table 1**. All crosses were carried out 25°C with Dcr-2 in the background unless indicated otherwise.

2.5.2 Larvae dissection and immunofluorescence

Third instar larvae were filleted and dissected in PBS on Sylgard plates. The protocol for fixation of larvae was in 4% paraformaldehyde with 1X PBS for 20 minutes. For integrin immunolabelling, larvae were fixed for only 10 minutes. Fixed fillets were washed two times in

1X PBS for 5 minutes each then washed three times in PBST (1X PBS, 0.1% Triton X-100) for 10 minutes each at room temperature. For immunofluorescence, samples were first transferred into blocking solution (4% heat-inactivated goat serum, 0.1% PBST) at 4°C overnight. All antibodies were diluted in blocking solution. For primary antibody incubation, samples were placed on an orbit shaker at 4°C overnight. Larvae fillets were then washed three times with PBST for 10 mins each and incubated with secondary antibody solution for two hours at room temperature. Lastly, samples were washed with PBST three times for 10 minutes each. Samples were equilibrated via glycerol series up to 90% glycerol and mounted with Vectashield antifade mounting medium (Vector Laboratories, Burlington, Canada). DAPI (1:1000 of 1 ug/mL) (Thermo Scientific) was added along with the secondary antibodies.

2.5.3 Imaging and Image processing

Fluorescent images of the peripheral nerves were taken with a DeltaVision microscope (Applied Precision, Mississauga, Canada) using a PlanApoN 60X oil immersion objective (NA=1.42) at 0.2 μm steps in the z-direction. Individual channels were deconvolved separately and merged back together with SoftWorx image processing software (SoftWorx, Toronto, Canada). Deconvolution is performed using a point spread function measured with a 0.2 μm fluorescent bead (Invitrogen, Toronto, Canada) in Vectashield Mounting Medium. The number of deconvolution iterations was set to terminate once the normalized error criterion for the constrained iterative algorithm begins to plateau. Orthogonal sections were generated using SoftWorx. Images of peripheral nerves were stitched using the Pairwise Stitching plugin (Preibisch et al., 2009) in Fiji (Schindelin et al., 2012). Images were further processed and compiled using Adobe Photoshop and Adobe Illustrator (Adobe Creative Cloud).

To measure the ventral nerve cord to body length ratio, ventral nerve cords were imaged using a DeltaVision microscope (Applied Precision, Mississauga, Canada) with a Plan 20X air objective (NA=0.4) at 1 µm steps in the z-direction. Body length was captured using an Axioplan-2 microscope (Carl Zeiss Canada, Toronto, Canada) with a Zeiss A-Plan 2.5X objective (NA=0.06) air objective. Images of VNC and larval body were stitched using the Pairwise Stitching plugin (Preibisch et al., 2009) in Fiji. Images were further processed and compiled using Adobe Photoshop and Adobe Illustrator (Adobe Creative Cloud).

Fluorescent images of brain lobes were acquired with an Olympus FV1000 Laser Scanning Confocal Microscope (Bioimaging Facility, UBC, Vancouver, Canada) using a UPLSAPO 30X silicone oil immersion objective (NA=1.05) at 0.73 µm steps. Digital zoom was optimized to ensure Nyquist sampling. Image stitching was achieved via the Pairwise Stitching plug-in (Preibisch et al., 2009) in Fiji (Schindelin et al., 2012). Images were further processed and compiled using, Adobe Photoshop and Adobe Illustrator (Adobe Creative Cloud).

Super-resolution images were acquired with a Zeiss LSM800 Confocal with Airyscan (Carl Zeiss Canada, Toronto, Canada) using a Plan-APOCHROMAT 63X oil immersion objective (NA = 1.4) at 3.5X digital zoom. Z-step collection and frame size was set to ensure Nyquist sampling. Laser intensity and master gain of each channel were optimized to ensure intensity spans 1/3 - 2/3 of the displayed histogram. Scan speed was set to 4 –7 µs/pixel. Raw images were further processed using ZEN 3.1 (blue edition, Carl Zeiss Canada, Toronto, Canada) and compiled using Adobe Photoshop and Adobe Illustrator (Adobe Creative Cloud).

2.5.4 Larval tracking

For each larval tracking session, multiple 3rd instar larvae were added to a fresh 2% agar plate. Food-safe dye was added to enhance contrast. Larval movements were recorded continuously for 60 seconds using a Canon VIXIA HF R800 video camera (Canon). The recorded movies were analyzed using Fiji plug-in wrmTrck (Nussbaum-Krammer et al., 2015; Brooks et al., 2016) to calculate speed and travel distance.

2.5.5 Larval survival assay

A set number of third instar larvae of the desired genotype were placed into fresh food vials. The number of pupae within each vial was counted after larvae ceased wandering. Each vial was then observed daily for two weeks after the first adult enclose. The newly enclosed adults were then separated by sex and observed for two more days. Adults that died within this 48-hour window were considered to be adult lethal.

2.5.6 Statistical analyses

All statistical analyses were conducted using GraphPad Prism 9 (GraphPad Software, La Jolla, CA). For larval locomotion assay (scatter plots) the difference in means between groups was analyzed using an ordinary parametric one-way ANOVA and Tukey *post hoc* test for multiple comparisons. For phenotype prevalence and VNC/body length ratio (bar plots), the difference in means of control and experimental larvae were analyzed using an ordinary parametric one-way ANOVA with Dunnett's *post-hoc* multiple comparison test. All graphs show mean and standard deviation (SD).

Table 2.1: Origins of the transgene and antibodies used in this study

Transgenes	Source or reference	Additional information
Sdc-RNAi-1 (GD13322)	RRID: VDRC_13322 (Dietzl et al., 2007)	
Sdc-RNAi-2 (KK107320)	RRID: VDRC_107320 (Dietzl et al., 2007)	
Sdc-shRNAi (HMC03265)	RRID: BDSC_51723	
w^{1118}	RRID: BDSC_3605	
repo-GAL4	RRID: BDSC_7415 (Sepp et al., 2001)	
46F-GAL4	(Xie and Auld, 2011)	
moody-GAL4	RRID: BDSC_90883 (Schwabe et al., 2005)	
nrv2-GAL4	RRID: BDSC_6799 (Sun et al., 1998)	
UAS-mCD8::RFP	RRID: BDSC_27398 Gifted by Dr. Elizabeth Davis	
UAS-mCD8::GFP	RRID: BDSC_5130 (Lee and Luo, 1999)	
UAS-Lifeact::GFP	RRID: BDSC_35544 (Riedl et al., 2008)	
UAS-NLS::GFP	RRID: BDSC_4775 Gifted by Dr. Douglas W. Allan	
UAS-Dcr-2	RRID: BDSC_57326 (Dietzl et al., 2007)	
LanA::GFP	RRID: VDRC_318155 (Sarov et al., 2016)	
vkg::GFP	RRID: VDSC_318167	

	(Sarov et al., 2016)
trol::GFP (*perlecan::GFP*)	RRID: DGRC_110807 (Morin et al., 2001)
NrxIV::GFP	RRID: BDSC_50798 (Sepp et al., 2001)
Sdc::GFP.PTT	(Buszczak et al., 2007)
Sdc::GFP.MI	RRID: BDSC_66373 (Nagarkar-Jaiswal et al., 2015)

Antibodies		**Dilution**
Mouse anti-αPS2	RRID: AB_528304 DSHB, Iowa City, IA	1:5
Mouse anti-βPS	RRID: AB_528310 DSHB, Iowa City, IA	1:10
Mouse anti-Futsch	RRID: AB_528403 DSHB, Iowa City, IA	1:2000
Rabbit anti-αPS3	Provided by Dr. Shigeo Hayashi (Wada et al., 2007)	1:100
Rabbit anti-cDCP-1	RRID: AB_2721060 Cell Signaling Technology, Danvers, MA	1:300
Rabbit anti-phosphohistone (H3-Ser10)	RRID: AB_880448 Abcam, Toronto, Canada	1:1000
Rabbit anti-zipper	Provided by Dr. Ken Prehoda (Liu et al., 2008)	1:2000
Rabbit anti-GFP	RRID: AB_221569 Invitrogen, Toronto, Canada	1:500
Chicken anti-GFP	RRID: AB_300798 Abcam, Toronto, Canada	1:1000
Rat anti-deadpan	RRID: AB_2687586	10 ug/mL

	Abcam, Toronto, Canada	
Goat anti-chick Alexa 488	RRID: AB_2534096 Invitrogen, Toronto, Canada	1:300
Goat anti-rabbit Alexa 488	RRID: AB_143165 Invitrogen, Toronto, Canada	1:300
Goat anti-rabbit Alexa 568	RRID: AB_2535730 Invitrogen, Toronto, Canada	1:300
Goat anti-rabbit Alexa 647	RRID: AB_2535812 Invitrogen, Toronto, Canada	1:300
Goat anti-mouse Alexa 488	RRID: AB_2534069 Invitrogen, Toronto, Canada	1:300
Goat anti-mouse Alexa 568	RRID: AB_2534072 Invitrogen, Toronto, Canada	1:300
Goat anti-mouse Alexa 647	RRID: AB_2535804 Invitrogen, Toronto, Canada	1:300
Goat anti-rat Alexa 488	RRID: AB_2534074 Invitrogen, Toronto, Canada	1:300

Chapter 3: Discussion

Active investigations into syndecan's structure, distribution, and function in cells and tissue have taken place since its first identification. Due to its ability to interact with a diverse range of ligands, syndecan has been implicated in many diseases and pathologies, with most focusing on cancer progression given syndecan's prominent role in regulating cell adhesion and motility (Beauvais and Rapraeger, 2004). Prior literature has highlighted syndecan's synergistic interactions with the integrin adhesion complex, as loss of syndecan reduces focal adhesion formation (Couchman, 2003). Additionally, syndecan is required for the activation of various growth factor signaling cascades, in particular by facilitating the assembly of growth factor-receptor complexes (Afratis et al., 2017). Syndecan is strongly expressed in both vertebrate and invertebrate nervous systems. However, the *in vivo* function of syndecan as a critical signaling relay in neural development has only scratched the surface, especially with regards to glia. Our primary goal for this thesis was to explore and characterize in-depth the requirement of Sdc in glial and its potential role in neural development by using *Drosophila melanogaster* as our model.

In Chapter 2 of this thesis, I identified novel aspects of Sdc modulation in the nervous system development *in vivo*. First of all, Sdc expressed by glia acts as a cell non-autonomous regulator of neuroblast niche within the optic lobe. Neuroblast population is negatively impacted when Sdc expression is reduced, this suggests glial Sdc promotes neuroblast expansion or maintenance within the optic lobe. Secondly, I showed that glial expression of Sdc in the peripheral nervous system is necessary for the radial ensheathment of axons and of the nerves as abnormalities were seen when Sdc is suppressed in all peripheral glia. I showed that Sdc is necessary for wrapping glia ensheathment, and without Sdc wrapping glia are unable to extend

their membranes to encapsulate nearby axons. Additionally, loss of Sdc leads to subperineurial glia abnormalities, including enlargement of the subperineurial membranes and diffusion of septate junction components. I characterized the whole nerve ensheathment defect of Sdc reduction in perineurial glia in the PNS and saw alterations in laminin deposition within the peripheral neural lamella correlated with the decrease population of perineurial glial cells in the PNS (but not the CNS). All together, these results led me to propose the following model: Sdc is present at PG cell membranes to bind and concentrate ECM proteins, such as laminin. This facilitates integrin's ability to efficiently bind the ECM ligands and promotes the radial ensheathment of perineurial glia. These findings demonstrated that Sdc is a necessary modulator of neural development and cell-ECM interaction *in vivo*.

3.1 Syndecan in glial and neural development

Chapter 2 of this thesis investigates the role of Sdc in the CNS and PNS of *Drosophila* glial development. The following section will address some of the unanswered questions and caveats that stemmed from our analysis.

3.1.1 Differential effects of RNAi reduction in Syndecan expression

One of the main questions raised from this study was the difference in phenotype penetrance associated with the three different Sdc-RNAi lines. The analysis of the CNS phenotypes suggested that *RNAi-1* was the strongest with *RNAi-2* intermediate and *shRNAi* the weakest. However, within the peripheral glia, instead of the expected linear decrease in severity and penetrance of the phenotypes from the three RNAis, I observed distinct effects between the different RNAi lines within the different glial layers, including perineurial glia and wrapping

glia. These distinct phenotypes generated by each RNAi line remains to be addressed. One potential cause of the differential effect I observed could be due to inconsistent RNAi knockdown efficacy of the *Sdc* messenger RNA (mRNA) levels, resulting in low penetrance of the phenotype. Alternatively, the expression of *RNAi-2* may provoke a compensatory mechanism within the cell, leading to an increase in the perineurial glia population in the PNS. To extend our RNAi results, I purpose using *Sdc* null mutations to determine if the phenotype associated with the RNAis are comparable to the loss of function *Sdc* mutants. Prior investigation into Sdc's *in vivo* function has characterized *Sdc* null mutants (**Fig. 3.1**). The *Sdc* mutant Sdc^{97}, Sdc^{23}, and *Df(2R)48*,*ubi-sara* (Johnson et al., 2004; Steigemann et al., 2004) were generated using imprecise P-element extension near the 5' of the gene which resulted in the complete absence of Sdc expression and matched the phenotypes generated by global expression of RNAi (Knox et al., 2011), but not specifically investigated in glia. I predict the *Sdc* null will reproduce the phenotypes I observed with *RNAi-1,* including the more severe penetrance and phenotype. The mutant analysis would allow me to confirm the RNAi phenotype I observed. Additionally, the use of genetic mutants will also test for potential off-target effects associated with RNAi.

Once confirmed, I can further capitalize on the *Sdc* mutants to map the key domains of the Sdc protein. For instance, the HS-GAG chain on the ectodomain is key to Sdc function (Xian et al., 2010), and I can test the function of these HS chains by ectopically express Sdc lacking the GAG chain attachments on the protein core (Chanana et al., 2009) to see if this transgene can rescue the *Sdc* null mutants. If the HS chains are critical for Sdc function, the construct lacking these HS-attachment sites should fail to rescue. Along the same lines, I can test the contribution of Sdc intracellular signaling by reintroducing a version of Sdc protein without the transmembrane or cytoplasmic tail in the *Sdc* mutant using the full transcript as the positive

control (Chanana et al., 2009). This would allow me to shed light on the protein domain that plays a role in Sdc-mediated function in neural and glial development.

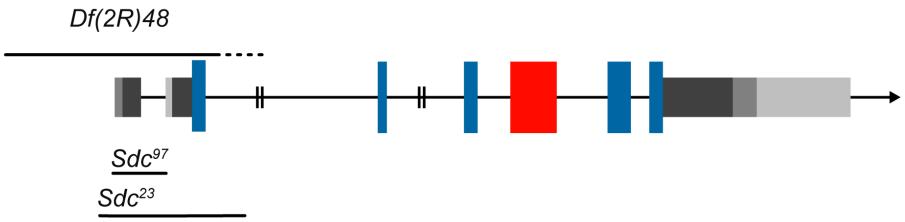

Figure 3.1: Schematic of *Drosophila Sdc* mutant.

Genomic structure of *syndecan* showing the null allele *Df(2R)48, ubi-sara*, and *sdc23* affects the first and second exons with *sdc97* affecting the first exon. The alleles are generated using imprecise P-element excision, with *Df(2R)48* deletion spanning a large segment of the genome, affecting a neighboring gene *sara,* rescued under ubiquitous expression. All mutants show little to no *sdc* expression confirmed by Western blots.

3.1.2 Syndecan and the neuroepithelium

I am interested in delineating the glia population responsible for the shrinkage of the outer proliferation zone resulting from the loss of Sdc. The brain lobe is composed of an interleaved network of neurons and glial processes, both expressing Sdc (Johnson et al., 2006). This poses a challenge to identify the Sdc expressing-glial populations. I can test a range of glial GAL4 drivers, including cortex glial GAL4 driver to test whether these cells plays a role in two ways: first by expressing Sdc-RNAi in these cells, second by rescuing Sdc function by

expressing transgenes in these cells in the *Sdc* null background. I purpose to use a *Sdc-GAL4* driver to test the pattern of expression to confirm which glial subtypes express Sdc (Nagarkar-Jaiswal et al., 2015). Preliminary results show this driver generates similar expression patterns to *Sdc::GFP.PTT*, including strong expression in wrapping glia in the PNS and the neuropile in the CNS. Therefore, it should allow me to reliably label a select population of Sdc expressing cells and determine whether they are glia or neuronal.

Both cortex glia and subperineurial glia have been implicated in the neuroepithelium-neuroblast transition, and each influencing neuroblast population in a unique manner. As previously mentioned, subperineurial glia expresses Serrated, a Notch ligand, that binds to the Notch receptor on the neuroepithelial membrane to regulate the spatial confinement of the proneural wave (Pérez-Gómez et al., 2013). Syndecan-3 is demonstrated to bind Notch ligands and enhance Notch signaling in vertebrate adult myogenesis, it would be interesting to see if *Drosophila* Sdc has the same conserved mechanism. I purpose to test whether Sdc can concentrate Serrate on the subperineurial membrane by utilizing a *SerD* (hypermorph) in a *Sdc* null background (Murata et al., 1996). The hypermorphic mutation increases Serrate protein function by eliminating the RNA degradation signal on the mRNA transcript, resulting in a gain of function phenotype. I predict this would rescue the neuroepithelium transition as I expect the absence of Sdc would reduce Notch signaling, thus dampen the hypermorphic function of the Se*rrate* allele.

The neuroepithelium transition can also be tuned by cortex glia through Notch-independent pathways that modulate growth and proliferation using various growth factor signaling, including EGF and FGF. In parallel, with vertebrate syndecan's contribution to EGFR activation, I purpose using a similar approach of dampening EGFR signaling by using a

hypomorphic version of the allele (*Egfr[t1]*) in a Sdc overexpression background (Clifford and Schüpbach, 1994). Vice versa, I can also test the reliance of Sdc of EGFR signaling by using a hypermorphic allele of EGFR (*Egfr[E3]*) in a *Sdc* null background (Brunner et al., 1994). I can further delineate the signaling pathway by overexpressing FGF or EGF ligands in the absence of Sdc, which could allow me to investigate whether Sdc is acting simply as a ligand reservoir or an integral component of the signaling complex. If the former idea is true, then the overabundance of growth factor ligand could override the requirement of Sdc by increasing bioavailability at the cell membrane. Moreover, it would be interesting to see whether Sdc is able to influence neuroepithelium indirectly by acting as a regulator of cortex glia growth and dissect apart the signaling mechanics of Sdc to EGFR signaling cascades.

3.1.3 Potential perineural glia tension differences between the CNS and PNS

Surprisingly, I observed that the failure of perineurial glia to ensheathe nerves in Sdc RNAi knockdown almost exclusively manifested in the PNS, more specifically within the nerve extension region. This is similar to the phenotype observed with loss of integrin in the perineurial glia (Xie and Auld, 2011). As the physical parameters from the extracellular environment exert a great degree of influence on cell behaviours, I hypothesized that the defective ensheathment by PG is caused by the topography change from the CNS to PNS, as perineurial glia are unable to respond to the increase in surface tension. Specifically I propose that with the transition from the CNS into the peripheral nerve, the surface tension experienced by the perineurial glia increases as an inverse relationship to the radius as per *LaPlace Law* (Prange, 2003). In other words, as the radius of the surface that the PG are migrating on moves from a large sphere to a narrow tube, the surface tension of the cell membrane increases. In this model perineurial glia can sense and

respond to this change in surface tension through Sdc and this leads to integrin activation and an increase in focal adhesion size/engagement to promote cell-ECM adhesion. This model is based on previous work in cultured human primary pluripotent stem cells where forces pulling on Sdc recruit α-actinin and PI3K activation in an EGFR dependent manner (Chronopoulos et al., 2020). Following the activation of PI3K, they observed a local accumulation of PIP_3, which is then propagated throughout the cell and binds to kindlin-2, an important integrin activator working in cooperation with talin, which ultimately leading to the activation of integrin and increased cell-ECM adhesion. By applying a PI3K inhibitor, or re-expression of kindlin-2 mutant lacking PIP3 binding site, the cell-wide upregulation of integrin is abolished when applying tension on Sdc (Chronopoulos et al., 2020). In our model, with Sdc knock down, the perineurial glia lose the ability to respond to the increase surface tension generated from the change in topography and are unable to upregulate focal adhesion formation and the subsequent ECM binding. This model would also explain why loss of Sdc in the PG only led the loss of perineurial glial processes in the PNS and not the CNS.

To test this hypothesis, I would quantify the mechanical force experienced by the perineurial glia *in vivo*. I propose utilizing a Förster resonance energy transfer (FRET) -based intracellular tension sensor modified from the endogenous *talin* gene (Lemke et al., 2019). The mechanical force is measured as the efficiency of fluorescent energy transfer between YPet and mCherry fluorescent proteins. Linking the two fluorophores is a mechanosensitive molecule incorporated within the Talin protein. As the cell experiences more force, the arrangement of Talin changes, leading to an increase in distance between the two fluorophores, in turn decreasing the FRET efficiency. I predict in a wild-type scenario that less FRET will be observed in the PNS than in the CNS within a given area. I predict that downregulating Sdc will lead to an

increase in the FRET efficiency in the PNS as the cell is unable to maintain the ensheathment tension than in the CNS.

Accompanying the perineurial glia radial ensheathment defect was an alteration in laminin deposition along the peripheral nerve. I hypothesized the non-uniform distribution of laminin is a consequence of reduced perineurial glia numbers. Normal laminin distribution in the neural lamella seen in *RNAi-2* knockdown larvae may resulted from the presence of normal and slightly increased number of PGs. In *Drosophila*, both hemocytes and perineurial glia are capable of producing laminin (Petley-Ragan et al., 2016; Sánchez-Sánchez et al., 2017). Thus, to determine the contribution of laminin in the PNS from the perineurial glia versus the hemocytes, I purpose to test the timing of laminin deposition. I would tag the *lanA* gene with a GFP-mCherry cassette containing protein-encoding reading frame arranged in opposing orientations flanked by inversion-oriented *FRT* sites, similar to *flybow* constructs (Hadjieconomou et al., 2011). Upon heat shock, flippase-mediated recombination would occur and convert the LanA::GFP tag to LanA::mCherry. Here, I would place the flippase under the control of *46F-GAL4* promoter, allowing recombination to take place within perineurial glial cells. If perineurial glia are the major contributor of laminin deposition in the PNS, I predict that major segments of the nerves will be covered in LanA::mCherry rather than LanA::GFP. Additionally, the result would be direct evidence that perineurial glia produce laminin, and what relative proportion of laminin is glial vs hemocyte produced. Moreover, this would allow me to visualize the perineurial glia contribution of laminin remaining upon Sdc knockdown or mutants, and determine the source of the laminin remnants I observed in the PNS.

3.1.4 Relationship of Syndecan and integrins in the perineurial glial layer

The synergistic interaction between syndecan and integrin *in vitro* has been well documented in various cell types. However, the synergistic cooperation *in vivo* is poorly documented. The syndecan-integrin (SDC-1 to -3) interactions are mediated by Sdc's ectodomain, and is independent of the HG-GAG chains (Beauvais et al., 2004). Yet, our results indicate Sdc and integrin do not co-localize, and it is unlikely the polypeptide chains of the two protein directly interact. Thus, I am curious to test whether they show genetic interaction in the *Drosophila* glia given the similar phenotypes observed with Sdc and integrin RNAi. I would like to confirm whether integrin or talin localization changes upon Sdc knockdown, and I predict by downregulating Sdc, there would be a decrease in integrin localization to the membrane. I would further examine this effect between Sdc and integrin by downregulating Sdc (using RNAi) in an integrin heteroallelic loss of function mutant (*mys[11]/+*) background to observe whether the Sdc lengthening of the VNC phenotype is enhanced. The alternative would be to downregulate integrin b-subunit with RNAi in a *Sdc* heteroallelic loss of function mutant.

A previous lab publication has shown Basigin (Bsg), an immunoglobulin domain transmembrane protein, acts as a negative regulator of integrin-mediated ECM adhesion by reducing integrin-ECM engagement, without affecting the ECM protein deposition in the matrix (Hunter et al., 2020). Our results suggest Sdc appears to be modulating integrin-mediated ECM adhesion. I am curious to know whether the lack of Sdc is working through the integrins or directly with the ECM or is functioning through Basigin. To test these ideas, I can reduce Sdc expression in a Bsg loss-of-function ($Bsg^{\Delta 265}$) background (Curtin et al., 2005). Lack of Bsg causes in the perineurial glia an over-engagement of the integrin pool with the ECM, resulting in

an accordion-like compression of the nerve (Hunter et al., 2020). Thus, I predict if Sdc is altering integrin-ECM engagement by downregulating Bsg this should counteract the loss of Sdc.

3.2 Conclusions

Syndecan's contribution to cellular function has been investigated in-depth *in vitro* through its association with integrin and growth factor receptor complexes, but the full breadth of Sdc's function has yet to be investigated *in vivo*. In this thesis, I have begun to illustrate the importance of Sdc as a cell surface receptor to mediate cell-cell, cell-ECM communication in the various neural and glial developmental processes in the *Drosophila* nervous system. However, our results also highlight many unknowns that require further investigation, including how Sdc and integrin functionally intersect if they do not co-localize; whether Sdc co-localizes with growth factor complexes; whether Sdc operates in a *cis*- or *trans*-configuration within the brain lobe to regulate the ligand concentration of the intended receptor. This thesis has demonstrated the capability of Sdc to influence cell behaviour during neural and glial development, though further investigation is required to concisely determine the molecular mechanisms of Sdc's influence.

Bibliography

Abram CL, Lowell CA (2009) The Ins and Outs of Leukocyte Integrin Signaling. Annu Rev Immunol 27:339–362.

Afratis NA, Nikitovic D, Multhaupt HAB, Theocharis AD, Couchman JR, Karamanos NK (2017) Syndecans – key regulators of cell signaling and biological functions. The FEBS Journal 284:27–41.

Andersen NF, Standal T, Nielsen JL, Heickendorff L, Borset M, Sørensen FB, Abildgaard N (2005) Syndecan-1 and angiogenic cytokines in multiple myeloma: correlation with bone marrow angiogenesis and survival. British Journal of Haematology 128:210–217.

Auld VJ, Broadie K, Goodman CS (1995) Gliotactin, a Novel Transmembrane Protein on Peripheral Gila, Is Required to Form the Blood-Nerve Barrier in Drosophila. Cell 81:757–767.

Avet-Rochex A, Kaul AK, Gatt AP, McNeill H, Bateman JM (2012) Concerted control of gliogenesis by InR/TOR and FGF signalling in the Drosophila post-embryonic brain. Development 139:2763–2772.

Avet-Rochex A, Maierbrugger KT, Bateman JM (2014) Glial enriched gene expression profiling identifies novel factors regulating the proliferation of specific glial subtypes in the Drosophila brain. Gene Expression Patterns 16:61–68.

Awasaki T, Lai S-L, Ito K, Lee T (2008) Organization and Postembryonic Development of Glial Cells in the Adult Central Brain of Drosophila. Journal of Neuroscience 28:13742–13753.

Babatz F, Naffin E, Klämbt C (2018) The Drosophila Blood-Brain Barrier Adapts to Cell Growth by Unfolding of Pre-existing Septate Junctions. Developmental Cell 47:697-710.e3.

Banerjee S (2006) Axonal Ensheathment and Septate Junction Formation in the Peripheral Nervous System of Drosophila. Journal of Neuroscience 26:3319–3329.

Banerjee S, Bhat MA (2008) Glial ensheathment of peripheral axons inDrosophila. J Neurosci Res 86:1189–1198.

Baron W, Shattil SJ, ffrench-Constant C (2002) The oligodendrocyte precursor mitogen PDGF stimulates proliferation by activation of αvβ3 integrins. The EMBO Journal 21:1957–1966.

Baumgartner S, Littleton JT, Broadie K, Bhat MA, Harbecke R, Lengyel JA, Chiquet-Ehrismann R, Prokop A, Bellen HJ (1996) A Drosophila Neurexin Is Required for Septate Junction and Blood-Nerve Barrier Formation and Function. Cell 87:1059–1068.

Beauvais DM, Burbach BJ, Rapraeger AC (2004) The syndecan-1 ectodomain regulates αv β3 integrin activity in human mammary carcinoma cells. J Cell Biol 167:171–181.

Beauvais DM, Rapraeger AC (2004) Syndecans in tumor cell adhesion and signaling. Reproductive Biology and Endocrinology:12.

Beauvais DM, Rapraeger AC (2010) Syndecan-1 couples the insulin-like growth factor-1 receptor to inside-out integrin activation. J Cell Sci 123:3796–3807.

Bernfield M, Götte M, Park PW, Reizes O, Fitzgerald ML, Lincecum J, Zako M (1999) Functions of Cell Surface Heparan Sulfate Proteoglycans. Annu Rev Biochem 68:729–777.

Brankatschk M, Dunst S, Nemetschke L, Eaton S (2014) Delivery of circulating lipoproteins to specific neurons in the Drosophila brain regulates systemic insulin signaling Ramaswami M, ed. eLife 3:e02862.

Brink DL, Gilbert M, Xie X, Petley-Ragan L, Auld VJ (2012) Glial Processes at the Drosophila Larval Neuromuscular Junction Match Synaptic Growth Dunaevsky A, ed. PLoS ONE 7:e37876.

Broadie K, Baumgartner S, Prokop A (2011) Extracellular matrix and its receptors in drosophila neural development. Devel Neurobio 71:1102–1130.

Brooks DS, Vishal K, Kawakami J, Bouyain S, Geisbrecht ER (2016) Optimization of wrMTrck to monitor Drosophila larval locomotor activity. Journal of Insect Physiology 93–94:11–17.

Brown NH (2000) Cell–cell adhesion via the ECM: integrin genetics in fly and worm. Matrix Biology 19:191–201.

Brunner D, Oellers N, Szabad J, Biggs WH, Zipursky SL, Hafen E (1994) A gain-of-function mutation in Drosophila MAP kinase activates multiple receptor tyrosine kinase signaling pathways. Cell 76:875–888.

Burgess WH, Maciag T (1989) THE HEPARIN-BINDING (FIBROBLAST) GROWTH FACTOR FAMILY OF PROTEINS. Annual Review of Biochemistry 58:575–606.

Buszczak M, Paterno S, Lighthouse D, Bachman J, Planck J, Owen S, Skora AD, Nystul TG, Ohlstein B, Allen A, Wilhelm JE, Murphy TD, Levis RW, Matunis E, Srivali N, Hoskins RA, Spradling AC (2007) The Carnegie Protein Trap Library: A Versatile Tool for Drosophila Developmental Studies. Genetics 175:1505–1531.

Campbell G, Göring H, Lin T, Spana E, Andersson S, Doe CQ, Tomlinson A (1994) RK2, a glial-specific homeodomain protein required for embryonic nerve cord condensation and viability in Drosophila. Development 120:2957–2966.

Carulli S, Beck K, Dayan G, Boulesteix S, Lortat-Jacob H, Rousselle P (2012) Cell Surface Proteoglycans Syndecan-1 and -4 Bind Overlapping but Distinct Sites in Laminin α3 LG45 Protein Domain *. Journal of Biological Chemistry 287:12204–12216.

Chanana B, Steigemann P, Jackle H, Vorbruggen G (2009) Reception of Slit requires only the chondroitin-sulphate-modified extracellular domain of Syndecan at the target cell surface. Proceedings of the National Academy of Sciences 106:11984–11988.

Chell JM, Brand AH (2010) Nutrition-Responsive Glia Control Exit of Neural Stem Cells from Quiescence. Cell 143:1161–1173.

Chen E, Hermanson S, Ekker SC (2004) Syndecan-2 is essential for angiogenic sprouting during zebrafish development. Blood 103:1710–1719.

Cheng B, Montmasson M, Terradot L, Rousselle P (2016) Syndecans as Cell Surface Receptors in Cancer Biology. A Focus on their Interaction with PDZ Domain Proteins. Front Pharmacol 7 Available at: http://journal.frontiersin.org/Article/10.3389/fphar.2016.00010/abstract [Accessed May 17, 2019].

Choi Y, Kwon M-J, Lim Y, Yun J-H, Lee W, Oh E-S (2015) Trans-regulation of Syndecan Functions by Hetero-oligomerization. Journal of Biological Chemistry 290:16943–16953.

Chronopoulos A, Thorpe SD, Cortes E, Lachowski D, Rice AJ, Mykuliak VV, Róg T, Lee DA, Hytönen VP, del Río Hernández AE (2020) Syndecan-4 tunes cell mechanics by activating the kindlin-integrin-RhoA pathway. Nat Mater Available at: http://www.nature.com/articles/s41563-019-0567-1 [Accessed March 2, 2020].

Chung H, Multhaupt HAB, Oh E-S, Couchman JR (2016) Minireview: Syndecans and their crucial roles during tissue regeneration. FEBS Letters 590:2408–2417.

Clause KC, Barker TH (2013) Extracellular matrix signaling in morphogenesis and repair. Current Opinion in Biotechnology 24:830–833.

Clifford R, Schüpbach T (1994) Molecular analysis of the Drosophila EGF receptor homolog reveals that several genetically defined classes of alleles cluster in subdomains of the receptor protein. Genetics 137:531–550.

Colognato H, Tzvetanova ID (2011) Glia unglued: How signals from the extracellular matrix regulate the development of myelinating glia. Devel Neurobio 71:924–955.

Corti F, Wang Y, Rhodes JM, Atri D, Archer-Hartmann S, Zhang J, Zhuang ZW, Chen D, Wang T, Wang Z, Azadi P, Simons M (2019) N-terminal syndecan-2 domain selectively enhances 6-O heparan sulfate chains sulfation and promotes VEGFA 165 -dependent neovascularization. Nature Communications 10:1562.

Couchman JR (2003) Syndecans: proteoglycan regulators of cell-surface microdomains? Nature Reviews Molecular Cell Biology 4:926–938.

Couchman JR, Gopal S, Lim HC, Nørgaard S, Multhaupt HAB (2015) Fell-Muir Lecture: Syndecans: from peripheral coreceptors to mainstream regulators of cell behaviour. International Journal of Experimental Pathology 96:1–10.

Coutinho-Budd JC, Sheehan AE, Freeman MR (2017) The secreted neurotrophin Spätzle 3 promotes glial morphogenesis and supports neuronal survival and function. Genes & Development 31:2023–2038.

Crest J, Diz-Muñoz A, Chen D-Y, Fletcher DA, Bilder D (2017) Organ sculpting by patterned extracellular matrix stiffness Spradling AC, ed. eLife 6:e24958.

Cui Y, Yang Y, Ni Z, Dong Y, Cai G, Foncelle A, Ma S, Sang K, Tang S, Li Y, Shen Y, Berry H, Wu S, Hu H (2018) Astroglial Kir4.1 in the lateral habenula drives neuronal bursts in depression. Nature 554:323–327.

Curtin KD, Meinertzhagen IA, Wyman RJ (2005) Basigin (EMMPRIN/CD147) interacts with integrin to affect cellular architecture. Journal of Cell Science 118:2649–2660.

Das S, Majid M, Baker AB (2016) Syndecan-4 enhances PDGF-BB activity in diabetic wound healing. Acta Biomaterialia 42:56–65.

De Luca M, Klimentidis YC, Casazza K, Moses Chambers M, Cho R, Harbison ST, Jumbo-Lucioni P, Zhang S, Leips J, Fernandez JR (2010) A Conserved Role for Syndecan Family Members in the Regulation of Whole-Body Energy Metabolism Bergmann A, ed. PLoS ONE 5:e11286.

De Rossi G, Whiteford JR (2013) Novel insight into the biological functions of syndecan ectodomain core proteins: Syndecan Ectodomains. BioFactors 39:374–382.

Delgado MG, Oliva C, López E, Ibacache A, Galaz A, Delgado R, Barros LF, Sierralta J (2018) Chaski, a novel Drosophila lactate/pyruvate transporter required in glia cells for survival under nutritional stress. Scientific Reports 8:1186.

Dietzl G, Chen D, Schnorrer F, Su K-C, Barinova Y, Fellner M, Gasser B, Kinsey K, Oppel S, Scheiblauer S, Couto A, Marra V, Keleman K, Dickson BJ (2007) A genome-wide transgenic RNAi library for conditional gene inactivation in Drosophila. Nature 448:151–156.

Doherty J, Logan MA, Tasdemir OE, Freeman MR (2009) Ensheathing Glia Function as Phagocytes in the Adult Drosophila Brain. Journal of Neuroscience 29:4768–4781.

DuFort CC, Paszek MJ, Weaver VM (2011) Balancing forces: architectural control of mechanotransduction. Nat Rev Mol Cell Biol 12:308–319.

Echtermeyer F, Streit M, Wilcox-Adelman S, Saoncella S, Denhez F, Detmar M, Goetinck P (2001) Delayed wound repair and impaired angiogenesis in mice lacking syndecan-4. J Clin Invest 107:R9–R14.

Egger B, Boone JQ, Stevens NR, Brand AH, Doe CQ (2007) Regulation of spindle orientation and neural stem cell fate in the Drosophila optic lobe. Neural Dev 2:1.

Egger B, Chell JM, Brand AH (2008) Insights into neural stem cell biology from flies. Philosophical Transactions of the Royal Society B: Biological Sciences 363:39–56.

Evans IR, Hu N, Skaer H, Wood W (2010) Interdependence of macrophage migration and ventral nerve cord development in Drosophila embryos. Development 137:1625–1633.

Faivre-Sarrailh C (2004) Drosophila contactin, a homolog of vertebrate contactin, is required for septate junction organization and paracellular barrier function. Development 131:4931–4942.

Feltri ML, Porta DG, Previtali SC, Nodari A, Migliavacca B, Cassetti A, Littlewood-Evans A, Reichardt LF, Messing A, Quattrini A, Mueller U, Wrabetz L (2002) Conditional disruption of β1 integrin in Schwann cells impedes interactions with axons. The Journal of Cell Biology 156:199–210.

Fernandes VM, Chen Z, Rossi AM, Zipfel J, Desplan C (2017) Glia relay differentiation cues to coordinate neuronal development in Drosophila. Science 357:886–891.

Filla MS, Dam P, Rapraeger AC (1998) The cell surface proteoglycan syndecan-1 mediates fibroblast growth factor-2 binding and activity. Journal of Cell Physiology 174:310–321.

Fiore VF, Ju L, Chen Y, Zhu C, Barker TH (2014) Dynamic catch of a Thy-1–α 5 β 1 +syndecan-4 trimolecular complex. Nature Communications 5:4886.

Frantz C, Stewart KM, Weaver VM (2010) The extracellular matrix at a glance. J Cell Sci 123:4195–4200.

Freeman MR (2015) Drosophila Central Nervous System Glia. Cold Spring Harb Perspect Biol 7 Available at: https://www.ncbi.nlm.nih.gov/pmc/articles/PMC4632667/ [Accessed December 30, 2020].

Freeman MR, Doherty J (2006) Glial cell biology in Drosophila and vertebrates. Trends in Neurosciences 29:82–90.

Genova JL, Fehon RG (2003) Neuroglian, Gliotactin, and the Na+/K+ ATPase are essential for septate junction function in Drosophila. Journal of Cell Biology 161:979–989.

Ginsberg MH, Partridge A, Shattil SJ (2005) Integrin regulation. Current Opinion in Cell Biology 17:509–516.

Granes F, Urena JM, Rocamora N, Vilaro S (2000) Ezrin links syndecan-2 to the cytoskeleton. J Cell Sci 113:1267–1276.

Grootjans JJ, Zimmermann P, Reekmans G, Smets A, Degeest G, Durr J, David G (1997) Syntenin, a PDZ protein that binds syndecan cytoplasmic domains. Proceedings of the National Academy of Sciences 94:13683–13688.

Hadjieconomou D, Rotkopf S, Alexandre C, Bell DM, Dickson BJ, Salecker I (2011) Flybow: genetic multicolor cell labeling for neural circuit analysis in Drosophila melanogaster. Nature Methods 8:260–266.

Harrison NJ, Connolly E, Gascón Gubieda A, Yang Z, Altenhein B, Losada Perez M, Moreira M, Sun J, Hidalgo A (2021) Regenerative neurogenic response from glia requires insulin-driven neuron-glia communication Bellen HJ, Banerjee U, Wang H, eds. eLife 10:e58756.

Hartenstein V (2011) Morphological diversity and development of glia in Drosophila. Glia 59:1237–1252.

Hindle SJ, Bainton RJ (2014) Barrier mechanisms in the Drosophila blood-brain barrier. Front Neurosci 8 Available at: https://www.frontiersin.org/articles/10.3389/fnins.2014.00414/full [Accessed January 26, 2021].

Hoffman MP, Nomizu M, Roque E, Lee S, Jung DW, Yamada Y, Kleinman HK (1998) Laminin-1 and Laminin-2 G-domain Synthetic Peptides Bind Syndecan-1 and Are Involved in Acinar Formation of a Human Submandibular Gland Cell Line. Journal of Biological Chemistry 273:28633–28641.

Hohenester E, Yurchenco PD (2013) Laminins in basement membrane assembly. Cell Adhesion & Migration 7:56–63.

Hortsch M, Margolis B (2003) Septate and paranodal junctions: kissing cousins. Trends in Cell Biology 13:557–561.

Hsueh Y-P, Yang F-C, Kharazia V, Naisbitt S, Cohen AR, Weinberg RJ, Sheng M (1998) Direct Interaction of CASK/LIN-2 and Syndecan Heparan Sulfate Proteoglycan and Their Overlapping Distribution in Neuronal Synapses. J Cell Biol 142:139–151.

Hunter AC, Petley-Ragan LM, Das M, Auld VJ (2020) Basigin Associates with Integrin in Order to Regulate Perineurial Glia and *Drosophila* Nervous System Morphology. J Neurosci 40:3360–3373.

Huveneers S, Danen EHJ (2009) Adhesion signaling - crosstalk between integrins, Src and Rho. Journal of Cell Science 122:1059–1069.

Isabella AJ, Horne-Badovinac S (2015) Dynamic regulation of basement membrane protein levels promotes egg chamber elongation in Drosophila. Dev Biol 406:212–221.

Johnson KG, Ghose A, Epstein E, Lincecum J, O'Connor MB, Van Vactor D (2004) Axonal Heparan Sulfate Proteoglycans Regulate the Distribution and Efficiency of the Repellent Slit during Midline Axon Guidance. Current Biology 14:499–504.

Johnson KG, Tenney AP, Ghose A, Duckworth AM, Higashi ME, Parfitt K, Marcu O, Heslip TR, Marsh JL, Schwarz TL, Flanagan JG, Van Vactor D (2006) The HSPGs Syndecan and Dallylike Bind the Receptor Phosphatase LAR and Exert Distinct Effects on Synaptic Development. Neuron 49:517–531.

Kaji T, Yamamoto C, Oh-i M, Fujiwara Y, Yamazaki Y, Morita T, Plaas AH, Wight TN (2006) The vascular endothelial growth factor VEGF165 induces perlecan synthesis via VEGF receptor-2 in cultured human brain microvascular endothelial cells. Biochimica et Biophysica Acta (BBA) - General Subjects 1760:1465–1474.

Kaksonen M, Pavlov I, Võikar V, Lauri SE, Hienola A, Riekki R, Lakso M, Taira T, Rauvala H (2002) Syndecan-3-deficient mice exhibit enhanced LTP and impaired hippocampus-dependent memory. Mol Cell Neurosci 21:158–172.

Kanai MI, Kim M-J, Akiyama T, Takemura M, Wharton K, O'Connor MB, Nakato H (2018) Regulation of neuroblast proliferation by surface glia in the Drosophila larval brain. Scientific Reports 8:3730.

Klass CM, Couchman JR, Woods A (2000) Syndecan-2 controls matrix assembly. Journal of Cell Science 113:493–506.

Knox J, Moyer K, Yacoub N, Soldaat C, Komosa M, Vassilieva K, Wilk R, Hu J, Vazquez Paz L de L, Syed Q, Krause HM, Georgescu M, Jacobs JR (2011) Syndecan contributes to heart cell specification and lumen formation during Drosophila cardiogenesis. Developmental Biology 356:279–290.

Kottmeier R, Bittern J, Schoofs A, Scheiwe F, Matzat T, Pankratz M, Klämbt C (2020) Wrapping glia regulates neuronal signaling speed and precision in the peripheral nervous system of Drosophila. Nat Commun 11:4491.

Kwon M-J, Jang B, Yi JY, Han I-O, Oh ES (2012) Syndecans play dual roles as cell adhesion receptors and docking receptors. FEBS Letters 586:2207–2211.

Lavery W, Hall V, Yager JC, Rottgers A, Wells MC, Stern M (2007) Phosphatidylinositol 3-Kinase and Akt Nonautonomously Promote Perineurial Glial Growth in Drosophila Peripheral Nerves. J Neurosci 27:279–288.

Lee T, Luo L (1999) Mosaic Analysis with a Repressible Cell Marker for Studies of Gene Function in Neuronal Morphogenesis. Neuron 22:451–461.

Leiserson WM, Forbush B, Keshishian H (2011) Drosophila glia use a conserved cotransporter mechanism to regulate extracellular volume. Glia 59:320–332.

Lemke SB, Weidemann T, Cost A-L, Grashoff C, Schnorrer F (2019) A small proportion of Talin molecules transmit forces at developing muscle attachments in vivo. PLOS Biology 17:e3000057.

Leonova EI, Galzitskaya OV (2013) Structure and functions of syndecans in vertebrates. Biochemistry (Moscow) 78:1071–1085.

Lin X, Buff E, Perrimon N, Michelson AM (1999) Role of HSPGs in FGF signaling. Development 126:3715–3723.

Liu S-L, Fewkes N, Ricketson D, Penkert RR, Prehoda KE (2008) Filament-dependent and -independent Localization Modes of *Drosophila* Non-muscle Myosin II. J Biol Chem 283:380–387.

Magnusson JP, Göritz C, Tatarishvili J, Dias DO, Smith EMK, Lindvall O, Kokaia Z, Frisén J (2014) A latent neurogenic program in astrocytes regulated by Notch signaling in the mouse. Science 346:237–241.

Mahalingam Y, Gallagher JT, Couchman JR (2007) Cellular Adhesion Responses to the Heparin-binding (HepII) Domain of Fibronectin Require Heparan Sulfate with Specific Properties*. Journal of Biological Chemistry 282:3221–3230.

Mahtouk K, Cremer FW, Rème T, Jourdan M, Baudard M, Moreaux J, Requirand G, Fiol G, De Vos J, Moos M, Quittet P, Goldschmidt H, Rossi J-F, Hose D, Klein B (2006) Heparan sulphate proteoglycans are essential for the myeloma cell growth activity of EGF-family ligands in multiple myeloma. Oncogene 25:7180–7191.

Martinek N, Shahab J, Saathoff M, Ringuette M (2008) Haemocyte-derived SPARC is required for collagen-IV-dependent stability of basal laminae in Drosophila embryos. Journal of Cell Science 121:1671–1680.

Masaki T, Matsumura K (2010) Biological Role of Dystroglycan in Schwann Cell Function and Its Implications in Peripheral Nervous System Diseases. Journal of Biomedicine and Biotechnology 2010:e740403.

Matzat T, Sieglitz F, Kottmeier R, Babatz F, Engelen D, Klambt C (2015) Axonal wrapping in the Drosophila PNS is controlled by glia-derived neuregulin homolog Vein. Development 142:1336–1345.

McKee KK, Yang D-H, Patel R, Chen Z-L, Strickland S, Takagi J, Sekiguchi K, Yurchenco PD (2012) Schwann cell myelination requires integration of laminin activities. Journal of Cell Science 125:4609–4619.

McLaughlin CN, Perry-Richardson JJ, Coutinho-Budd JC, Broihier HT (2019) Dying Neurons Utilize Innate Immune Signaling to Prime Glia for Phagocytosis during Development. Developmental Cell 48:506-522.e6.

Melendez-Vasquez C, Carey DJ, Zanazzi G, Reizes O, Maurel P, Salzer JL (2005) Differential expression of proteoglycans at central and peripheral nodes of Ranvier. Glia 52:301–308.

Melom JE, Littleton JT (2013) Mutation of a NCKX Eliminates Glial Microdomain Calcium Oscillations and Enhances Seizure Susceptibility. J Neurosci 33:1169–1178.

Meyer S, Schmidt I, Klämbt C (2014) Glia ECM interactions are required to shape the Drosophila nervous system. Mechanisms of Development 133:105–116.

Milner R, Wilby M, Nishimura S, Boylen K, Edwards G, Fawcett J, Streuli C, Pytela R, ffrench-Constant C (1997) Division of Labor of Schwann Cell Integrins during Migration on Peripheral Nerve Extracellular Matrix Ligands. Developmental Biology 185:215–228.

Mochizuki M, Güç E, Park AJ, Julier Z, Briquez PS, Kuhn GA, Müller R, Swartz MA, Hubbell JA, Martino MM (2020) Growth factors with enhanced syndecan binding generate tonic signalling and promote tissue healing. Nat Biomed Eng 4:463–475.

Morante J, Vallejo DM, Desplan C, Dominguez M (2013) Conserved miR-8/miR-200 Defines a Glial Niche that Controls Neuroepithelial Expansion and Neuroblast Transition. Developmental Cell 27:174–187.

Morgan MR, Humphries MJ, Bass MD (2007) Synergistic control of cell adhesion by integrins and syndecans. Nature Reviews Molecular Cell Biology 8:957–969.

Morin X, Daneman R, Zavortink M, Chia W (2001) A protein trap strategy to detect GFP-tagged proteins expressed from their endogenous loci in Drosophila. Proceedings of the National Academy of Sciences 98:15050–15055.

Munesue S, Kusano Y, Oguri K, Itano N, Yoshitomi Y, Nakanishi H, Yamashina I, Okayama M (2002) The role of syndecan-2 in regulation of actin-cytoskeletal organization of Lewis lung carcinoma-derived metastatic clones. Biochem J 363:201–209.

Murata T, Ogura K, Murakami R, Okano H, Yokoyama KK (1996) hiiragi, a gene essential for wing development in Drosophila melanogaster, affects the Notch cascade. Genes Genet Syst 71:247–254.

Nagarkar-Jaiswal S, DeLuca SZ, Lee P-T, Lin W-W, Pan H, Zuo Z, Lv J, Spradling AC, Bellen HJ (2015) A genetic toolkit for tagging intronic MiMIC containing genes. eLife 4 Available at: https://elifesciences.org/articles/08469 [Accessed April 2, 2019].

Nakano R, Iwamura M, Obikawa A, Togane Y, Hara Y, Fukuhara T, Tomaru M, Takano-Shimizu T, Tsujimura H (2019) Cortex glia clear dead young neurons via Drpr/dCed-

6/Shark and Crk/Mbc/dCed-12 signaling pathways in the developing Drosophila optic lobe. Developmental Biology 453:68–85.

Nave K-A, Salzer JL (2006) Axonal regulation of myelination by neuregulin 1. Current Opinion in Neurobiology 16:492–500.

Nave K-A, Trapp BD (2008) Axon-Glial Signaling and the Glial Support of Axon Function. Annu Rev Neurosci 31:535–561.

Nguyen MU, Kwong J, Chang J, Gillet VG, Lee RM, Johnson KG (2016) The Extracellular and Cytoplasmic Domains of Syndecan Cooperate Postsynaptically to Promote Synapse Growth at the Drosophila Neuromuscular Junction McCabe BD, ed. PLOS ONE 11:e0151621.

Nussbaum-Krammer CI, Neto MF, Brielmann RM, Pedersen JS, Morimoto RI (2015) Investigating the Spreading and Toxicity of Prion-like Proteins Using the Metazoan Model Organism C. elegans. JoVE:52321.

Okina E, Grossi A, Gopal S, Multhaupt HAB, Couchman JR (2012) Alpha-actinin interactions with syndecan-4 are integral to fibroblast–matrix adhesion and regulate cytoskeletal architecture. The International Journal of Biochemistry & Cell Biology 44:2161–2174.

Olofsson B, Page DT (2005) Condensation of the central nervous system in embryonic Drosophila is inhibited by blocking hemocyte migration or neural activity. Developmental Biology 279:233–243.

Parkhurst SJ, Adhikari P, Navarrete JS, Legendre A, Manansala M, Wolf FW (2018) Perineurial Barrier Glia Physically Respond to Alcohol in an Akap200-Dependent Manner to Promote Tolerance. Cell Reports 22:1647–1656.

Pastor-Pareja JC, Xu T (2011) Shaping Cells and Organs in Drosophila by Opposing Roles of Fat Body-Secreted Collagen IV and Perlecan. Developmental Cell 21:245–256.

Pereanu W, Shy D, Hartenstein V (2005) Morphogenesis and proliferation of the larval brain glia in Drosophila. Developmental Biology 283:191–203.

Pereira JA, Benninger Y, Baumann R, Gonçalves AF, Özçelik M, Thurnherr T, Tricaud N, Meijer D, Fässler R, Suter U, Relvas JB (2009) Integrin-linked kinase is required for radial sorting of axons and Schwann cell remyelination in the peripheral nervous system. Journal of Cell Biology 185:147–161.

Pérez-Gómez R, Slováková J, Rives-Quinto N, Krejci A, Carmena A (2013) A Serrate–Notch–Canoe complex mediates essential interactions between glia and neuroepithelial cells during Drosophila optic lobe development. J Cell Sci 126:4873–4884.

Petley-Ragan LM, Ardiel EL, Rankin CH, Auld VJ (2016) Accumulation of Laminin Monomers in Drosophila Glia Leads to Glial Endoplasmic Reticulum Stress and Disrupted Larval Locomotion. Journal of Neuroscience 36:1151–1164.

Pickup MW, Mouw JK, Weaver VM (2014) The extracellular matrix modulates the hallmarks of cancer. EMBO reports 15:1243–1253.

Pisconti A, Cornelison DDW, Olguín HC, Antwine TL, Olwin BB (2010) Syndecan-3 and Notch cooperate in regulating adult myogenesis. Journal of Cell Biology 190:427–441.

Prange HD (2003) LAPLACE'S LAW AND THE ALVEOLUS: A MISCONCEPTION OF ANATOMY AND A MISAPPLICATION OF PHYSICS. Advances in Physiology Education 27:34–40.

Preibisch S, Saalfeld S, Tomancak P (2009) Globally optimal stitching of tiled 3D microscopic image acquisitions. Bioinformatics 25:1463–1465.

Rapraeger AC (2001) Molecular interactions of syndecans during development. Seminars in Cell & Developmental Biology 12:107–116.

Rapraeger AC, Ell BJ, Roy M, Li X, Morrison OR, Thomas GM, Beauvais DM (2013) Vascular endothelial-cadherin stimulates syndecan-1-coupled insulin-like growth factor-1 receptor and cross-talk between αVβ3 integrin and vascular endothelial growth factor receptor 2 at the onset of endothelial cell dissemination during angiogenesis. The FEBS Journal 280:2194–2206.

Rawson JM, Dimitroff B, Johnson KG, Rawson JM, Ge X, Van Vactor D, Selleck SB (2005) The Heparan Sulfate Proteoglycans Dally-like and Syndecan Have Distinct Functions in Axon Guidance and Visual-System Assembly in Drosophila. Current Biology 15:833–838.

Read RD (2018) Pvr receptor tyrosine kinase signaling promotes post-embryonic morphogenesis, and survival of glia and neural progenitor cells in Drosophila. Development 145 Available at: https://dev.biologists.org/content/145/23/dev164285 [Accessed March 6, 2021].

Reiland J, Rapraeger AC (1993) Heparan sulfate proteoglycan and FGF receptor target basic FGF to different intracellular destinations. Journal of Cell Science 105:1085–1093.

Riedl J, Crevenna AH, Kessenbrock K, Yu JH, Neukirchen D, Bista M, Bradke F, Jenne D, Holak TA, Werb Z, Sixt M, Wedlich-Soldner R (2008) Lifeact: a versatile marker to visualize F-actin. Nature Methods 5:605–607.

Rogers KW, Schier AF (2011) Morphogen gradients: from generation to interpretation. Annu Rev Cell Dev Biol 27:377–407.

Roper JA, Williamson RC, Bass MD (2012) Syndecan and integrin interactomes: large complexes in small spaces. Current Opinion in Structural Biology 22:583–590.

Saab AS et al. (2016) Oligodendroglial NMDA Receptors Regulate Glucose Import and Axonal Energy Metabolism. Neuron 91:119–132.

Sánchez-Sánchez BJ, Urbano JM, Comber K, Dragu A, Wood W, Stramer B, Martín-Bermudo MD (2017) Drosophila Embryonic Hemocytes Produce Laminins to Strengthen Migratory Response. Cell Reports 21:1461–1470.

San-Juán BP, Baonza A (2011) The bHLH factor deadpan is a direct target of Notch signaling and regulates neuroblast self-renewal in Drosophila. Developmental Biology 352:70–82.

Saoncella S, Echtermeyer F, Denhez F, Nowlen JK, Mosher DF, Robinson SD, Hynes RO, Goetinck PF (1999) Syndecan-4 signals cooperatively with integrins in a Rhodependent manner in the assembly of focal adhesions and actin stress fibers. PNAS 96:2805–2810.

Sarov M et al. (2016) A genome-wide resource for the analysis of protein localisation in Drosophila. eLife 5:e12068.

Schindelin J, Arganda-Carreras I, Frise E, Kaynig V, Longair M, Pietzsch T, Preibisch S, Rueden C, Saalfeld S, Schmid B, Tinevez J-Y, White DJ, Hartenstein V, Eliceiri K, Tomancak P, Cardona A (2012) Fiji: an open-source platform for biological-image analysis. Nat Methods 9:676–682.

Schulz JG, Ceulemans H, Caussinus E, Baietti MF, Affolter M, Hassan BA, David G (2011) Drosophila syndecan regulates tracheal cell migration by stabilizing Robo levels. EMBO reports 12:1039–1046.

Schwabe T, Bainton RJ, Fetter RD, Heberlein U, Gaul U (2005) GPCR Signaling Is Required for Blood-Brain Barrier Formation in Drosophila. Cell 123:133–144.

Sepp KJ, Auld VJ (2003) Reciprocal Interactions between Neurons and Glia Are Required for *Drosophila* Peripheral Nervous System Development. J Neurosci 23:8221–8230.

Sepp KJ, Schulte J, Auld VJ (2000) Developmental dynamics of peripheral glia in Drosophila melanogaster. Glia 30:122–133.

Sepp KJ, Schulte J, Auld VJ (2001) Peripheral Glia Direct Axon Guidance across the CNS/PNS Transition Zone. Developmental Biology 238:47–63.

Skeath JB, Wilson BA, Romero SE, Snee MJ, Zhu Y, Lacin H (2017) The extracellular metalloprotease AdamTS-A anchors neural lineages in place within and preserves the architecture of the central nervous system. Development 144:3102–3113.

Smart AD, Course MM, Rawson J, Selleck S, Van Vactor D, Johnson KG (2011) Heparan sulfate proteoglycan specificity during axon pathway formation in the Drosophila embryo. Developmental Neurobiology 71:608–618.

Somjen GG (1988) Nervenkitt: Notes on the history of the concept of neuroglia. Glia 1:2–9.

Song Z, McCall K, Steller H (1997) DCP-1, a Drosophila Cell Death Protease Essential for Development. Science 275:536–540.

Spéder P, Brand AH (2014) Gap Junction Proteins in the Blood-Brain Barrier Control Nutrient-Dependent Reactivation of Drosophila Neural Stem Cells. Developmental Cell 30:309–321.

Spéder P, Brand AH (2018) Systemic and local cues drive neural stem cell niche remodelling during neurogenesis in Drosophila Banerjee U, ed. eLife 7:e30413.

Spindler SR, Ortiz I, Fung S, Takashima S, Hartenstein V (2009) Drosophila cortex and neuropile glia influence secondary axon tract growth, pathfinding, and fasciculation in the developing larval brain. Developmental Biology 334:355–368.

Spring J, Paine-Saunders SE, Hynes RO, Bernfield M (1994) Drosophila syndecan: conservation of a cell-surface heparan sulfate proteoglycan. Proceedings of the National Academy of Sciences 91:3334–3338.

Steigemann P, Molitor A, Fellert S, Jäckle H, Vorbrüggen G (2004) Heparan Sulfate Proteoglycan Syndecan Promotes Axonal and Myotube Guidance by Slit/Robo Signaling. Current Biology 14:225–230.

Steinfeld R, Van Den Berghe H, David G (1996) Stimulation of fibroblast growth factor receptor-1 occupancy and signaling by cell surface-associated syndecans and glypican. J Cell Biol 133:405–416.

Stepp MA, Gibson HE, Gala PH, Iglesia DDS, Pajoohesh-Ganji A, Pal-Ghosh S, Brown M, Aquino C, Schwartz AM, Goldberger O, Hinkes MT, Bernfield M (2002) Defects in keratinocyte activation during wound healing in the syndecan-1-deficient mouse. Journal of Cell Science 115:4517–4531.

Stepp MA, Pal-Ghosh S, Tadvalkar G, Pajoohesh-Ganji A (2015) Syndecan-1 and Its Expanding List of Contacts. Advances in Wound Care 4:235–249.

Stork T, Bernardos R, Freeman MR (2012) Analysis of Glial Cell Development and Function in Drosophila. Cold Spring Harbor Protocols 2012:pdb.top067587-pdb.top067587.

Stork T, Engelen D, Krudewig A, Silies M, Bainton RJ, Klämbt C (2008) Organization and Function of the Blood–Brain Barrier in Drosophila. J Neurosci 28:587–597.

Stork T, Sheehan A, Tasdemir-Yilmaz OE, Freeman MR (2014) Neuron-Glia Interactions through the Heartless FGF Receptor Signaling Pathway Mediate Morphogenesis of Drosophila Astrocytes. Neuron 83:388–403.

Sun D, Mcalmon KR, Davies JA, Merton B, Hay ED (1998) Simultaneous loss of expression of syndecan-1 and E-cadherin in the embryonic palate during epithelial-mesenchymal transformation. International Journal of Developemental Biology 42:733–736.

Takada Y, Ye X, Simon S (2007) The integrins. Genome Biology 8:215.

Tepass U, Fessler LI, Aziz A, Hartenstein V (1994) Embryonic origin of hemocytes and their relationship to cell death in Drosophila. Development 120:1829–1837.

Theocharis AD, Karamanos NK (2019) Proteoglycans remodeling in cancer: Underlying molecular mechanisms. Matrix Biol 75–76:220–259.

Theocharis AD, Skandalis SS, Gialeli C, Karamanos NK (2016) Extracellular matrix structure. Adv Drug Deliv Rev 97:4–27.

Volkenhoff A, Weiler A, Letzel M, Stehling M, Klämbt C, Schirmeier S (2015) Glial Glycolysis Is Essential for Neuronal Survival in Drosophila. Cell Metabolism 22:437–447.

von Hilchen CM, Bustos AE, Giangrande A, Technau GM, Altenhein B (2013) Predetermined embryonic glial cells form the distinct glial sheaths of the Drosophila peripheral nervous system. Development 140:3657–3668.

Wada A, Kato K, Uwo MF, Yonemura S, Hayashi S (2007) Specialized extraembryonic cells connect embryonic and extraembryonic epidermis in response to Dpp during dorsal closure in Drosophila. Developmental Biology 301:340–349.

Wallquist W, Patarroyo M, Thams S, Carlstedt T, Stark B, Cullheim S, Hammarberg H (2002) Laminin chains in rat and human peripheral nerve: Distribution and regulation during development and after axonal injury. The Journal of Comparative Neurology 454:284–293.

Wallquist W, Plantman S, Thams S, Thyboll J, Kortesmaa J, Länngergren J, Domogatskaya A, Ögren SO, Risling M, Hammarberg H, Tryggvason K, Cullheim S (2005) Impeded Interaction between Schwann Cells and Axons in the Absence of Laminin α4. J Neurosci 25:3692–3700.

Wang H, Jin H, Rapraeger AC (2015) Syndecan-1 and Syndecan-4 Capture Epidermal Growth Factor Receptor Family Members and the α3β1 Integrin Via Binding Sites in Their Ectodomains: NOVEL SYNSTATINS PREVENT KINASE CAPTURE AND INHIBIT α6β4-INTEGRIN-DEPENDENT EPITHELIAL CELL MOTILITY*. Journal of Biological Chemistry 290:26103–26113.

Wang H, Leavitt L, Ramaswamy R, Rapraeger AC (2010) Interaction of Syndecan and α6β4 Integrin Cytoplasmic Domains: REGULATION OF ErbB2-MEDIATED INTEGRIN ACTIVATION *. Journal of Biological Chemistry 285:13569–13579.

Wang W, Liu W, Wang Y, Zhou L, Tang X, Luo H (2011) Notch signaling regulates neuroepithelial stem cell maintenance and neuroblast formation in Drosophila optic lobe development. Developmental Biology 350:414–428.

Wilgus TA (2012) Growth Factor–Extracellular Matrix Interactions Regulate Wound Repair. Advances in Wound Care 1:249–254.

Woods A, Longley RL, Tumova S, Couchman JR (2000) Syndecan-4 Binding to the High Affinity Heparin-Binding Domain of Fibronectin Drives Focal Adhesion Formation in Fibroblasts. Archives of Biochemistry and Biophysics 374:66–72.

Woods A, Oh E-S, Couchman JR (1998) Syndecan proteoglycans and cell adhesion. Matrix Biology 17:477–483.

Wu ZL, Zhang L, Yabe T, Kuberan B, Beeler DL, Love A, Rosenberg RD (2003) The Involvement of Heparan Sulfate (HS) in FGF1/HS/FGFR1 Signaling Complex *. Journal of Biological Chemistry 278:17121–17129.

Xian X, Gopal S, Couchman JR (2010) Syndecans as receptors and organizers of the extracellular matrix. Cell and Tissue Research 339:31–46.

Xie X, Auld VJ (2011) Integrins are necessary for the development and maintenance of the glial layers in the Drosophila peripheral nerve. Development 138:3813–3822.

Yamada M, Sekiguchi K (2015) Molecular Basis of Laminin–Integrin Interactions. In: Current Topics in Membranes, pp 197–229. Elsevier. Available at: https://linkinghub.elsevier.com/retrieve/pii/S1063582315000605 [Accessed January 25, 2021].

Yamashita H, Goto A, Kadowaki T, Kitagawa Y (2004) Mammalian and Drosophila cells adhere to the laminin α4 LG4 domain through syndecans, but not glypicans. Biochemical Journal 382:933–943.

Yang N, Friedl A (2016) Syndecan-1-Induced ECM Fiber Alignment Requires Integrin αvβ3 and Syndecan-1 Ectodomain and Heparan Sulfate Chains Cukierman E, ed. PLoS ONE 11:e0150132.

Yildirim K, Petri J, Kottmeier R, Klämbt C (2019) Drosophila glia: Few cell types and many conserved functions. Glia 67:5–26.

Yu W-M, Feltri ML, Wrabetz L, Strickland S, Chen Z-L (2005) Schwann Cell-Specific Ablation of Laminin γ1 Causes Apoptosis and Prevents Proliferation. J Neurosci 25:4463–4472.

Yu W-M, Yu H, Chen Z-L, Strickland S (2009) Disruption of laminin in the peripheral nervous system impedes nonmyelinating Schwann cell development and impairs nociceptive sensory function. Glia 57:850–859.

Yuan X, Sipe CW, Suzawa M, Bland ML, Siegrist SE (2020) Dilp-2–mediated PI3-kinase activation coordinates reactivation of quiescent neuroblasts with growth of their glial stem cell niche. PLOS Biology 18:e3000721.

Yurchenco PD, Quan Y, Colognato H, Mathus T, Harrison D, Yamada Y, O'Rear JJ (1997) The α chain of laminin-1 is independently secreted and drives secretion of its β- and γ-chain partners. PNAS 94:10189–10194.

Zang Y, Wan M, Liu M, Ke H, Ma S, Liu L-P, Ni J-Q, Carlos Pastor-Pareja J (2015) Plasma membrane overgrowth causes fibrotic collagen accumulation and immune activation in Drosophila adipocytes. eLife 4:e07187.

Appendix: Supplemental figures

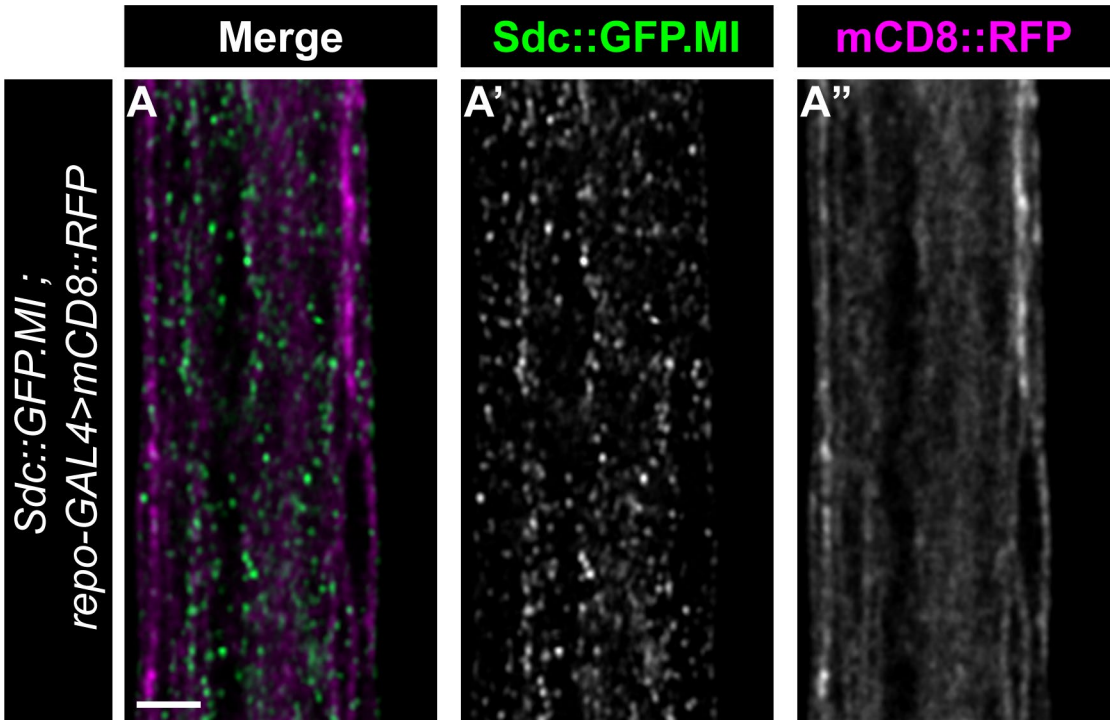

Supplemental Figure A.1: Syndecan's expression in the peripheral nerve

(**A**) Longitudinal cross-section of a 3rd instar larval peripheral nerve in which the all glia are labeled with membrane-bound mRFP (mCD8::RFP, magenta) driven by *repo-GAL4*. Sdc:: GFP.MI (green) localization is visualized using an anti-GFP antibody. I observed similar distribution of Sdc::GFP.MI puncta along the glial membranes comparing to Sdc::GFP.PTT. Scale bar, 2 μm.

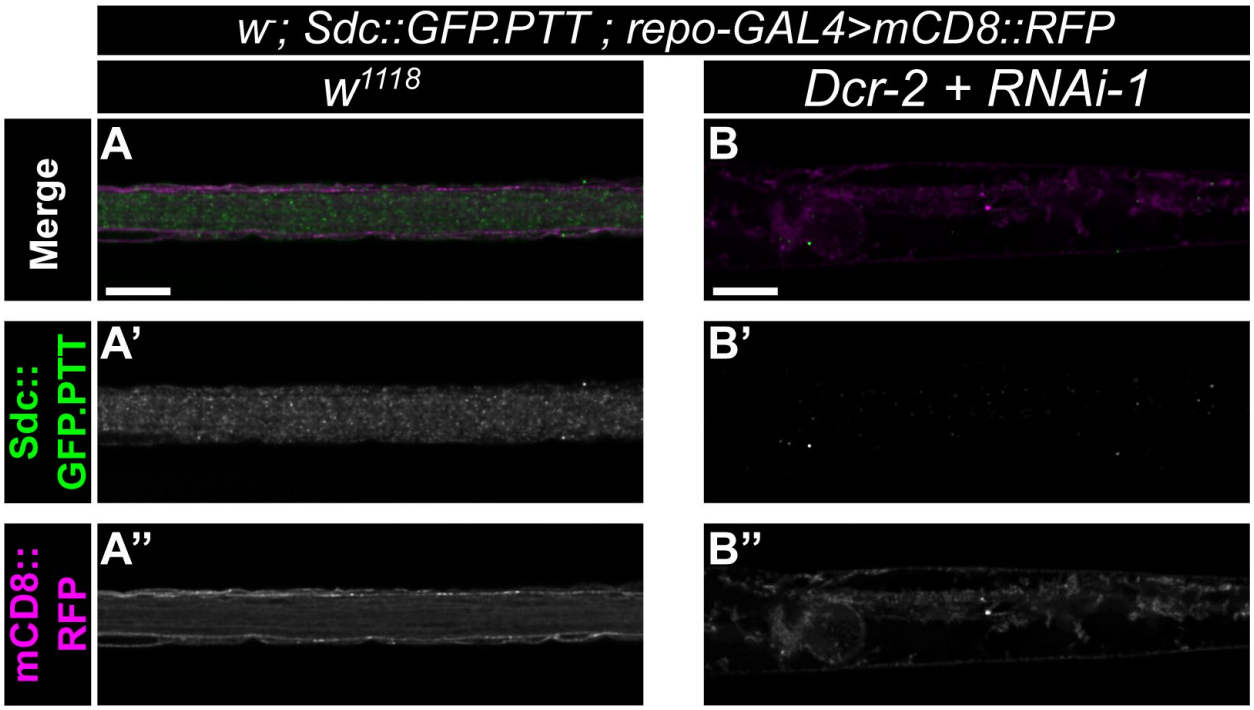

Supplemental Figure A.2: Syndecan RNAi effectively reduce Syndecan expression

(**A-B**) Representative longitudinal cross-section images of peripheral nerve in control (w^{1118}) (A-A") and *Dcr2+RNAi-1* (B-B"). Pan glial membranes are marked with mCD8::RFP (magenta) under the control of repo-GAL4. Syndecan expression is visualized by Sdc::GFP.PTT (green), enhanced by anti-GFP antibody. Note the almost absence of Sdc staining in *Dcr-2 + RNAi-1* (B'), showing the RNAi-1 is capable of robustly reduce Sdc expression.